

IDENTIFICATION AND CHARACTERIZATION OF MONOOXYGENASE
ENZYMES INVOLVED IN 1,4-DIOXANE DEGRADATION IN *PSEUDONOCARDIA*
SP. STRAIN ENV478, *MYCOBACTERIUM* SP. STRAIN ENV421, AND *NOCARDIA*
SP. STRAIN ENV425

by

HISAKO MASUDA

A Dissertation submitted to the
Graduate School-New Brunswick Rutgers,
The State University of New Jersey

And

The Graduate school of Biomedical Sciences
University of Medicine and Dentistry of New Jersey
in partial fulfillment of the requirements

for the degree of

Doctor of Philosophy

Graduate Program in Microbiology and Molecular Genetics

written under the direction of

Professor Gerben J Zylstra

And approved by

New Brunswick, New Jersey

May, 2009

ABSTRACT OF THE DISSERTATION

IDENTIFICATION AND CHARACTERIZATION OF MONOOXYGENASE
ENZYMES INVOLVED IN 1,4-DIOXANE DEGRADATION IN *PSEUDONOCARDIA*
SP. STRAIN EVN478, *MYCOBACTERIUM* SP. STRAIN ENV421, AND *NOCARDIA*
SP. STRAIN ENV425
AND IDENTIFICATION AND CHARACTERIZATION OF *AQUABACTERIUM*
NJENSIS NOV.

by HISAKO MASUDA

Dissertation director: Professor Gerben J. Zylstra

The first part of this dissertation deals with the identification and analysis of oxygenases possibly involved in a biodegradation of a possible human carcinogen, 1, 4-dioxane.

The cometabolic oxidations of 1, 4-dioxane in three gram positive bacteria were analyzed. In *Mycobacterium* sp. ENV421 and *Nocardia* sp. ENV425, 1, 4-dioxane is oxidized during growth on propane. Three putative propane oxidizing enzymes (alkane monooxygenase, soluble diiron monooxygenase, and cytochrome P450) were identified in both strains. While in strain ENV425 only soluble diiron monooxygenase was expressed after growth on propane, in strain ENV421 all three genes were expressed. Although 1,4-dioxane oxidation activity could not be detected in heterologous host gene expression studies, aliphatic oxidation activity was observed with cytochrome P450 CYP153 from strain ENV421.

In strain *Pseudonocardia* sp. ENV478, 1, 4-dioxane oxidation activity was induced in the presence of tetrahydrofuran (THF). A THF-inducible soluble diiron monooxygenase was identified in strain ENV478. The oxygenase gene was transcribed in a complex operonic fashion yielding multiple transcripts with varying lengths. A gene knockdown experiment using antisense technology was employed to show that this gene is essential in THF and 1,4-dioxane degradation.

The second part of this dissertation dealt with the isolation and characterization of a novel solid alkane-utilizing β -*Proteobacterium*, *Aquabacterium njensis* sp. nov.

A novel liquid and solid alkane-degrading bacterium was isolated from hydrocarbon-contaminated soil in New Jersey, USA. The morphological, genomic, and metabolic properties of this organism were examined, including, observation with scanning electron microscopy, DNA-DNA hybridization, and nutritional screening of mainly aliphatic compounds as the sole source of carbon for growth. The preliminary screen of known alkane oxidation enzymes identified two alkane monooxygenase (AlkB) genes in the HMGZ-01 strain.

Sequence analysis of 16S rRNA showed that it has the highest similarity to the members of the genus *Aquabacterium*. The ability to hydrolyze urea and gelatin, NaCl tolerance, substrate utilization pattern and anaerobic growth distinguish the isolated strain from other members of this genus. We proposed the new species, *Aquabacterium njensis*, to be created with a single member and a type strain (HMGZ-01^T).

ACKNOWLEDGEMENTS

First and foremost, I would like to express my gratitude to my thesis advisor, Dr. Gerben Zylstra. Without his extensive knowledge and his patience, this project would not have been possible.

I also wish to thank Drs. Costantino Vetriani, Theodore Chase, and Joan Bennett for serving on my thesis committee and reviewing my dissertation in a professional and objective manner.

I would like to thank Dr. and Mrs. Boyd Woodruff, the Department of Biochemistry and Microbiology and the Biotech Center for providing funding to support my graduate research.

I would like to thank fellow graduate students, lab members and colleagues, Yolanda Hom, Victoria Swiss, Colleen Guerin, Cecilia Della Valle, Maria Fisher-Cruz, Lizbeth Romero, Ruyang Han, Elyse Rodgers-Vieira and Maria Rivera. Thanks for being around when I most needed you. I also want to thank Jong-Chan Chae and Hung-Kuang Chang for helpful discussions and technical support. I thank Laurie Seliger and Michael Murillo for timely providing me materials and sequencing results. I would like to thank Kevin McClay and Dr. Robert Steffan for fruitful collaboration on the 1,4-dioxane project.

I would like also like to thank my family. I thank my husband, daughter, parents, sister, grandparents, uncles and aunt for their faith and support. I would like to give my special thanks to my mom for giving me an inspiration to pursue a career and to be a great mother. I thank Katie for being cute and cheerful.

I would finally like to thank Peter for his love, support, patience and comfort.

None of this was possible without him.

TABLE OF CONTENTS

ABSTRACT OF THE DISSERTATION	ii
ACKNOWLEDGEMENTS	iv
TABLE OF CONTENTS	vi
LIST OF TABLES	xii
LIST OF ILLUSTRATIONS	xiv
PART-A	
1.0 INTRODUCTION	1
1.1 Properties and biodegradation of 1,4-dioxane	1
1.2 Review of organisms studied	5
1.3 Oxygenases	7
1.3.1 Reaction mechanism of C-H oxidation by oxygenases	7
1.3.2 Oxygenases involved in degradation of cyclic, linear, and branched ethers	8
1.3.3 Oxygenases may be involved in tetrahydrofuran degradation. . .	11

1.3.4	Oxygenases involved in short chain alkane and ether degradation	14
1.3.5	Alkane monooxygenase	15
1.3.6	Cytochrome P450	19
1.3.7	Soluble diiron monooxygenase	22
1.3.8	Oxygenases involved in propane degradation	30
2.0	Methods	34
2.1	Bacterial strains, culture conditions and vectors	34
2.2	Nucleic acid techniques.	35
2.3	Chemical, biochemical analysis.	40
3.0	1,4-Dioxane oxidation in <i>Mycobacterium</i> sp. strain ENV421.	44
3.1	N-terminal protein sequencing of propane-induced proteins in <i>Mycobacterium</i> sp. strain ENV421	44
3.2	Identification and analysis of alkane monooxygenase (AlkB) in <i>Mycobacterium</i> sp. ENV421	47
3.2.1	Sequence analysis of alkane monooxygenase (<i>alkB</i>) gene cluster in <i>Mycobacterium</i> sp. strain ENV421	47
3.2.2	Propane-mediated induction of the <i>alkB</i> gene in <i>Mycobacterium</i> sp. strain ENV421	53
3.2.3	Heterologous expression of alkane monooxygenase of <i>Mycobacterium</i> sp. strain ENV421	53

3.3	Identification and analysis of cytochrome P450 (CYP153) in <i>Mycobacterium</i> sp. strain ENV421	56
3.3.1	Sequence analysis and propane mediated induction of cytochrome P450 gene cluster in <i>Mycobacterium</i> sp. strain ENV421	56
3.3.2	Heterologous expression of cytochrome P450	61
3.4	Identification and analysis of a soluble diiron monooxygenase (PMO) in <i>Mycobacterium</i> sp. strain ENV421	77
3.4.1	Sequence analysis of propane monooxygenase gene cluster in <i>Mycobacterium</i> sp. strain ENV421	77
3.4.2	Propane-mediated induction of the propane monooxygenase gene in <i>Mycobacterium</i> sp. strain ENV421	78
3.4.3	Heterologous gene expression of putative PMO	80
3.5	Alcohol dehydrogenases in <i>Mycobacterium</i> sp. strain ENV421	80
3.6	Genetic manipulation of <i>Mycobacterium</i> sp. ENV421	44
3.7	Discussion	44
4.0	1,4-dioxane oxidation in <i>Pseudonocardia</i> sp. strain ENV478	91
4.1	Sequence analysis of 16S rRNA gene in <i>Pseudonocardia</i> sp. strain ENV478	92
4.2	Identification and analysis of putative tetrahydrofuran monooxygenase in <i>Pseudonocardia</i> sp. strain ENV478	92
4.2.1	Sequence analysis of tetrahydrofuran monooxygenase gene cluster in <i>Pseudonocardia</i> sp. strain ENV478	92

4.2.2	THF-mediated induction of the THF monooxygenase gene in <i>Pseudonocardia</i> sp. strain ENV478	94
4.2.3	Transcript analysis of THF monooxygenase gene in <i>Pseudonocardia</i> sp. strain ENV478	99
4.2.4	Analysis of the origin of multiple <i>thm</i> transcripts in <i>Pseudonocardia</i> sp. strain ENV478.	104
4.2.5	Genetic manipulation of <i>Pseudonocardia</i> sp. strain ENV478 . .	111
4.2.6	Gene knockdown of <i>thmB</i> in <i>Pseudonocardia</i> sp. strain ENV478	111
4.3	Alkane monooxygenase (AlkB) gene cluster in <i>Pseudonocardia</i> sp. strain ENV478	115
4.4	Identification and analysis of cytochrome P450 gene cluster in <i>Pseudonocardia</i> sp. strain ENV478	115
4.5	Discussion.	116
5.0	1,4-dioxane oxidation in <i>Rhodococcus</i> sp. strain ENV425	122
5.1	Identification and analysis of propane monooxygenase in <i>Rhodococcus</i> sp. strain ENV425	122
5.1.1	Sequence analysis of propane monooxygenase gene cluster in <i>Rhodococcus</i> sp. strain ENV425	122
5.1.2	Propane-mediated induction of propane monooxygenase gene cluster in <i>Rhodococcus</i> sp. strain ENV425	125
5.1.3	Heterologous expression of putative PMO in <i>E. coli</i> BL21 . . .	125

5.2	Identification and analysis of alkane monooxygenase (AlkB) and cytochrome P450 gene in <i>Rhodococcus</i> sp. strain ENV425	127
5.3	Discussion.	127
5.4	Conclusion for PART-A.	128

PART-B

6.0	Isolation and characterization of <i>Aquabacterium njensis</i> sp. nov., a novel member of the β - <i>Proteobacteria</i> active in liquid and solid alkane degradation	132
6.1	Introduction	133
6.2	Methods	135
6.2.1	Bacterial strains, media and culture conditions.	135
6.2.2	Morphological and physiological characterization.	136
6.2.3	Molecular techniques.	137
6.3	Results	138
6.3.1	Morphology and colony characteristics.	138
6.3.2	Physiological properties.	140
6.3.3	Substrate utilization.	142
6.3.4	Electron acceptor.	143
6.3.5	DNA-DNA hybridization.	143
6.3.6	Phylogenetic analysis of 16S rRNA sequence.	143
6.3.7	Phylogenetic analysis of <i>alkB</i>	145
6.4	Discussion	145

REFERENCES.	151
------------------	-----

Curriculum Vita.	162
-----------------------	-----

LIST OF TABLES

Table 1. List of members of a genus <i>Pseudonocardia</i> and their ability to oxidize 1,4-dioxane.	12
Table 2. List of genes known to be involved in alkane degradation pathway in <i>Pseudomonas putida</i> GP01.	16
Table 3. Subunit composition of soluble diiron monooxygenase sub-families.	24
Table 4. List of phenol hydroxylases	28
Table 5. List of 4-component alkene/aromatic hydroxyases	28
Table 6. List of N-terminal protein sequences of propane-induced proteins in <i>Mycobacterium</i> sp. strain ENV421.	46
Table 7. Properties of <i>alk</i> gene products in <i>Mycobacterium</i> sp. strain ENV421.	50
Table 8. Properties of <i>aphG</i> , <i>aphH</i> , and <i>aphI</i> gene products identified in <i>Mycobacterium</i> sp. strain ENV421.	60
Table 9. List of genes identified in <i>prm</i> gene cluster and their predicted functions.	64
Table 10. The list of known limonene hydroxylases.	85
Table 11. List of genes identified in <i>thm</i> gene cluster and their predicted functions.	93
Table 12. Efficiency of primers for amplifying <i>thmB</i> or 16S rRNA gene in Quantitative RT-PCR reactions	96
Table 13. Δ Ct values and relative amounts of <i>thmB</i> mRNA in <i>Pseudonocardia</i> sp. strain ENV478 cells grown on different carbon sources.	98
Table 14. Efficiency of primers for amplifying 16S rRNA and intragenic or intergenic fragment of <i>thm</i> genes in quantitative RT-PCR reactions.	108

Table 15. List of genes identified in <i>prm</i> gene cluster from <i>Nocardia</i> sp. strain ENV425 and their predicted functions.	123
Table 16. Summary of three oxygenases in <i>Mycobacterium</i> sp. strain ENV421, <i>Pseudonocardia</i> sp. strain ENV478 and <i>Nocardia</i> sp. strain ENV425.	129
Table 17. Summary of physiological characteristics of <i>Aquabacterium njensis</i> HMGZ01 ^T <i>Aquabacterium</i> , <i>A. citratiphilum</i> sp. B4 ^T , <i>A. parvum</i> sp. B6 ^T , and <i>A. commune</i> sp. B8 ^T	141
Table 18. List of alkane monooxygenases with known substrate range.	146

LIST OF ILLUSTRATIONS

Figure 1. Proposed 1,4-dioxane degradation pathway	2
Figure 2. Phylogenetic analysis of 16S rRNA sequences of <i>Pseudonocardia</i> sp. strain ENV478 and THF degrading <i>Pseudonocardia</i> strains.	12
Figure 3. Proposed tetrahydrofuran (THF) degradation pathway	13
Figure 4. The gene organization and functions of gene products in alkane degradation pathway in <i>Pseudonocardia putida</i> GPo1	16
Figure 5. Structure of alkane monooxygenase system	17
Figure 6. Gene organization of <i>alk</i> genes in various organisms	17
Figure 7. Structure and gene organization of cytochrome P450 complex in <i>Mycobacterium</i> sp. strain HXN-1500, <i>Acinetobacter</i> sp. OC4 and <i>Gordonia</i> sp. TF6.	21
Figure 8. Phylogenetic analysis of α subunit of soluble diiron monooxygenases ...	23
Figure 9. Structure of soluble diiron monooxygenase.	23
Figure 10. Gene organization of soluble diiron monooxygenase subfamilies.	24
Figure 11. Propane degradation pathway	31
Figure 12. Protein expression pattern of <i>Mycobacterium</i> sp. strain ENV421 after the growth on propane or on succinate	46
Figure 13. Phylogenetic analysis of the alkane monooxygenase (AlkB) gene identified in <i>Mycobacterium</i> sp. strain ENV421.	48
Figure 14. The organization of the alkane monooxygenase gene cluster in <i>Mycobacterium</i> sp. strain ENV421.	50

Figure 15. Phylogenetic tree of oxidoreductases for soluble diiron monooxygenase, cytochrome P450 and alkane monooxygenases.	52
Figure 16. RT-PCR analysis of <i>alkB</i> expression in <i>Mycobacterium</i> sp. ENV421 after growth on propane or succinate.	54
Figure 17. The octane oxidation activity of <i>E.coli</i> BL21 recombinant clone expressing AlkBFG of ENV421 and AlkTFG of <i>Pseudomonas putida</i>	57
Figure 18. Southern blot analysis of cytochrome P450 genes in <i>Mycobacterium</i> sp. strain ENV421	57
Figure 19. Expression pattern of cytochrome P450 gene in <i>Mycobacterium</i> sp. strain ENV421 after growth on propane or succinate.	59
Figure 20. Phylogenetic analysis of cytochrome P450 hydroxylase gene from <i>Mycobacterium</i> sp. strain ENV421.	59
Figure 21. Gene order and gene composition of the cytochrome P450 gene cluster from <i>Mycobacterium</i> sp. strain ENV421	60
Figure 22. Pigment formation by <i>E. coli</i> recombinant clone expressing cytochrome P450 from <i>Mycobacterium</i> sp. strain ENV421BL21	62
Figure 23. The analysis of blue and pink pigments produced by <i>E. coli</i> recombinant clone expressing cytochrome P450 from <i>Mycobacterium</i> sp. strain ENV421 using thin layer chromatography.	62
Figure 24. UV-visible spectroscopy of blue pigment produced by recombinant <i>E.coli</i> clone expressing cytochrome P450 from <i>Mycobacterium</i> sp. strain ENV421 and indigo standard	63
Figure 25. UV-visible spectroscopy of pink pigment produced by recombinant <i>E.coli</i>	

clone expressing	63
Figure 26. UV-visible spectroscopy of indigo and indirubin	63
Figure 27. Various indole oxidation products	64
Figure 28. The biotransformation of limonene to perillyl alcohol by cytochrome P450 from <i>Mycobacterium</i> sp. strain ENV421.	66
Figure 29. The biotransformation of cymene to <i>p</i> -cymen-7-ol by cytochrome P450 from <i>Mycobacterium</i> sp. strain ENV421	67
Figure 30. The biotransformation of 4-ethyltoluene to 4-(ethylphenyl)methanol by cytochrome P450 from <i>Mycobacterium</i> sp. strain ENV421.	68
Figure 31. The biotransformation of octylbenzene by cytochrome P450 from <i>Mycobacterium</i> sp. strain ENV421	69
Figure 32. The biotransformation of heptylbenzene by cytochrome P450 from <i>Mycobacterium</i> sp. strain ENV421	70
Figure 33. The biotransformation of hexylbenzene by cytochrome P450 from <i>Mycobacterium</i> sp. strain ENV421	71
Figure 34. The biotransformation of pentylbenzene by cytochrome P450 from <i>Mycobacterium</i> sp. strain ENV421	72
Figure 35. The biotransformation of n-butylbenzene by cytochrome P450 from <i>Mycobacterium</i> sp. strain ENV421	73
Figure 36. The biotransformation of propylbenzene by cytochrome P450 from <i>Mycobacterium</i> sp. strain ENV421	74
Figure 37. The biotransformation of octane to 1-octanol by cytochrome P450 from <i>Mycobacterium</i> sp. strain ENV421.	75

Figure 38. Summary of biotransformation assay of aliphatic compounds by cytochrome P450 from <i>Mycobacterium</i> sp. strain ENV421.	76
Figure 39. Phylogenetic analysis of two soluble diiron monooxygenase genes identified in <i>Mycobacterium</i> sp. strain ENV421	79
Figure 40. Two soluble diiron monooxygenase genes identified in <i>Mycobacterium</i> sp. strain ENV421.	79
Figure 41. The multiple sequence alignment of N-terminal sequence of a propane induced 42kDa protein in strain ENV421 and zinc-alcohol dehydrogenases	81
Figure 42. Phylogenetic analysis of alcohol dehydrogenases identified in <i>Mycobacterium</i> sp. strain ENV421.	81
Figure 43. Enzymatic oxidation product of limonene.	85
Figure 44. Gene composition and gene organization of an operon containing putative THF monooxygenase and dehydrogenases in <i>Pseudonocardia</i> sp. strain ENV478.	93
Figure 45. RT-PCR analysis of <i>thmB</i> gene expression in THF or succinate grown ENV478.	96
Figure 46. RT-PCR analysis of THF-induced <i>thm</i> genes.	100
Figure 47. The positions of 5' ends of mRNA identified by 5' RACE Assay.	102
Figure 48. Alignment of sequences upstream of <i>thm</i> genes in <i>Pseudonocardia</i> sp. strain ENV478.	102
Figure 49. The inverted repeats downstream of <i>thmA</i> and <i>thmC</i> in <i>Pseudonocardia</i> sp. strain ENV478.	103

Figure 50. Transcription pattern of <i>thm</i> gene clusters in <i>Pseudonocardia</i> sp. strain ENV478.	103
Figure 51. The primer design for <i>thm</i> transcript analysis in <i>Pseudonocardia</i> sp. strain ENV478.	107
Figure 52. The primers for <i>thm</i> transcript analysis of in strain ENV478.	107
Figure 53. The predicted result of RT- PCR reaction in two different scenarios for the origin of multiple <i>thm</i> transcripts.	108
Figure 54. Relative level of <i>thmA</i> and <i>thmB</i> intergenic region and <i>thmB</i> intragenic region 0, 2, and 6 min after halting transcription by an addition of rifampicin.	110
Figure 55. The growth curve of wild-type and <i>thmA</i> and <i>thmB</i> knockdown mutant strains of <i>Pseudonocardia</i> sp. strain ENV478 on THF.	114
Figure 56. 1,4-dioxane degradation by wild-type and <i>thmB</i> knockdown mutant strains of <i>Pseudonocardia</i> sp. strain ENV478.	114
Figure 57. Transcription pattern of <i>thm</i> gene clusters in <i>Pseudonocardia</i> sp. strain K1 (Thiemer et al., 2003).	119
Figure 58. The predicted combination of <i>thm</i> transcripts in <i>Pseudonocardia</i> sp. strain ENV478.	119
Figure 59. Phylogenetic analysis of soluble diiron monooxygenase α -subunit from <i>Nocardia</i> sp. strain ENV425.	123
Figure 60. Gene organization of propane monooxygenase gene cluster in <i>Nocardia</i> sp. strain ENV425.	124
Figure 61. Gene expression analysis of <i>alkB</i> , soluble diiron monooxygenase, and cytochrome P450 in <i>Nocardia</i> sp. strain ENV425 after growth	

on propane.	126
Figure 62. Gene expression analysis of soluble diiron monooxygenase and cytochrome P450 in response to NDMA (N -nitrosodimethylamine) in <i>Nocardia</i> sp. strain ENV425.	126
Figure 63. Phylogenetic and gene organization analysis of soluble diiron monooxygenase α -subunit identified in <i>Mycobacterium</i> sp. strain ENV421, <i>Pseudonocardia</i> sp. strain ENV478 and <i>Nocardia</i> sp. strain ENV425.	131
Figure 64. Scanning electron microscopy of <i>Aquabacterium njensis</i> HMGZ01 ^T	139
Figure 65. Phylogenetic analysis of 16S rRNA gene of <i>Aquabacterium njensis</i> sp. HMGZ01 ^T and other β -proteobacteria strains.	144
Figure 66. Phylogenetic analysis of <i>alkB</i> protein sequences in <i>Aquabacterium njensis</i> HMGZ01 ^T , <i>Aquabacterium</i> , <i>A. citratiphilum</i> sp. B4 ^T , <i>A. parvum</i> sp. B6 ^T , and <i>A. commune</i> sp. B8 ^T	146

PART-A

1.0 INTRODUCTION

1.1 Properties and biodegradation of 1,4-dioxane

The cyclic ether 1, 4-dioxane is an organic solvent widely used as a stabilizing agent in chemical syntheses involving chlorinated compounds. It is miscible in water, and contamination of ground water with 1,4-dioxane is a growing human health concern (DeRosa et al, 1996). 1,4-dioxane is a suspected carcinogen. Studies in mice have shown the formation of micronuclei in bone marrow and liver upon exposure to 1,4-dioxane (Roy et al, 2005).

There are few studies describing the biodegradation of 1,4-dioxane. For several decades, the studies were limited to metabolic intermediate analysis in rats and humans (Braun and Young, 1977; Young et al, 1976; Young et al., 1977).

In rats, two major 1,4-dioxane metabolic intermediates were discovered by two independent researchers: β -hydroxyethoxyacetic acid (β -HEAA) and *p*-dioxane-2-one (Braun et al., 1977; Woo et al, 1977). These two compounds are related, and the product of lactonization of β -HEAA is *p*-dioxane-2-one. Based on the pH conditions of the experiments, the two molecules can interconvert abiotically.

There are two predicted pathways for the formation of β -HEAA/*p*-dioxane-2-one as summarized in Figure 1: 1) β -oxidation followed by oxidation of hydroxyl groups on the hydroxyaldehyde intermediate (Figure 1, line 2), and 2) hydrolysis of 1,4-dioxane which results in the formation of diethylene glycol, followed by an oxidation of alcohol group (Figure 1, line 3).

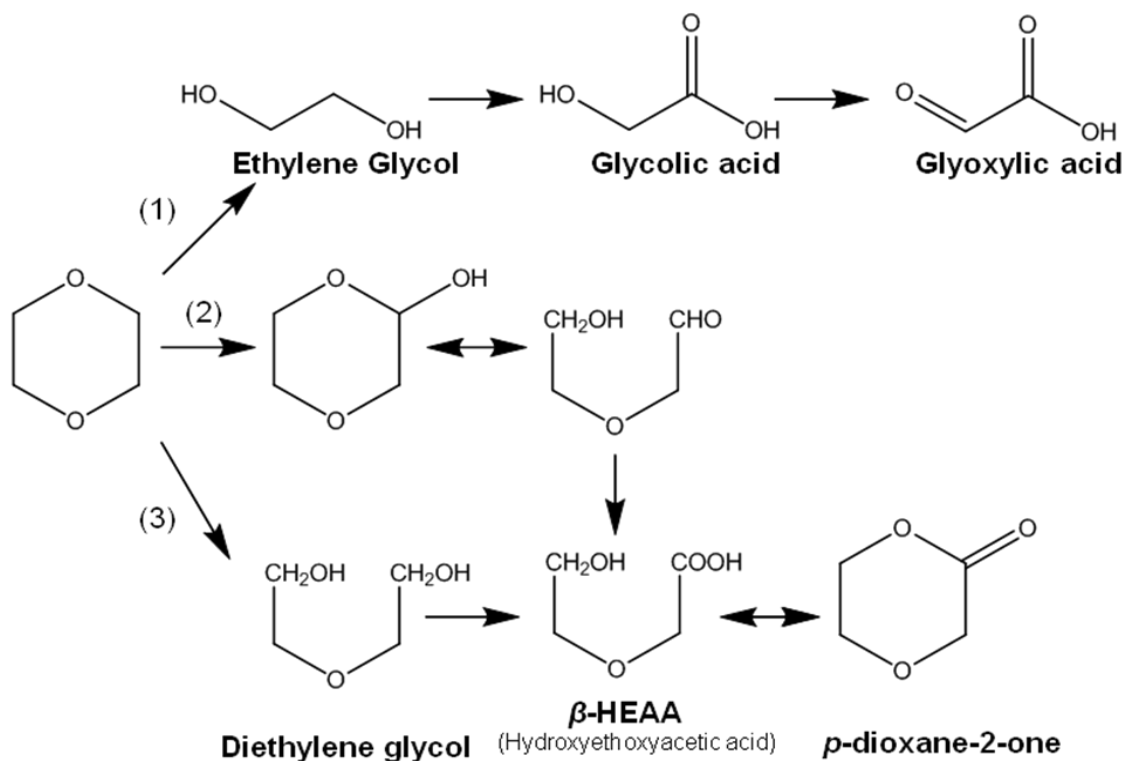


Figure 1. **Proposed 1,4-dioxane degradation pathway.** (1) In yeast *Cordyceps sinensis*, ethylene glycol, glycolic acid, and glyoxylic acid were identified as a degradation product of 1,4-dioxane (Nakamiya et al, 2005). (2, 3) In rats and humans, β-hydroxyethoxyacetic acids have been identified as an intermediate (Woo et al, 1977). The degradation pathway can start either by (2) hydroxylation by oxygenase or (3) hydrolysis of 1,4-dioxane.

1,4-Dioxane degradation by both mixed and pure cultures of bacteria and fungi has started to be examined recently (Nakamiya et al., 2005; Parales et al., 1994). Very few pure cultures of fungi and bacteria capable of utilizing 1,4-dioxane as a sole carbon source have been isolated. *Cordyceps sinensis* is the only yeast strain that can utilize 1,4-dioxane as a sole carbon source. The possible degradation pathway in *C. sinensis* was postulated based on analysis of intermediates, which was different from what was observed in rats (Nakamiya et al., 2005). In *C. sinensis*, 1,4-dioxane degradation initiates with the formation of two ethylene glycol molecules (Nakamiya et al., 2005). Ethylene glycol will be further degraded to glycolic acid, which will then be turned into glyoxylic acid (Figure 1). Glyoxylic acid will be funneled into the central energy metabolism. The enzyme responsible for transformation of 1,4-dioxane to two ethylene glycol molecules is unknown.

An *Actinomycete* strain, CB1190, recently renamed as *Pseudonocardia dioxanivorans*, and *Pseudonocardia benzenivorans* are the only known bacteria that are capable of mineralization and growth with 1,4-dioxane as a sole carbon source (Parales et al., 1994; Mahendra et al., 2006). However, no information on intermediates or enzymes involved in the degradation pathway is available.

Although discovery of bacteria capable of utilizing 1,4-dioxane as the sole source of carbon is rare, 1,4-dioxane degradation via a cometabolic process in tetrahydrofuran (THF) grown bacteria seems to be a common phenomenon (Vainberg et al., 2006; Mahendra et al., 2006). Tetrahydrofuran is a cyclic ether and structural analog of 1,4-dioxane.

Based on the proposed pathways of 1,4-dioxane degradation in yeasts and rats, it is proposed that biodegradation of 1,4-dioxane in bacteria is most likely initiated through either direct hydrolysis of ether bonds, or by destabilization of the bonds by introduction of an oxygen atom.

In cyclic ether-degrading *Rhodococcus* and *Pseudonocardia* strains, it was observed that the initial step of cyclic ether degradation is an oxidation of the compound at the carbon adjacent to the oxygen, a process called 2-hydroxylation (Bernhardt and Diekmann, 1991; Thiemer et al., 2003). 2-Hydroxylation forms an unstable hemiacetal, which spontaneously dismutates to an alcohol and an aldehyde, which subsequently results in ether bond cleavage. Since both THF and 1,4-dioxane are cyclic ether, the initial degradation step of these compounds is also expected to be 2-hydroxylation. Also, due to their structural similarity, one enzyme is likely to be responsible for oxidation of both THF and 1,4-dioxane.

1,4-Dioxane degradation in three high-GC gram-positive strains was examined in this study. In all strains, 1,4-dioxane was degraded through a cometabolic process after growth on other substrates. The specific details of 1,4-dioxane degradation in these organisms will be described later. In all strains, 1,4-dioxane cannot be completely mineralized and provide a carbon source for cells, indicating either absence of the enzyme(s) necessary for catabolism of degradation intermediates and/or lack of ability to induce their gene expression under 1,4-dioxane degrading conditions.

Thus, the focus of our study was to elucidate the enzyme involved in the initial rate-limiting oxidation step of 1,4-dioxane in these organisms. The above mentioned studies on cyclic ether degradation by fungi and bacteria lead us to hypothesize that

oxidation of 1,4-dioxane is also performed by oxygenases and oxidation happens at the carbon next to an oxygen.

Two strategies were taken to discover the putative 1,4-dioxane oxygenases. First, transposon based-mutagenesis was attempted to identify mutants that lost the ability to oxidize 1,4-dioxane. However, none of the transposon donors tested yielded any mutants. A reverse genetic approach was then used to identify the oxygenases. We choose several putative oxygenases to investigate either through a proteomics approach or through a literature search of oxygenases with the desired catalytic capability and substrate range. The identification schemes will be described in later sections. The presence of these genes was screened for using PCR with degenerate primers. Their expression pattern was then examined using RT-PCR and quantitative RT-PCR. The 1,4-dioxane oxidation activity of these gene products were confirmed by heterologous expression or by gene knockdown experiment.

1.2 Review of organisms studied

Mycobacterium sp. strain ENV421 is a gram-variable, acid-fast, filamentous organism, and the 16S rRNA sequence showed that it is most closely related to members of the genera *Mycobacterium* sp. ENV421 was isolated from uncontaminated turf soil by enrichment culture with propane as a sole carbon and energy source (Steffan et al., 1997). It grows on 1-propanol, but not on 2-propanol, suggesting the propane-oxidizing oxygenase carries out terminal oxidation of propane to form 1-propanol, which can be further metabolized for growth. Studies on strain ENV421 were originally focused on its

ability to degrade MTBE (Steffan et al., 1997). Strain ENV421 oxidizes MTBE at 9.2 nmol/min/mg through cometabolic oxidation after growth on propane. Since both MTBE and 1,4-dioxane oxidation occur only after growth on propane, the enzyme responsible for propane oxidation is most likely also important in both 1,4-dioxane and MTBE oxidation.

Pseudonocardia sp. strain ENV478 was originally isolated as a tetrahydrofuran (THF) degrader by Dr. Robert Steffan and Mr. Kevin McClay at Shaw Corp (Lawrenceville, NJ). After growth on THF, strain ENV478 can oxidize a variety of ethers: THF (63 mg/h/g total suspended solids [TSS]), 1,4-dioxane (21 mg/h/g TSS), 1,3-dioxolane (0.1 mg/h/g TSS), *bis*-2-chloroethylether (BCEE) (12 mg/h/g TSS), and methyl-*tert*-butyl ether (MTBE) (9.1 mg/h/g TSS) (Vainberg et al., 2006). The degradation of 1,4-dioxane occurs after growth not only on THF but also on non-ether substrates, such as sucrose, lactate, yeast extract, 2-propanol, and propane. The rate of 1,4-dioxane oxidation by THF grown cells is faster than that of cells grown on other substrates. When both THF and 1,4-dioxane are added to the medium, the oxidation of 1,4-dioxane starts after THF is completely utilized. This indicates the possibility that 1,4-dioxane and THF competes for the same enzyme and that the enzyme has a higher affinity for THF. The 16S rRNA sequence shares 97% sequence identity to a known THF degrader, *Pseudonocardia* sp. K1 (Kampfer et al., 2006; Kohlweyer et al., 2000). Due to this high similarity, it was predicted that the two organisms may use the same enzyme system for THF oxidation. This will be further discussed in later sections.

Strain ENV425 is a gram-variable, acid fast, filamentous, rod-shaped organism that forms red to orange colonies on MSB or rich media. It was identified by 16S rRNA

sequence analysis as a member of the *Nocardia* genus. Strain ENV425 has been studied for its ability to degrade MTBE via cometabolism. The highest MTBE degradation rate was observed after growth on propane (4.6nmol/min/mg) (Steffan et al., 1997; Smith et al., 2003; Liu et al., 2001). In the absence of oxygen, no degradation of MTBE was observed, suggesting the role of oxygenase in MTBE degradation (Steffan et al., 1997). In previous studies, an oxygenase responsible for MTBE oxidation had been proposed. Carbon monoxide difference spectrum and inhibitor studies were consistent with the presence of a cytochrome P450 enzyme in propane grown cells (Steffan et al., 1997). Another study suggested the involvement of an alkane monooxygenase in MTBE degradation in strain ENV425 (Smith et al., 2003).

Strain ENV425 grows on both 1-propanol and 2-propanol. This growth pattern suggests that their putative propane oxygenases can possibly oxidize propane at both terminal and sub-terminal positions. The oxygenase that is responsible for propane oxidation in strain ENV425 had not been identified. 1,4-dioxane oxidation in strain ENV425 occurs after growth on propane indicating the involvement of a putative propane monooxygenase in 1,4-dioxane degradation.

1.3 Oxygenases

1.3.1 Reaction mechanism of C-H oxidation by oxygenases

The replacement of carbon-bound hydrogen with a hydroxyl group is a difficult reaction (Groves et al., 2006). Enzymatic hydroxylation of hydrocarbons has thus

attracted great attention. So far, enzymes known to catalyze this reaction are limited. The list of enzymes includes heme-containing oxygenase (cytochrome P450), and non-heme oxygenase (AlkB, sMMO, T4moH, XylM) (Groves et al., 2006).

Although the structure of the catalytic center is different, the reaction mechanism of these enzymes is conserved: activation of molecular oxygen to hydrogen peroxide by irons at the active center, followed by an incorporation of one of the oxygen atoms into the substrate.

Cytochrome P450 and chloroperoxidase (CPO) use an iron-protoporphyrin IX center, which is coordinated to a cysteine thiolate, to activate molecular oxygen (in P450) or hydrogen peroxide (in CPO). The reaction starts through the oxidation of iron (III) to a reactive oxoiron (IV)-porphyrin cation radical intermediate. Non-heme diiron hydroxylases initiate a reduction of dioxygen via a di-ferrous form of the enzyme, forming a peroxo-Fe(III)-Fe(III) state. During substrate activation, both heme and non-heme enzymes go through formation and rearrangement of radical and cationic intermediates (Groves et al., 2006).

1.3.2 Oxygenases involved in degradation of cyclic, linear, and branched ethers

Both 1,4-dioxane and tetrahydrofuran (THF) are cyclic ethers. The degradation of ether compounds are known to involve activation of ether bonds followed by their scission. Since the ether bond is a high energy bond and hard to activate enzymatically, few enzymes responsible for ether bond scission have been discovered. Several

mechanisms for the enzymatic cleavage of ether bonds have been proposed. The list of known possible mechanisms includes hydroxylation by oxygenases or by cytochrome P450, hydroxyl shift, hydrolysis, anaerobic cleavage of methyl-aryl ethers, and oxidation or reduction by C-O lyase (White et al., 1996).

Ethers can be categorized as dialkyl ether, alkyl aryl ether, and diaryl ether (Kim et al., 2004), and 1,4-dioxane and THF are classified as dialkyl ethers. Historically, study on ether bond scission was limited to aromatic ethers (=aryl ethers) and some alkyl ethers: phenoxyacetic acid and lignin related ethers (Pieper et al., 1990). Recently, more studies on linear and cyclic ethers have been conducted. A characteristic of ether oxidation is the formation of an unstable hemiacetal after oxygenation of the carbon next to the oxygen by an oxygenase (Kim et al., 2004). It has been known that dialkyl ethers and alkyl ethers are oxidized through monooxygenation, while diaryl ethers are oxidized by dioxygenation reaction.

Some bacterial and fungal strains are shown to be capable of oxidation of dialkyl ethers, and in some cases possible oxygenases capable of ether oxidation have been identified. *Burkholderia cepacia* strain G4/PR1, containing a variety of monooxygenases including toluene-2-monooxygenase and toluene-4-monooxygenase, can oxidize diethyl ether, butyl methyl ether, diethyl sulfide, and 2-chloroethyl ethyl ether (Hur et al., 1997). Ammonia monooxygenase of *Nitrosomonas europaea* was suggested to oxidize dimethyl ether (Hyman et al., 1994).

Some liquid or gas alkane degraders are also capable of ether oxidation. Octane-grown *Pseudomonas putida* GPo1, which has a membrane-bound alkane monooxygenase, can oxidize methyl tert-butyl ether (MTBE) (Smith and Hyman, 2004). *Mycobacterium*

austroafricanum IFP 2012 can also oxidize tertiary butanol (TBA) (Lopes Ferreira et al., 2007). A variety of propane degraders are capable of oxidizing a variety of alkylethers: methyl tert-butyl ether, ethyl tert-butyl ether, and tert-amyl methyl ether (Steffan et al., 1997). Five *Mycobacterium* strains can degrade Trichloroethylene (TCE) through cometabolic oxidation after growth on propane. A fungal *Graphium* strain utilizes butane and diethyl ether, and can oxidize MTBE through co-oxidation using P450 (Hardison et al., 1997).

MTBE is one of the most well studied non-aromatic ethers regarding its biodegradation pathway. MTBE regulons have been characterized in two organisms that can grow on MTBE as a carbon source. In the MTBE growing strain *Methylibium petroleiphilum* PM1, the MTBE regulon contains *alkB* (Hristova, et al., 2007). On the other hand, in another alkane-utilizing *Mycobacterium austroafricanum* IFP2012 strain, MdpB protein, which belongs to the glucose-methanol-choline oxidoreductase family, has been shown to be important for MTBE oxidation (Lopes Ferreira et al., 2006).

Most known MTBE oxidation reactions are through cometabolic processes. Co-metabolism of MTBE is found in bacteria growing on propane, butane, camphor, pentane, and cyclohexane (Francois et al., 2002). Notably, there are several bacteria that seem to show a correlation between MTBE degradation and short chain alkane degradation (Garnier et al., 1999; Smith et al, 2003), particularly propane degraders. For example, propane-grown *Mycobacterium vaccae* JOB5 cometabolically degrades MTBE (Smith et al, 2003). The enzyme has not yet been characterized, but the range of substrates this enzyme is capable of oxidizing is known to include several short chain alkanes.

Besides AlkB in *Pseudomonas putida* GPo1, so far the only known enzymes for MTBE degradation belong to the cytochrome P450 family (Chauvaux et al., 2001; Hardison, 1997).

1.3.3 Oxygenases may be involved in tetrahydrofuran degradation

THF, unlike 1,4-dioxane, supports growth of many bacteria found in environment (personal communication, Mr. Kevin McClay). All THF degraders identified so far belong to the gram positive *Rhodococcus*, *Gordonia*, or *Pseudonocardia* genera. In the genus *Pseudonocardia*, THF is a growth substrate for a number of its members (Figure 2). The oxidation activity towards 1,4-dioxane, however, varies greatly in this genus (Table 1). *P. dioxynovorans* and *P. benzenivorans* can utilize both THF and 1,4-dioxane. *Pseudonocardia* sp. strain K1 and strain ENV478 can oxidize 1,4-dioxane through a co-metabolic process but cannot grow on 1,4-dioxane as a sole carbon source. Interestingly, THF utilizing *P. sulfidoxydans* and *P. hydrocarbonoxydans* strains have no activity towards 1,4-dioxane (Mahendra et al., 2006).

The THF degradation pathway was recently proposed by Thiemer and his colleagues based on the putative function of genes that are located adjacent to the THF-induced monooxygenase genes in *Pseudonocardia* sp. strain K1 (Thierner et al. 2003). The list of genes included succinate-semialdehyde dehydrogenase (ThmS), putative 4-hydroxybutyraldehyde dehydrogenase (ThmH), and several ORFs with unknown function. The proposed pathway is shown in Figure 3. The multicomponent THF monooxygenase initiates the degradation of THF by adding a hydroxyl group to the

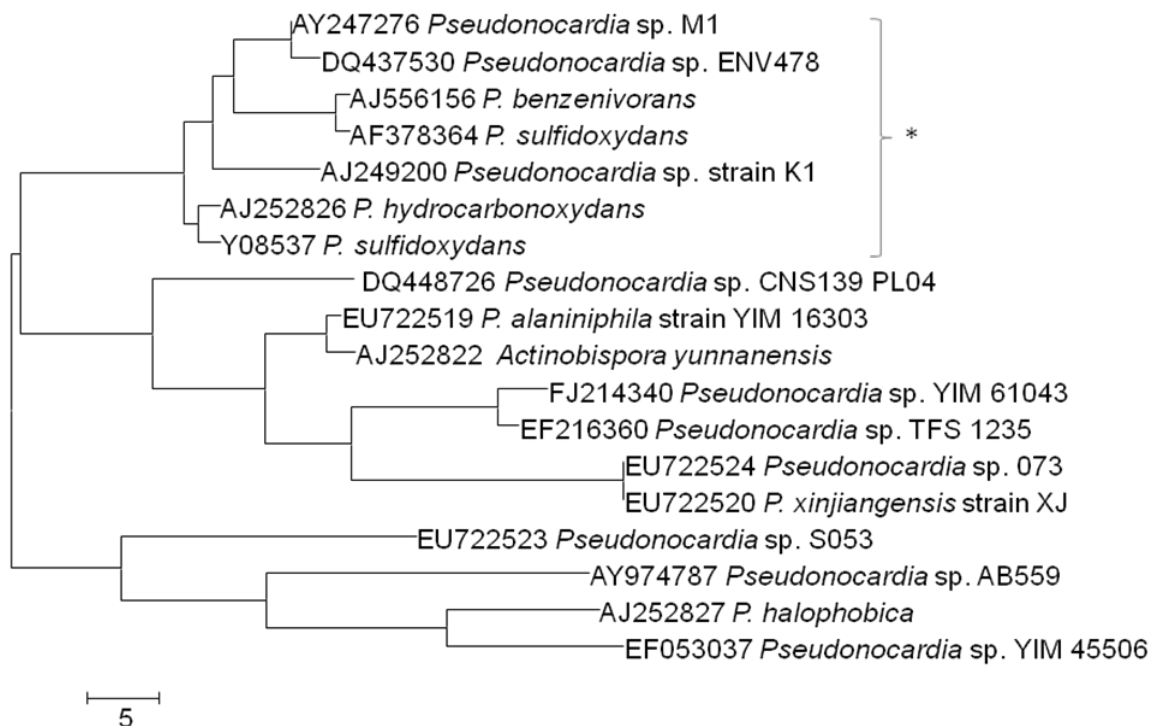


Figure 2. **Phylogenetic analysis of 16S rRNA sequences of *Pseudonocardia* sp. strain ENV478 and THF degrading *Pseudonocardia* strains.** All of known THF-utilizing *Pseudonocardia* strains (labeled with *) are clustered in a subgroup containing strain ENV478.

Table 1. **List of members of a genus *Pseudonocardia* and their ability to oxidize 1,4-dioxane.** All *Pseudonocardia* strains listed here have capability to utilize THF.

Strain	1,4-dioxane utilization	Reference
<i>Pseudonocardia dioxanivorans</i>	Growth substrate	Parales et al., 1994
<i>Pseudonocardia benzenivorans</i>	Growth substrate	Mahendra et al., 2006
<i>Pseudonocardia</i> sp. strain K1	Oxidize cometabolically	Thierner et al., 2001
<i>Pseudonocardia</i> sp. strain ENV478	Oxidize cometabolically	Vainberg et al., 2006
<i>Pseudonocardia sulfidoxydans</i>	Not observed	Mahendra et al., 2006
<i>Pseudonocardia hydrocarbonoxydans</i>	Not observed	Mahendra et al., 2006
<i>Pseudonocardia</i> sp. M1	Not tested	

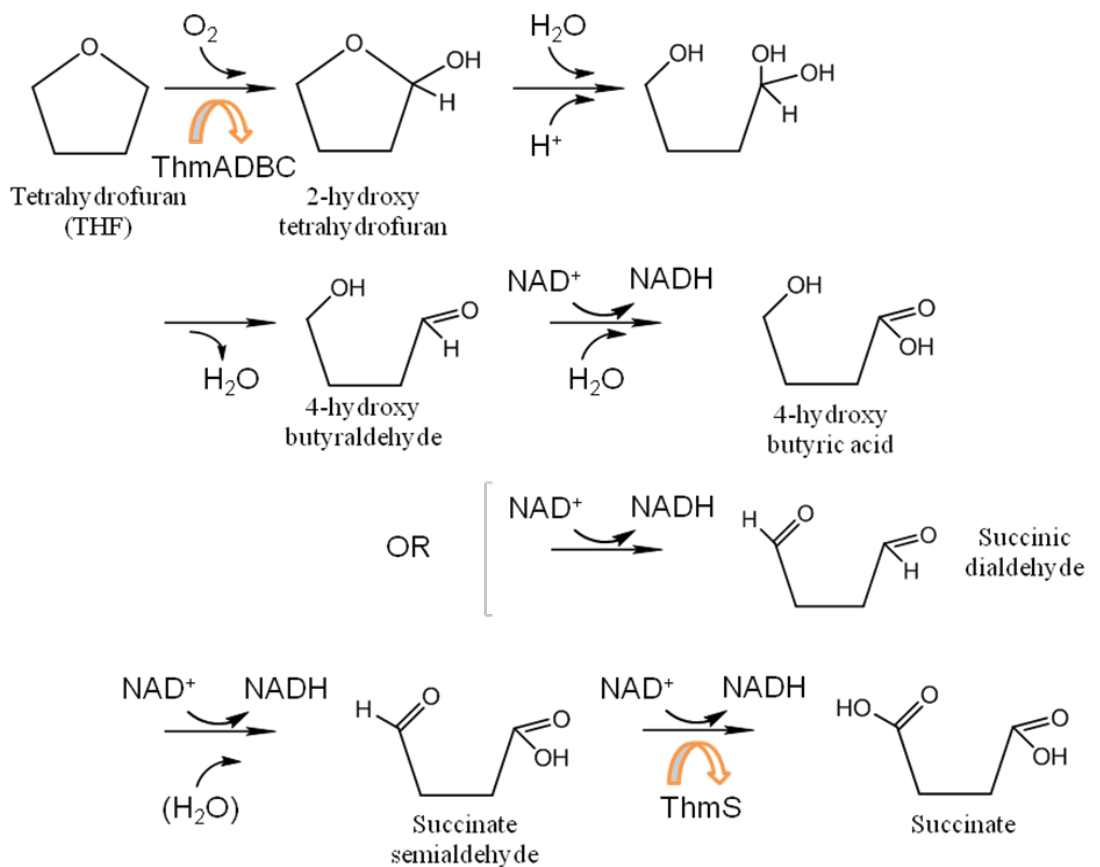


Figure 3. **Proposed tetrahydrofuran (THF) degradation pathway.** Oxidation of tetrahydrofuran by oxygenase forms 2-hydroxytetrahydrofuran. Unstable hemiacetal undergoes spontaneous atomic rearrangements and results in scission of ether bond. A proposed intermediate, succinate semialdehyde, is proposed to be oxidized by ThmS to form succinate (Thierner et al., 2001).

carbon adjacent to the oxygen. The product, 2-hydroxytetrahydrofuran, is proposed to be degraded enzymatically or abiotically to 4-hydroxybutyrate which in turn is converted to succinate semialdehyde. ThmS converts succinate semialdehyde to succinate, which subsequently enters the TCA cycle.

Phylogenetically, the α -subunit of the THF-induced monooxygenase is related to non-heme diiron monooxygenases (BMMs), including soluble methane monooxygenase (sMMO) and propane monooxygenase (PMO). Since reaction mechanisms are well conserved in BMMs, THF-MO can also catalyze similar reactions, namely, monooxygenation of a carbon atom in an organic compound. The observation that a majority of bacteria degrading linear ethers contain THF monooxygenase homologs also supports the possible involvement of THF monooxygenase in THF oxidation (Kim et al., 2007). Although the gene expression of this operon is regulated by THF, there is no direct evidence that this monooxygenase participates in THF oxidation.

1.3.4 Oxygenases involved in short chain alkane and ether degradation

Strains ENV421 and ENV425 oxidize 1,4-dioxane cometabolically after growth on propane. Here, I will review enzyme systems known to be involved in gaseous or liquid linear alkane and ether oxidation in bacteria.

Linear alkanes can be categorized into several groups based on the groups of enzymes capable of attacking the carbon: methane (C_1), short chain (C_2 - C_4), medium/long chain (C_5 - C_{16}), and long chain (C_{17} and longer). Propane is a three-carbon linear chain alkane, belonging to the short chain alkane group. There are several enzymes

known to catalyze short chain alkane oxidation reactions in bacteria. Soluble methane monooxygenase (sMMO), particulate methane monooxygenase (pMMO), propane monooxygenase (PMO), butane monooxygenase (BMO), and alkane hydroxylase related monooxygenase (*alkB*) (Leahy et al., 2003; van Beilen and Funhoff, 2007).

1.3.5 Alkane monooxygenase

AlkB, a membrane bound-alkane monooxygenase enzyme, is the first and best characterized system for liquid alkane hydroxylation. In *P. putida* GPo1, sets of genes necessary to convert alkanes to Co-A derivatives through a series of oxidation steps have been identified (Table 2, Figure 4) (van Beilen et al., 1994). The initial step of alkane oxidation is catalyzed by a multicomponent monooxygenase. The hydroxylase consists of 3 subunits: hydroxylase (*alkB*), rubredoxin (*alkGF*) and rubredoxin reductase (*alkT*) (Figure 5). The electrons from NADH are transferred from *alkT* to *alkGF*, and then to the active center of *alkB*. At the catalytic center of *alkB*, molecular oxygen is activated by an iron group and, combined with an electron, oxidizes alkanes at their terminal carbon. The substrate specificity is determined solely by the *alkB* component.

AlkB is most similar to other membrane bound iron enzymes, such as xylene monooxygenase (XylM) and stearyl-CoA desaturase. Eight catalytically essential histidine residues are conserved in these enzymes. Based on these conserved histidine sites in the AlkB enzyme sequence, degenerate primers were developed. These primers are used for screening presence of *alkB* in various alkane degraders. Using this primer, *alkB* has been identified in a number of medium (C₆-C₁₁) to long (C₁₂-C₁₆) liquid alkane

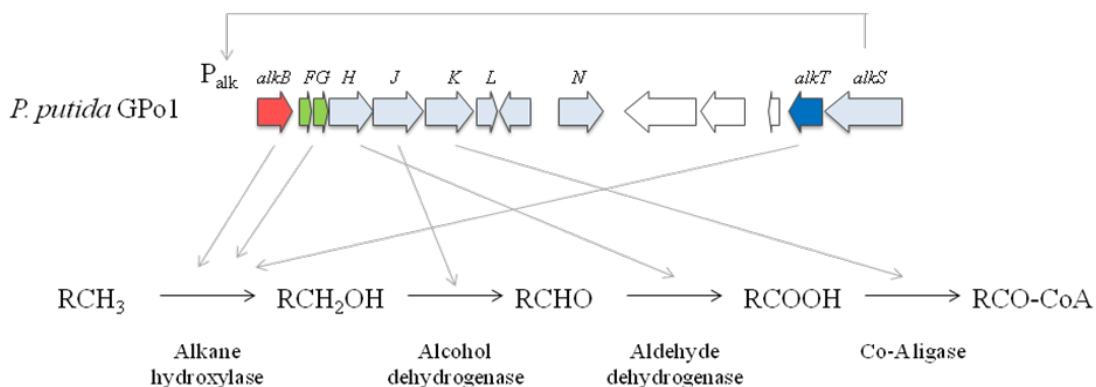


Figure 4. **The gene organization and functions of gene products in alkane degradation pathway in *Pseudonocardia putida* GPo1.** The *alk*-genes are organized in two clusters: the *alkBFGJKL* and the *alkST*. The arrows indicate the point of action of each gene product in alkane oxidation pathway. The function of each gene product is : AlkBFGT: monooxygenase; AlkJ: alcohol dehydrogenase; AlkH: aldehyde dehydrogenase; AlkK: CoA-ligase. AlkL: outermembrane protein, AlkN : plasma membrane protein involved in chemotaxis, AlkS: transcriptional regulator of the *alkB* operon.

Table 2. **List of genes known to be involved in alkane degradation pathway in *Pseudomonas putida* GP01.** (van Beilen et al., 1992)

Gene	Function of encoded protein
<i>alkB</i>	Hydroxylase of monooxygenase
<i>alkFG</i>	Rubredoxin of monooxygenase
<i>alkH</i>	Aldehyde dehydrogenase
<i>alkJ</i>	Alcohol dehydrogenase
<i>alkK</i>	Acyl-CoA synthetase
<i>alkL</i>	Outer membrane protein
<i>alkM</i>	Methyl-accepting chemotaxis protein
<i>alkS</i>	Regulator
<i>alkT</i>	Rubredoxin reductase of monooxygenase

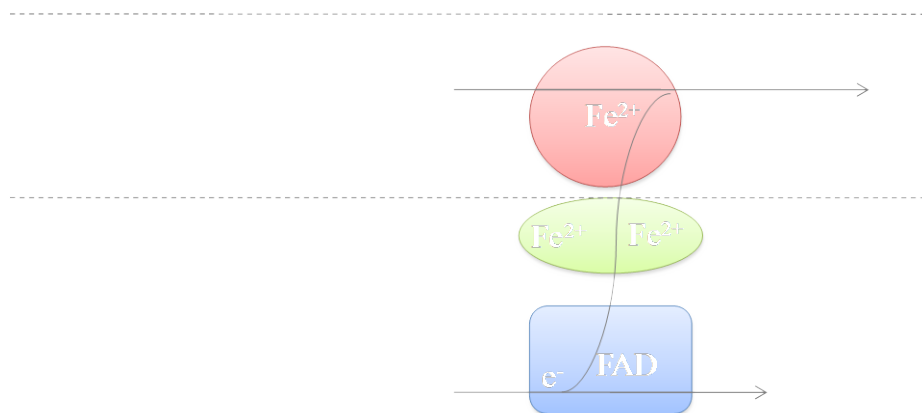


Figure 5. **Structure of alkane monooxygenase system.** The monooxygenase consists of three subunits: membrane-bound hydroxylase (AlkB), rubredoxins (AlkFG), and rubredoxin reductase (AlkT).

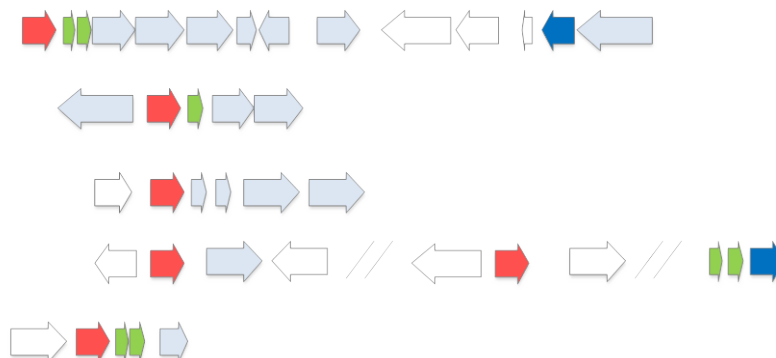


Figure 6. **Gene organization of *alk* genes in various organisms.** Monooxygenase components are indicated in dark grey and other enzymes known to be involved in alkane degradation pathways are colored in light grey. Organizations of *alkB* and its neighboring genes in *P. putida* GPo1, *A. borkumensis* AP1, *P. fluorescens* CHA0, *P. aeruginosa* PAO1, and *M. tuberculosis* H37Rv were compared (Stover et al., 2000; Smits et al., 2002). Genes are abbreviated as: *alkB*: alkane hydroxylase; *alkF*: rubredoxin 1; *alkG*: rubredoxin 2; *alkH*: aldehyde dehydrogenase; *alkJ*: alcohol dehydrogenase; *alkK*: acyl coenzyme A (acyl –CoA) synthetase; *alkL*: outer membrane protein; *alkS*: regulatory protein; *alkT*: rubredoxin reductase; *ompP1*: putative transporter of alkanes; *yafH*: acyl-CoA dehydrogenase; *alkU*: regulatory protein.

degraders, both gram negative and gram positive strains (Smits et al., 1999; Andreoni et al., 2000; van Beilen et al., 2007). In some strains, multiple distinct *alkB* homologues are present; sometimes 3 to 5 copies (van Beilen et al., 2002). Each seems to have a different role, i.e. having a different substrate range or expressed in different growth phases (van Beilen et al., 2002; Marin et al., 2003).

The gene organization differs significantly among different organisms. In *P. putida* GPo1, most of the *alk* genes are present in one operon, except for a regulator (*alkS*) and rubredoxin reductase (*alkT*) (Figure 6). In other organisms, particularly in gram positive bacteria, only *alkB* and rubredoxin genes are clustered together as an operon.

Originally, *alkB* was found for its ability to hydroxylate medium chain alkanes (van Beilen et al., 1994). Recent analysis of other *alkB* encoded enzymes revealed their wider substrate ranges including long/short chain alkanes and other types of hydrocarbons. AlkB from *P. fluorescens* CHAO can oxidize long chain alkanes (C₁₂-C₁₆), while AlkB in *Mycobacterium austroafricanum* IFP 2012 can possibly oxidize alkanes with wider chain lengths (C₂-C₁₆). AlkB from strain GPo1 was also found to have activity towards short chain alkanes, i.e. propane and butane, in addition to alkanes with medium chain length. Amino acid positions that are important in determining substrate range were identified through mutation analysis (van Beilen et al., 2005). The residues responsible for discriminating alkanes with different chain length are also identified through the same method (Rojo, 2005).

Propane and butane inhibit MTBE oxidation by alkane-grown *Pseudomonas putida* GPo1, implying that propane, MTBE, and octane are oxidized by the same

enzyme, most likely by AlkB (Smith and Hyman, 2004) (Johnson and Hyman, 2006).

Mycobacterium austroafricanum IFP 2012 has an *alkB* gene whose expression is induced by gaseous and liquid alkanes (C₂-C₁₆) and by TBA. *Mycobacterium austroafricanum* strain IFP2014, IFP2173, and IFP2009 also degrade TBA and other ethers after growth on C₂-C₁₆ alkanes (Lopes Ferreira et al., 2007).

1.3.6 Cytochrome P450

Cytochrome P450 is a family of proteins found across the kingdoms (Bacteria, Archaea, and Eukaryotes). A number of P450s have been identified in the human genome, and they are responsible for oxygenation of a variety of natural products or drugs, including steroids, fatty acids, eicosanoids, procarcinogens, mutagens, and xenobiotics (Omura, 1999). There are more than 1000 different enzymes that belong to this family, and they are categorized into more than 100 subgroups (Nelson et al., 1996). The P450 hydroxylases contain a heme group at their active center, which plays a role in transferring an electron from one (class II) or two (Class I) electron transport proteins to organic substrates. Unlike membrane bound eukaryotic cytochrome P450 (530 amino acid long), the bacterial P450 enzymes are typically soluble proteins with a length of about 400 amino acids.

Recently, the first native bacterial cytochrome P450 that is capable of oxidizing alkanes was discovered in *Acinetobacter* sp. EB104 (Maier et al., 2001). This formed a new family, CYP153, and its homologues are found in other alkane degrading bacteria (Asperger et al., 1981; Kubota et al., 2005; van Beilen et al., 2006; Fujii et al., 2006).

They are induced by a variety of hydrocarbons and have activity toward other organic compounds such as limonene (van Beilen et al, 2005). It is also noted that this system requires ferredoxin and ferredoxin reductase components. Like other bacterial cytochrome P450s, CYP153 is a soluble protein (Eremina et al., 1987) having a high tendency to aggregate and a relatively high apparent molecular weight of 52-53.6 kDa (Figure 7) (Muller et al., 1989).

From the first discovery of this family, an increasing number of CYP153 have been shown to be involved in the hydroxylation of liquid alkanes and other organic compounds, which was enabled by ease of stable expression in *E. coli* (Fujii et al., 2006; van Beilen et al., 2005; Nodate et al., 2006). CYP153 from *Acinetobacter* sp. OC4 was the first of these enzymes to show octane oxidizing activity in *E. coli* (Fujii et al., 2006). CYP153 from *Alcanivorax borkumensis* SK2 can also convert octane to 1-octanol (Nodate et al., 2006). In *Mycobacterium* sp. HXN-1500, CYP153 can oxidize both mid-chain alkanes (C₆₋₁₁) and limonene (van Beilen et al., 2005). So far activity of these enzymes towards short-chain alkanes or ethers has not been observed.

While eight tertiary structures of eukaryotic P450s are available (CYP101, 102, CYP108, CYP107A1, CYP55A, CYP119, CYP2C5 and Mt CYP51), there are only three bacterial cytochrome P450 enzymes available so far (P450CAM, CYP101, P450 BM3). Comparison of this data indicates that despite a high divergence in amino acid sequence, the tertiary structures are very conserved. Although x-ray structures of the CYP153 family have not yet been solved, the possible structure of the CYP153 can be predicted using homology modeling. This is helpful for mechanistic understanding of alkane hydroxylation, since there is no structure information on other alkane monooxygenases.

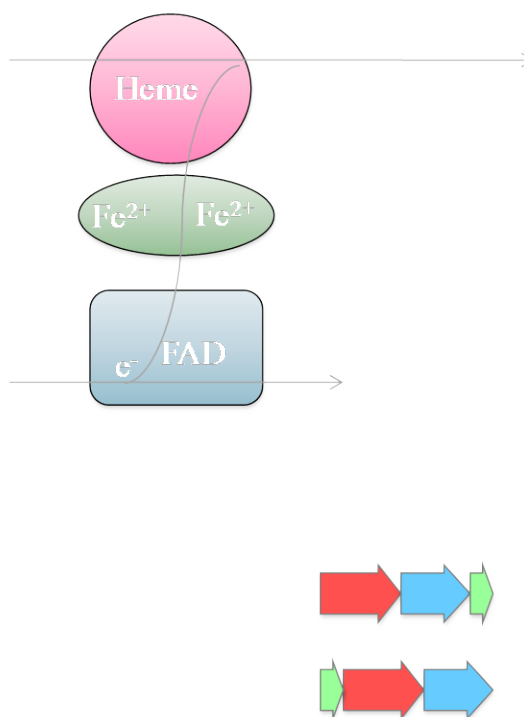


Figure 7. **Structure and gene organization of cytochrome P450 complex in *Mycobacterium* sp. strain HXN-1500, *Acinetobacter* sp. OC4 and *Gordonia* sp. TF6.** A) Monooxygenase is composed of three components: Hydroxylase (AphG), ferredoxin (AphI), and ferredoxin reductase (AphH). B) The three genes are organized in an operon (Fujii et al., 2006; van Beilen et al., 2005).

Other cytochrome P450s can be engineered to have alkane hydroxylation activity. For instance, cytochrome P450 BM3, whose native substrates are fatty acids, does not have any activity towards alkanes. Cytochrome P450 BM3's variants with a mutation at some active site residues had become capable of hydroxylating alkanes, cycloalkanes, and indole (Feenstra et al., 2007; Appel et al., 2001).

1.3.7 Soluble diiron monooxygenase

Soluble diiron monooxygenase (BMMs) is a family of non-heme, di-iron enzymes known to use molecular oxygen to hydroxylate a variety of organic compounds including phenol, toluene, methane, alkenes, and chlorinated compounds (Notomista et al., 2003). BMMs are divided into at least 6 sub-families based on the phylogenetic analysis of the protein sequence of the α -subunit (Figure 8). Members of each sub-family share the same gene composition and gene order for hydroxylase subunits (Figure 9, 10). The members of each subfamily also share similar substrate ranges.

Subunits of all known BMMs are transcribed from a single operon. Four components of BMMs that are found in all BMMs are large hydroxylase α subunit, β subunit, reductase (N) and a coupling protein (R). α and β subunits form a tetramer, called H complex, and the complex brings about hydroxylating activity. An additional subunit, γ , is present in some BMMs. The γ subunit stabilizes the $\alpha\beta$ tetramer by interacting with them and forms an $(\alpha\beta\gamma)_2$ hexamer. N contains a ferredoxin-like domain (N-terminus) and an NAD(P)H dependant reductase domain (C-terminus). Together with R, N mediates recharging of the di-iron center of hydroxylase. Between the sub-families,

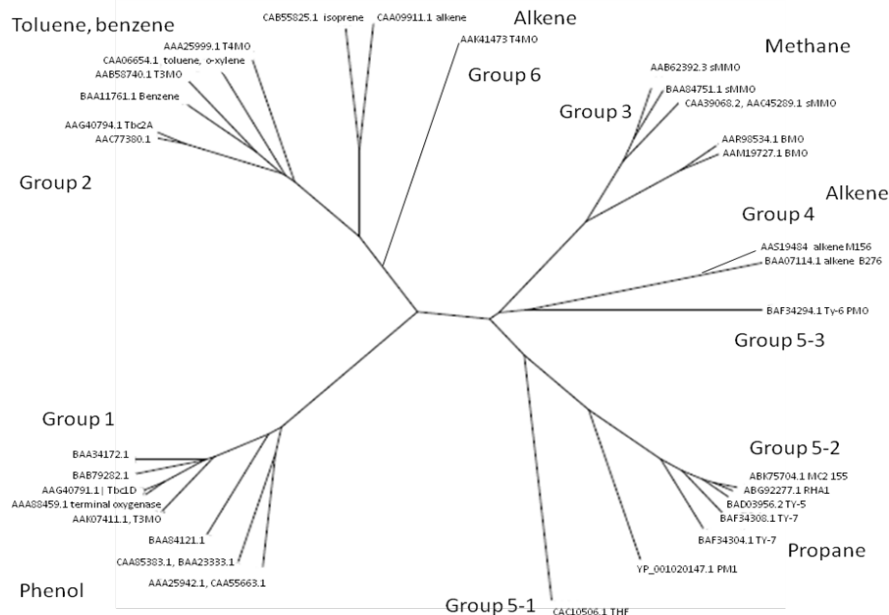


Figure 8. **Phylogenetic analysis of α subunit of soluble diiron monooxygenases.**

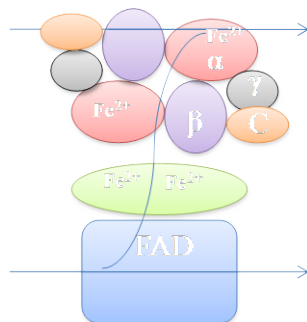


Figure 9. **Structure of soluble diiron monooxygenase complex.** A) Monooxygenase is composed of multiple subunits. All subfamilies carry α , β , and coupling subunits and a reductase. Some families have extra subunits, such as γ subunit or an external ferredoxin that mediate transfer of electrons from a reductase to a hydroxylase (Notomista et al., 2003). Genes are abbreviated as: α , β , γ , C: α , β , γ , and coupling subunits of a hydroxylase, respectively; F: ferredoxin; F-R: ferredoxin reductase.

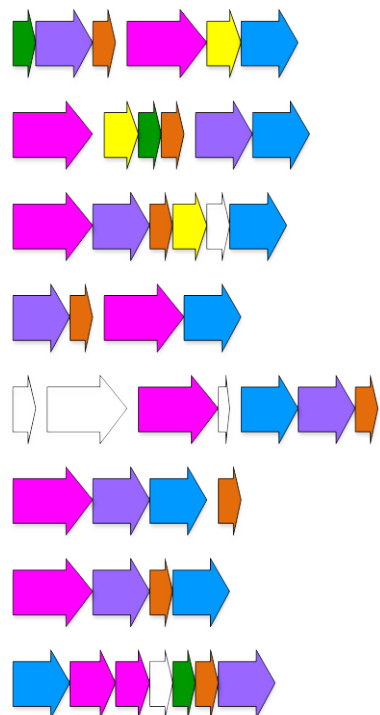


Figure 10. **Gene organization of soluble diiron monooxygenase subfamilies.** Group 1: phenol monooxygenase; group 2: Toluene/benzene monooxygenase; group 3: soluble methane monooxygenase; group 4: alkene monooxygenase; group 5-1: putative tetrahydrofuran monooxygenase; group 5-2, 3 propane monooxygenase; group 6: archeal alkene monooxygenase. Genes are abbreviated as: α , β , γ , C: α , β , γ , and coupling subunits of hydroxylase, respectively; F: ferredoxin; F-R: ferredoxin reductase.

Table 3. **Subunit composition of soluble diiron monooxygenase sub-families.**

Subfamily	Subunits					
	α^*	β^*	γ^*	C*	F*	F-R*
1	+	+	+	+	+	+
2	+	+	+	+	+	+
3	+	+	+	+	-	+
4	+	+	-	+	-	+
5	+	+	-	+	-	+
6	+*1	+	-	+	+	+

* The abbreviations are designated as described in Figure 10.

*1 The N-terminus and C-terminus parts of α subunit are transcribed separately in subfamily-6 (She et al., 2001).

the composition of hydroxylase subunits varies (Table 3). Group 1, 2 and 3 have only α , β and coupling subunits. Group 4, 5, and 6 carry another subunit, γ . An electron transfer protein, ferredoxin, is required only in group 1, 2, and 6 (Notomista et al., 2003).

The amino acid sequences of the β subunit and the amino acid sequences of the N-terminal portion of the α subunit share some sequence homology (Leafy et al, 2003). It has been suggested that α and β subunits share a common ancestor and throughout their evolution, α retained its catalytic center and activity while β only retained a structural role. Also, the interaction between hydroxylases and reductases is mediated through the C-terminus domain of the α subunit whose homologous sequence is not present in the β subunit.

Gene duplication of α subunits is predicted to have occurred earlier in the evolution of BMM rather than after the formation of BMM operons. The phylogenetic tree constructed using protein sequences of ferredoxin reductases appears different from that of α and β subunits. This indicates that the reductase was recruited to the operon at a different time in the history of enzyme evolution, independently from the α and β subunits. The γ subunit is a short peptide with varying length and no apparent sequence similarities between the enzymes. This way of enzyme evolution may explain the plasticity and modularity of this enzyme. And this feature may contribute to rapid emergence of new bacterial strains which grow in contaminated environment (Notomista et al., 2003).

Because of the fact that hydroxylation activity is present only in the α subunit, protein sequences of the α subunit were used for phylogenetic analysis throughout my project. Each subfamily of BMMs will be briefly reviewed next.

Soluble methane monooxygenase (sMMO) is best characterized member of the BMMs. They are found in a limited fraction of methanotrophs. Methanotrophs utilize two systems for oxidizing methane: soluble methane monooxygenase (sMMO) and particulate methane monooxygenase (pMMO). While all methanotrophs possess pMMO, few of them have sMMO (Murrell et al., 2000-1). Since pMMO is only expressed and active when the copper concentration is sufficiently high, it has been speculated that carrying sMMO gives bacteria a selective advantage in lower copper environments (Murrell et al., 2000-2). These two enzymes are not phylogenically related; pMMO is related to ammonia monooxygenase while sMMO is a member of BMMs. Another difference between the two enzymes is that pMMOs have a narrow substrate range while sMMOs are capable of hydroxylating a variety of substrates, mainly hydrocarbons i.e. substituted methanes, alkanes, cycloalkanes, alkenes, haloalkenes, ethers, and aromatic and heterocyclic hydrocarbons. (Grosse et al., 1999; Colby et al., 1977; Green et al., 1989; Fox et al., 1990). The crystal structure is available for sMMO from *Mc. capsulatus* Bath and *Ms. trichosporium* OB3b (Woodland et al., 1984; Lund et al., 1985; Lund et al., 1985; Fox et al., 1985). Biochemical analysis showed that the hydroxylase contains three subunits ($\alpha\beta\gamma$)₂. Besides core subunits, the operon contains another ORF with unknown function (*orfY*), which is unique to this family.

Alkene monooxygenase is the second subfamily of BMMs. There are only two known members of this family, found in *Mycobacterium* sp. M156 and *Gordonia rubripertincta*. This enzyme can oxidize low molecular-mass alkenes to their corresponding epoxides (Fosdike et al., 2005). It is shown to oxidize C₃-C₅ (Allen et al.,

1999). Gene organization is similar to that of sMMO except for the fact that the hydroxylase consists of only 2 subunits ($\alpha\beta$). It does not have *orfY*.

There are few studies on the members of the third BMM family, phenol monooxygenase (Table 4). All of these enzymes are capable of oxidizing phenol and methylphenol. Further, toluene *o*-monooxygenase (TOM) can oxidize ethers, aromatic hydrocarbons, and polycyclic aromatic hydrocarbons, including diethyl ether, dichloroethylene, vinyl chloride, naphthalene, benzene, catechol, 1,2,3-trihydroxybenzene, naphthalene and fluorene (Tao et al., 2004; Tao et al., 2005). Utilization of some of these substrates was also observed in other members of this subfamily. The enzyme consists of a 3 component hydroxylase ($\alpha\beta\gamma$), reductase, and an effector protein.

The fourth subfamily is 4-component alkene/aromatic monooxygenase. The substrate range of the enzymes in this family overlaps with that of other subfamilies (Table 5). For example, toluene-4-monooxygenase (TMO), toluene 3-monooxygenase (TBU), and toluene/*o*-xylene monooxygenase (TOU) oxidize toluene and other unactivated aromatic compounds. Some members also have activity toward phenol. TMOs have broader substrate range: acetanilide, chlorobenzene, ethylbenzene, TCE, 1,2-dichloroethane, chloroform, C₃-C₈ alkenes, but no phenolic compounds (Yen et al., 1991; McClay et al., 1996; McClay et al., 2000).

This family of enzymes can catalyze a wide variety of oxidation reactions with wide regiospecificity. For example, toluene can be hydroxylated at 1) *m*-, 2) *p*-, or 3) *o*- and *m*- or *p*- position by TBU, TMO, and TOU, respectively (Yen et al., 1991, McClay et al., 1996, 2000; McClay et al., 1996; Bertoni et al., 1998). In addition to hydroxylation,

Table 4. List of Phenol hydroxylases

Enzyme	Strain	Reference
Toluene-4-monooxygenase (TMO)	<i>Pseudomonas mendocina</i> KR1	Yen et al., 1991, McClay et al., 1996, 2000
Toluene-3-monooxygenase (TBU)	<i>Ralstonia pickettii</i> PKO1	Byrne et al., 1995; McClay et al., 1996
Toluene/o-xylene monooxygenase (TOU)	<i>Pseudomonas stutzeri</i> OX1	Bertoni et al., 1998
Phenol hydroxylase (PHL)	<i>Ralstonia eutropha</i> JMP134	Ayoubi and Harker, 1998
Alkene monooxygenase (AAM)	<i>Xanthobacter</i> Py2	Small et al., 1997
Isoprene monooxygenase	<i>Rhodococcus</i> sp. strain AD45	van Hylckama Vlieg et al., 2000

Table 5. List of 4-component alkene/aromatic hydroxyases.

Enzyme	Strain	Reference
Phenol hydroxylase (DMP)	<i>Pseudomonas</i> CF600	Shingler, 1989; Shields, 1989
Toluene o-monooxygenase (TOM)	<i>Burkholderia vietnamiensis</i> G4	Shingler, 1989; Shields, 1989; Newman and Wackett, 1997; Tao et al., 2004, 2005; McClay et al., 1996
Toluene/benzene 2-monooxygenase	<i>Burkholderia cepacia</i> JS150	Johnson and Olsen, 1995
Phenol monooxygenase	<i>Comamonas testosteroni</i> R5 and <i>Ralstonia eutropha</i> E2	Teramoto, 1999

this group of enzymes can also catalyze epoxidation reactions. TMO and alkene monooxygenase (AAM) in *Xanthobacter* sp. Py2 can oxidize short chain alkenes (Small et al., 1997). Although group 4 alkene monooxygenases (AMO) are also capable of alkene oxidation, they have different subunit composition from TMO and AAM (no Rieske-like ferredoxin). This may indicate converging evolution for alkene epoxidation. Activity towards chlorinated hydrocarbons such as TCE is also noted.

Unlike enzyme systems for mid-chain alkane or for methane degradation, enzymes capable of oxidizing short-chain alkanes are not very well studied. There is only one characterized butane monooxygenase (BMO) from *Pseudomonas butanovora* (Arp et al., 1999). BMO is most similar to sMMO in gene order, amino acid sequence, and ability to oxidize methane. BMO has a wider range of substrates that it can oxidize. While sMMO can only oxidize short chain alkanes, BMO can oxidize medium chain alkanes also. BMO from *Pseudomonas butanovora* oxidizes C₂-C₈ alkanes (Doughty et al., 2006). A cyclic alkane, cyclohexane, is another substrate known to be oxidized by BMO. Activity towards ethers is not known.

Propane monooxygenase (PMO) is a new family of BMMs that are recently identified. Details will be discussed in the following section. As described in earlier an section, THF-induced monooxygenase found in *Pseudonocardia* sp. strain K1 is also a member of BMM, forming a new subfamily by itself.

1.3.8 Oxygenases involved in propane degradation

Propane degraders are widespread in nature (Steffen et al., 1997). But the phylogenetic distribution of propane degraders seem to be limited to the Gram-positive *Corynebacterium* - *Nocardia* - *Mycobacterium* - *Rhodococcus* complex (Malachowsky et al., 1994, Ashraf et al., 1994).

The first example of propane oxidation was studied in *Rhodococcus rhodochrous* (Macmichael and Brown, 1987). The extent of these studies was to show that the catabolism of propane by *Nocardia paraffinicum* (*Rhodococcus rhodochrous*) involved CO₂ fixation after its oxidation to propionic acid. For more than a decade, genetic studies of propane oxidation were limited and failed to identify propane monooxygenases. Despite the lack of purified propane monooxygenase, the propane degradation pathway was known to be initiated by the hydroxylation of propane to form propanol. The oxidation could happen at the terminal and/or sub-terminal carbon, forming 1-propanol or 2-propanol, respectively (Figure 11) (Ashraf et al., 1994).

Due to an increase in interest in biodegradation and the wide range of substrates propane-grown cells can oxidize, the catalytic capability of a number of propanotrophs has started to be studied in recent years. Several propane degraders were shown to oxidize MTBE and other ethers, as discussed earlier (Steffan et al., 1997). Propane is a competitive inhibitor of MTBE degradation by alkane grown *P. putida* GPo1 (Johnson and Hyman, 2006). *Mycobacterium vaccae* JOB5 and five other *Mycobacterium* strains can oxidize TCE after growth on propane (Wackett et al., 1989). In *Rhodococcus erythropolis* 3/89, a propane-inducible enzyme was shown to catalyze epoxidation of

Figure 11. **Propane degradation pathway.** Propane is first oxidized by oxygenase to form 1-propanol and/or 2-propanol, which will be further oxidized by dehydrogenases (Ashraf et al., 1994).

gaseous alkenes and hydroxylation of aromatic hydrocarbons (Kulikova and Bezborodov, 2001).

There are recent studies that link the propane degrading activity of organisms to a medium chain alkane monooxygenase (AlkB) system. *Pseudomonas putida* GP01 has an alkane oxygenase that degrades liquid alkanes and a variety of methylated substrates (Smith and Hyman, 2004). Octane growing cells can cometabolically degrade methyl tert-butyl ether (MTBE). Induction studies showed that the enzyme involved in this pathway is most likely an alkane monooxygenase. Although propane does not support cell growth, propane can competitively inhibit the MTBE degradation activity of *Pseudomonas putida* GP₀₁. This suggests that the same enzyme degrades propane and MTBE. *Mycobacterium austroafricanum* IFP 2012 can grow on MTBE, alkanes C₂ to C₁₆. Expression of AlkB is induced by propane, hexane, hexadecane, and TBA (Lopes Ferreira et al., 2007). Another BMM enzyme, BMO from *Pseudomonas butanovora*, have shown to oxidize alkanes C₂-C₈, including propane (Doughty et al., 2006). But propane is not a native substrates in any of these enzymes and propane does not support the growth of the cells who possess these enzymes.

Recently, the first enzyme involved in propane degradation was characterized by a gene knockout approach, and the nucleotide sequence of the genes was determined, in *Gordonia* sp. strain TY-5 (Kotani et al., 2003). A monooxygenase, two alcohol dehydrogenases (*adh1*, *adh2*), and an aldehyde dehydrogenase (*adh3*) have been identified in this organism. The amino acid sequence of propane monooxygenase showed it belongs to BMMs. Particularly, it is most similar to that of sMMO and BMO. Interestingly, it is also similar to the putative THF monooxygenase in *Pseudonocardia* sp.

strain K1 (Figure 8). Propane monooxygenase, however, is very different from the well characterized liquid-alkane monooxygenase (AlkB) in its protein sequence and cellular localization. The wild-type strain TY-5 grows on propane and alkanes with chain length C_{13-22} . A mutant that lost the functional β -subunit of the hydroxylase can no longer grow on propane (Kotani et al., 2003). In another study with *Rhodococcus* strain RHA-1, a PMO deletion mutant also lost its ability to grow on propane (Sharp et al., 2007).

Since the discovery of PMO in strain TY-5, an increasing number of PMO-type sequences were identified in propane utilizing organisms (Kotani et al., 2006, Sharp et al., 2007). For example, in *Mycobacterium* sp. TY-6 and *Pseudonocardia* sp. TY-7, a putative propane monooxygenase was induced by C_2 - C_4 alkanes, and not by methane (C_1) (Kotani et al., 2006).

2.0 Methods

2.1 Bacterial strains, culture conditions and vectors

Three strains of bacteria, *Mycobacterium* sp. strain ENV421, *Pseudonocardia* sp. strain ENV478, and *Rhododoccus* sp. strain ENV425, were isolated by Dr. Robert Steffan and Mr. Kevin McClay at Shaw Corp. and were used throughout this work.

Mycobacterium sp. ENV421, *Pseudonocardia* sp. ENV478, and *Rhododoccus* sp. ENV425 were grown on Tryptic Soy Broth (Difco Inc, MD) or MSB medium (Stanier et al. 1966), to which a carbon source (10 mM) was added, at 30°C under constant shaking at 100 rpm. When propane was used as a carbon source, a 500 ml flask containing 100 ml of MSB medium under a gas mixture (propane: air=1:1), and sealed with a rubber stopper, was shaken at 30°C.

Escherichia coli DH5 α was used for gene cloning and was usually grown on LB medium (Difco Inc, MD) in the presence of ampicillin (100 μ g/ml), gentamicin (15 μ g/ml), tetracycline (15 μ g/ml), or kanamycin (50 μ g/ml) when necessary. pGEM-3Zf(+), pGEM-T, pALTER_Ex2 (Promega, Madison, WI), pBluescript II SK(+), pET-3a (Stratagene, La Jolla, CA), modified pQE-30 (Qiagen, Valencia, CA) and pNV18 (Chiba et al. 2007) were used as cloning or expression vectors.

Competent cells of *E. coli* for chemical transformation were prepared as follows. The overnight culture was added to fresh LB medium so that it would have a cell density of OD₆₀₀ 0.05. Cells were grown at 37°C with constant agitation (100 rpm) until they reached an OD₆₀₀ of 0.3 to 0.7. The cells were placed on ice for 30 min and then subjected to centrifugation at 1600 x g at 4°C for 7 min. Cells were resuspended in

chilled 10 ml CaCl_2 solution (60 mM CaCl_2 , 15% (v/v) glycerol, 10 mM PIPES, pH 7.0). They were centrifuged again at $1600 \times g$ at 4°C for 7 min and resuspended in 2 ml CaCl_2 solution.

About 1 μg of DNA was added to 50 μl of competent cells and the suspension of cells was placed on ice for 30 min. Then it was placed in 42°C water bath for 30 seconds and 250 μl LB medium was added immediately. It was then incubated at 37°C with constant agitation for 1 hour before plated onto LB medium with appropriate antibiotics.

Competent cells of *Pseudonocardia* sp. strain ENV478 for electroporation were prepared by the following method. Cells were grown until mid-exponential phase, incubated at room temperature or on ice for 30 min, and harvested by centrifugation. The cell pellet was resuspended in 10% glycerol solution. 1 μl of plasmid DNA was added to 50 μl of competent cell immediately before electroporation. The BioRad gene pulser with the condition of 25 μF , 200 Ω and 1.25kV was used for introducing plasmids into strain ENV478. After electroporation, 250 μl of Tryptic Soy Broth (Difco, Franklin Lakes, NJ) was added and then incubated at 30°C without agitation for 3 hour. Cells were plated on Tryptic Soy Agar (BD DifcoTM, Franklin Lakes, NJ) containing 50 $\mu\text{g}/\text{ml}$ kanamycin.

2.2 Nucleic acid techniques

Genomic DNA of *Mycobacterium* sp. ENV421, *Pseudonocardia* sp. ENV478, *Rhododoccus* sp. ENV425 and *E.coli* was isolated from bacterial cells using the UltraCleanTM Microbial DNA Isolation Kit (Mo Bio Laboratories, Inc. CA) following the directions of the manufacturer.

Plasmid DNA from *E. coli* was isolated with the NucleoSpin plasmid Miniprep kit (BD Biosciences, CA). Isolation from ENV478 required an additional step of incubating cells with 10 mg lysozyme at 30°C for 20 min before starting the isolation using the kit.

PCR and inverse PCR were performed using Taq polymerase (Invitrogen, Carlsbad, CA) in order to examine the presence of the gene and to obtain the entire sequence of a gene/operon. In order to clone a DNA fragment for heterologous expression, the proof reading pfu polymerase was used for amplification (Invitrogen, Carlsbad, CA).

The PCR products were purified by NucleoTrap purification kit (BD Biosciences, USA) according to the manufacture's protocol, and the sequences were determined by primer-walking.

To obtain the gene fragment encoding oxygenases from the chromosomal DNA of *Mycobacterium* sp. ENV421, *Pseudonocardia* sp. ENV478, and *Rhododoccus* sp. ENV425, PCR was performed with degenerative oligonucleotide primers for each enzyme family.

AlkB F: AATACHGSVCAYGAGCTCRGYCAYAAR

R: GCRTGRTGATCAGARTGHCGYTG

Cytochrome P450 F: GTSGGCGGCAACGACACSAC

R: GCASCGGTGGATGCCGAAGCCRAA

Diiron Monooxygenase F: ATGGAAGCGGAGAAGGA

R: CTGGCCGATGAGGGTCTTGC

To obtain the DNA sequence of upstream or downstream regions, inverse-PCR was performed (Ochman et al., 1988)

Throughout the study, agarose gel electrophoresis was performed in 1% agarose gel made with 0.5x TAE buffer (40 mM Tris, 20 mM acetate, 2 mM EDTA).

Southern hybridization was carried out following. 200 ng of genomic DNA was digested with various restriction enzymes and separated on 1% agarose gel. The agarose gel was treated with depurination solution (0.25 N HCl), denaturation solution (1.5 M NaCl, 0.5 M NaOH), and neutralization solution (1 M Tris-base, 1 M NaCl, pH 5.0) for 15 min each at gentle agitation. The gel and nylon membrane were equilibrated with transfer solution (20x SSC : 3 M NaCl, 0.3 M trisodium citrate) for 10 min before transfer. DNA was transferred to nylon membrane using Tyler Research Instruments. Transfer was carried out for at least three hours. The complete transfer of DNA to the nylon membrane was confirmed by staining the agarose gel with ethidium bromide and visual observation under UV light. The DNA and the nylon membrane were cross-linked by exposure to UV light for 2 min.

Southern hybridization was performed as recommended by the supplier for the DIG non-radioactive nucleic acid labeling and detection system (Bioehringer Mannheim, Germany). The hybridization probe was synthesized using PCR DIG probe synthesis kit (Roche, Nutley, NJ). It was denatured by boiling for 2 min then cooled rapidly on ice. The nylon membrane was incubated with the probe in hybridization buffer (5x SSC, 1% blocking stock solution, 0.1% N-lauroyl sarcosine, 0.02% SDS) for at least 6 hours at 68°C with constant agitation. The membrane was washed with 2x wash buffer (2x SSC, 0.1% SDS) at room temperature and then with 0.1x wash buffer (0.1x SSC, 0.1% SDS) at

68°C. The membrane was incubated with 1% blocking solution for 30 min. The membrane was incubated with anti-DIG-Ap conjugate then washed twice. BCIP (5-bromo-4-chloro-3'-indoly phosphate *p*-toluidine salt) and NBT (nitro-blue tetrazolium chloride) were added and incubated in dark until bands appeared. When the bands with appropriate intensity appeared, the membrane was washed with dH₂O and air-dried.

Nucleotide sequences were determined with the ABI PRISM 3100 Genetic Analyzer (Applied Biosystems, USA). The sequence was compared with existing sequences in the GenBank database by performing a BLAST search (Altschul, 1997). Multiple alignments of homologous sequences were generated by Clustal W alignment using the Lasergene software (DNASTAR, inc., USA). Pairwise sequence comparisons were performed using BLAST2 sequences (Tatusova et al. 1999). Phylogenetic and molecular evolutionary analyses were conducted using MEGA version 4 (Tamura et al., 2007).

Total RNA from the bacterial cells was isolated with an RNeasy Mini kit (Qiagen, Hilden, Germany) with some modifications (personal communication, Dr. E. Kim). In summary, overnight cell cultures in 50 ml of MSB medium with 10 mM carbon source were harvested, and resuspended in 50 ml of fresh MSB medium containing 10 mM carbon source, so that fresh cultures would have O.D.₆₀₀ 0.05. Cells were incubated at 30°C until they reached an O.D.₆₀₀ of 0.4. A negative control was prepared by adding succinate or glucose to a final concentration of 10 mM. Harvested cells were treated with 30 mg lysozyme at 37°C for 20min. The cells were incubated with Trizol and chloroform solution (5:1 mix), and then washed by chloroform solution. RNA was precipitated with isopropyl alcohol at -70°C for 1h. The RNA was washed with 70 % ethanol. RNA was

dissolved in RNase-free water, and then the sample was digested with DNaseI and further purified with RNeasy Mini kit.

The RT-PCR reaction was performed using QIAGEN OneStep RT-PCR Kit (Valencia, CA). In order to determine whether there was DNA contamination in the RNA sample, PCR with Taq polymerase was performed prior to RT-PCR. The RT-PCR amplification cycle is as follows. (1) 50°C for 30 min, (2) 30 cycles of 94°C for 30 sec, 55°C for 30 sec, 72°C for 30 second, and (3) 72°C for 5 min. In a negative control, the first step, formation of cDNA with reverse transcriptase, was omitted. In each reaction, 5 ng of RNA sample was added.

Real time quantitative reverse transcriptase PCR (QRT-PCR) was carried out with a 7300 Real-Time PCR System (Applied Biosystems, Foster City, CA) following the manufacture's protocol. The reaction was set up using TaqMan® Reverse Transcription Reagents (Applied Biosystems, Foster City, CA)

The transcription start sites, upstream of *orfY*, *thmS*, and *thmB*, were determined by 5' RACE assay (Invitrogen, USA) following the manufacture's instruction. RNA extracted from THF-grown cells was used for the study.

2.3 Chemical, and biochemical analyses

Cytoplasmic and membrane proteins extracts were prepared from propane-grown or succinate-grown cells during exponential growth phase with Sigma ProteoPrep Universal Extraction Kit (SIGMA, Saint Louis, Missouri) following the manufacture's instruction. The purified proteins were separated with SDS-PAGE.

SDS-PAGE was performed with 7% acrylamide gells with stacking gel 4x buffer (0.5 M Tris pH 6.8) or resolving gel 4x buffer (1.5 M Tris pH 6.8), 0.1% SDS, 0.05% ammonium persulfate, and 0.067% TEMED. Samples were loaded with Laemmli loading buffer (80 mM Tris-Cl pH 6.8, 2% SDS, 10% glycerol, 5.3% β -mercaptoethanol, and 0.02% bromophenol blue). Gels were run in 1x PAGE running buffer (25 mM Tris-base, 0.25 M glycine, and 0.1% SDS, pH 8.3) at 25 mA for 5 hour. For visualization of proteins on the gel, colloidal Coomassie staining was performed. A staining solution consisted of 1.6% ortho-phosphoric acid, 8% ammonium sulfate, 0.08% CBB G250, 20% methanol, and excess stain was destained with distilled water.

For protein sequencing, unstained proteins on the polyacrylamide gel were electroblotted onto a PDVF membrane by the following method. Transfer buffer (25 mM Tris-base, 192 mM glycine, 20% methanol) was made and chilled to 4°C. Gels were equilibrated in the transfer buffer for 15 min and then soaked in methanol, water, and then in transfer buffer for 2 min each. Foams and filter papers were also soaked in transfer buffer before assembly. Proteins were blotted to membrane over night at 25V. The membrane was then stained using amido black (0.1% amido black and 10% glacial acetic acid) for 1 hour and was destained by 5% acetic acid to reduce the background.

Propane induced protein bands were cut out from the membrane and then subjected to N-terminal sequencing by the protein sequencing facility at Iowa State University.

The biotransformation of compounds by recombinant *E. coli* strains were examined using resting cells, which were prepared as following. An overnight culture of the cells in 50 ml of MSB medium with 10 mM carbon source was harvested, and

resuspended in 50 mL of fresh MSB medium containing 10 mM carbon source, so that the fresh culture would have O.D.₆₀₀ 0.05. It was incubated at 30°C or 37°C until it reached O.D.₆₀₀ 0.5. Cells were harvested and collected by centrifugation. The cell pellet was resuspended in 50 mM phosphate buffer (pH 7.0). It was subjected to centrifugation again and resuspended in fresh phosphate buffer to a final volume of 25 ml. In addition to 10 mM glucose and appropriate antibiotics, the compound of interest was supplied either directly into the medium (1% vol/vol) or as a gas. The culture was incubated overnight at 30 °C with constant agitation. The culture was subjected to centrifugation to remove cellular material and the supernatant was extracted with ethyl acetate twice. Ethyl acetate was evaporated with vacuum in a rotary evaporator. Upon completion of evaporation, residual material was resuspended with 1.75 ml ethyl acetate and kept frozen at -20°C until further analysis.

The metabolites were analyzed by gas-chromatography-mass spectrometry using a HP 5890 gas chromatograph with a HP 5971 mass-selective detector (Agilent Technologies, Wilmington, DE, USA) and a DB-5MS fused silica column (0.25mm by 30m, with 0.2 µm film thickness, J&W Scientific, Folsom, CA). 1 µl of sample was injected. Detector temperature was 280 °C and injection temperature was 250 °C. When alkylbenzenes were analyzed, oven temperature was programmed as 60°C for 1 min, 10°C/min to 300°C, and 300°C for 1 min. For detection of octane and its metabolites, oven temperature was programmed as 40°C for 1 min, 20°C/min to 230°C, and 230°C for 0.5min.

The degradation of 1,4-dioxane and THF in wildtype and knockdown mutant strains of *Pseudonocardia* sp. strain ENV478 was analyzed by biotransformation assay in

a similar manner as described above. Cells were grown on TSA media until it reached OD 0.3. Cells were subjected to centrifugation and resuspended in 50mM phosphate buffer (pH 7.0). Cell suspension was divided into three test tubes and sealed with a rubber stopper. Three samples without an addition of cells were used to monitor abiotic cause of 1,4-dioxane and THF disappearance. 1ml of sample was removed at each time point and extracted with 1.5ml ethylether containing 100mM benzene as a internal control. Organic layer was removed and dried with sodium sulfate. Samples were kept frozen at -20 °C until ready for analysis. The amount of 1,4-dioxane and THF was measured by GC-FID with DB5 column (0.24mm by 30m, with 0.25µm film thickness). Oven temperature was programmed for 40°C for 1 min, 20°C/min to 230°C, and 230°C for 0.5min. The amount of 1,4-dioxane and THF in each sample was calibrated to that of benzene.

GC-MS analysis of 1,4-dioxane was performed by our collaborators at Shaw Corp. 1 µl of the culture medium containing 1,4-dioxane was injected into a Varian 3400 gas chromatograph (Varian, Walnut Creek, CA) equipped with a 30-m capillary Vocol column (Supelco, Inc., Bellefonte, Pa.) and a flame ionization detector. The injector and detector temperatures were maintained at 180°C and 220°C, respectively, whereas the column temperature was programmed to increase from 85°C to 140°C at a rate of 50°C/min.

Thin layer chromatography was performed to analyze the indole oxidation products. Pigments were extracted from cells by first resuspending pigment forming cells in an equal volume mixture of MSB medium and chloroform. The chloroform layer was removed and evaporated with a stream of nitrogen. The dried pigment pellet was

dissolved in 100 μ l chloroform. All of the extract was applied to a polyester-backed silica gel thin-layer chromatography plate (250 μ m-thick layer, Whatman Ltd., Maidstone, Kent, England). The pigments were resolved on TLC plates with a solvent mixture of 50% toluene, 25% acetone, and 25% chloroform.

3.0 1,4-dioxane oxidation in *Mycobacterium* sp. strain ENV421

Abstract:

Strain ENV421 oxidizes 1,4-dioxane only after growth on propane. As discussed earlier, an oxygenase which is responsible for the initial step of the propane degradation pathway is proposed to be important in 1,4-dioxane oxidation. Because 1,4-dioxane oxidation occurred after growth on propane but not on succinate, we hypothesized that only propane can induce transcription of an enzyme that is responsible for 1,4-dioxane oxidation.

In order to identify an oxygenase involved in 1,4-dioxane and propane oxidation, we utilized two strategies. First, because the enzyme is specifically induced by propane and not by succinate, we looked for propane-induced proteins by SDS-PAGE. We also looked for three oxygenases that are possibly capable of propane and 1,4-dioxane oxidation using PCR with degenerate primers. The presence of these candidate genes and their expression pattern in strain ENV421 were examined by PCR and RT-PCR. The functions of the encoded proteins were then examined by heterologous expression in *E. coli*.

3.1 N-terminal protein sequencing of propane-induced proteins in *Mycobacterium* sp. strain ENV421

Purified total cytoplasmic and membrane proteins from propane-grown or succinate-grown cells were separated by one dimensional SDS-PAGE. Three propane-

induced proteins with sizes of approximately 42 kDa, 51 kDa, and 56 kDa were identified (Figure 12). These bands were cut out from the PDVF membrane and were subjected to N-terminal protein sequencing. N-terminal sequencing allowed the identification of the N-terminal 20-amino acids of each protein. The 42 kDa and 56 kDa bands contained two proteins with different abundance (Table 6).

The more abundant 56 kDa protein had no sequence similarity to known proteins in the database. The less abundant 56kDa protein had highest similarity to the N-terminal sequence of a putative aldehyde dehydrogenase from *Nocardia farcinica* IFM 10152.

The N-terminal sequence of the 51 kDa protein was identical to that of cytochrome P450 from *Mycobacterium* sp. HXN1500. This result is consistent with the RT-PCR result with cytochrome P450 primers, which will be described later.

The 42 kDa band also contained two proteins. The more abundant protein had an N-terminal sequence similar to a number of zinc-type alcohol dehydrogenases from gram-positive strains, such as *Frankia alni* ACN14a or *M. tuberculosis* H37Rv. It also contained a protein most similar to glyceraldehyde-3-phosphate dehydrogenase, type I from *Mycobacterium* sp. MCS, albeit at low abundance.

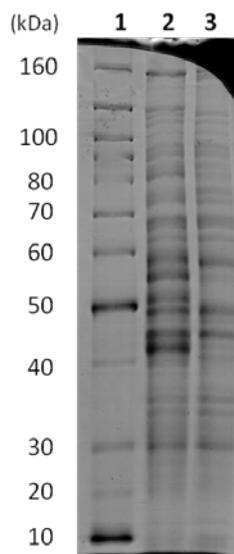


Figure 12. **Protein expression pattern of *Mycobacterium* sp. strain ENV421 after the growth on propane or on succinate.** ENV421 cells were grown in MSB medium with propane or succinate as a sole carbon source until mid-exponential phase. Total cytosolic proteins were extracted by Proteoprep kit and separated on SDS-PAGE gel. Gel was stained with commassie blue. Lane 1: protein molecular weight marker; lane 2 cytosolic protein extracted from propane grown cells; lane 3: cytosolic protein extracted from succinate grown cells.

Table 6. **List of N-terminal protein sequences of propane-induced proteins in *Mycobacterium* sp. strain ENV421.**

Size (kDa)	Protein sequence of N-terminus	Protein with highest similarity	Organisms
55*	TFLSIDIPETLQTFLRRASN	No	N/A
55	GVVSPGVEGSIVDAADGYDA	Aldehyde dehydrogenase	<i>Nocardia farcinica</i> IFM 10152
51	TEMTVAASDATNAAYGMALE	Cytochrome P450	<i>Mycobacterium</i> sp. HXN-1500
42*	MKTRAAVLFEAGKPFVVVEL	Alcohol dehydrogenase	<i>M. tuberculosis</i> H37Rv
42	TIRVGVNG	glyceraldehyde-3-phosphate dehydrogenase, type I	<i>Mycobacterium</i> sp. MCS

*

indicate the sequences of proteins that were more abundant.

3.2. Identification and analysis of alkane monooxygenase (AlkB) in *Mycobacterium* sp. ENV421

3.2.1. Sequence analysis of alkane monooxygenase (*alkB*) gene cluster in *Mycobacterium* sp. strain ENV421

Alkane monooxygenase is the most well studied enzyme of alkane oxidation. A number of alkane-degrading bacteria are known to have one or more *alkB* gene clusters. The degenerate primers that amplify a fragment of *alkB* gene from various organisms, including gram positive bacteria, were developed by Dr. Jong-Chang Chae at Dr. Zylstra's lab. PCR amplification with 30 cycles of 94°C for 30 sec, 55°C for 45 sec, and 72°C for 30 sec, followed by 5 min at 72°C yielded a product. Southern blot analysis using the *alkB* PCR fragment as a probe showed only one band, indicating *Mycobacterium* sp. ENV421 contains only one alkane monooxygenase (data not shown).

The deduced amino acid sequence of the PCR product showed high sequence similarity to *alkB* from various gram positive bacteria belonging to *Mycobacterium*, *Rhodococcus* and *Gordonia*, with highest similarity with *alkB* from *Mycobacterium* sp. Rv37R (96% identify) (figure 13). These homologues of ENV421's *alkB* sequences were determined through genome sequencing projects of the organisms. Alkane oxidation activity in these organisms or activity of these *alkB* genes in heterologous hosts has not been examined experimentally.

The DNA sequence neighboring *alkB* was determined. There are at least five putative open reading frames (ORFs) encoded in the same orientation: cationic

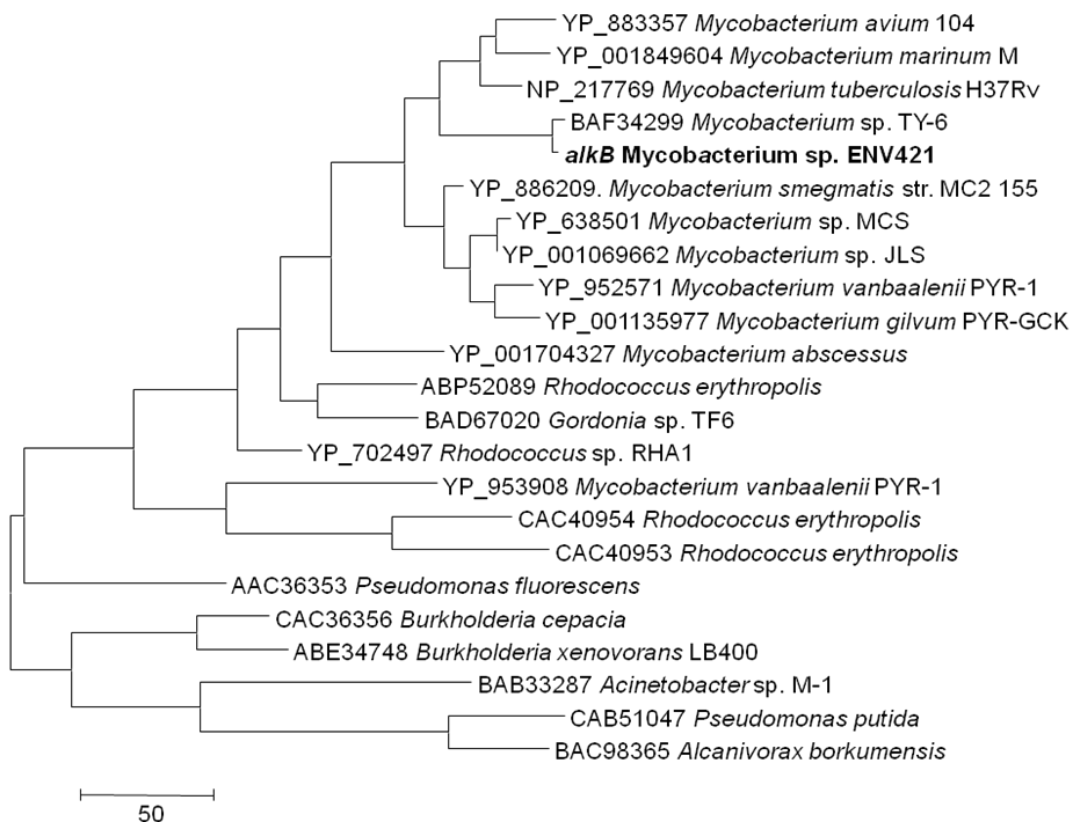


Figure 13. **Phylogenetic analysis of alkane monooxygenase (AlkB) gene identified in *Mycobacterium* sp. strain ENV421.**

transporter, alkane monooxygenase (*alkB*), two putative rubredoxins (*alkGF*) and a homologue of *P. putida*'s regulator for *alkB* system (*alkU*). (Figure 14, Table 7). These five genes are expected to be transcribed in the same orientation and gene organization is conserved in other organisms. On the other hand, the organization of genes surrounding these five ORFs is not conserved, and genes are seemingly not related to alkane metabolism. A rubredoxin reductase, another essential subunit of alkane hydroxylase complex, is not present in this region.

This gene organization is different from that of the canonical alkane monooxygenase clusters from *P. putida* GPo1 (Figure 4). In *P. putida* GPo1, *alkB* and *alkGF* is present in a large operon containing other *alk* genes involved in the downstream reaction of alkane degradation. Alkane is serially oxidized to form alkyl alcohol, alkyl aldehyde, and then alkyl acid using these gene products. The *alkB* operon of strain ENV421 does not contain these extra *alk* genes. The gene organization of *alkB* in strain ENV421 is identical to that of that of *M. tuberculosis* H37Rv and other *Mycobacterium* strains (Figure 6).

Alkane monooxygenase consists of three subunits: AlkB, AlkGF, and AlkT. All components are shown to be essential for exhibiting an enzyme activity. In order to find rubredoxin reductase (AlkT) in strain ENV421, degenerate primers were created based on the catalytically important residues among known AlkT proteins. DNA sequencing of the PCR product yielded sequence of a number of reductases. None of them had high sequence similarity to *P. putida*'s *alkT*. This result can be explained by high sequence conservation of residues involved in co-factor binding in various reductase families. The

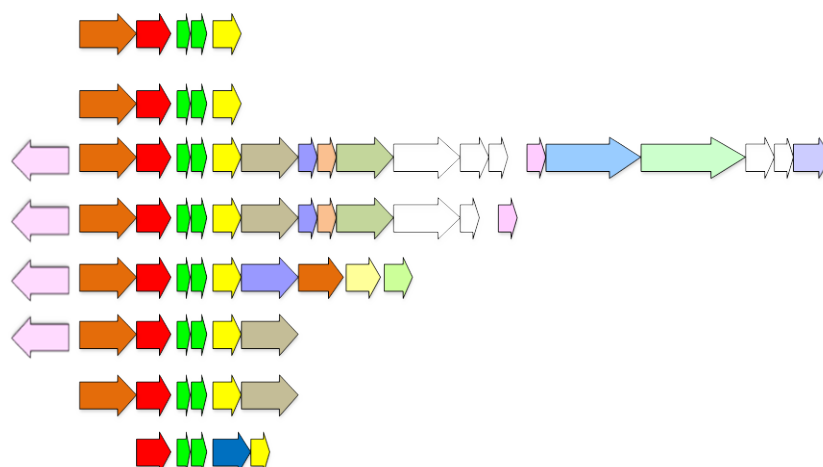


Figure 14. **The organization of alkane monooxygenase gene cluster in *Mycobacterium* sp. strain ENV421.** DNA sequence of approximately 3kb fragment including *alkB* was obtained. The *alkB* from *Mycobacterium* sp. ENV421 was found in close proximity to a cationic transporter, ferredoxin for alkane hydroxylase (*alkFG*), and putative transcription regulator for *alk* system (*alkU*). List of genes present in regions flanking *alk* genes are: 1: hypothetical protein with FAD-binding site, 2: Adenosylhomocysteinase, 3: Thymidylate kinase, 4: Response regulators, 5: Signal transduction histidine kinase, 6,7,8 : hypothetical proteins, 9: Sigma 54 modulation protein, 10: protein translocase, 11: drug transporter, 12,13: hypothetical proteins, 14: cation transporter, 15: amidohydrolase, 16: Triacylglycerol lipase, 17: GAF sensor protein, 18: TPR_2 repeat protein. In *Rhodococcus* sp. RHA1 and *Gordonia* sp. TF6, ferredoxin reductase (*alkT*) was found between *alkFG* and *alkU*.

Table 7. **Properties of *alk* gene products in *Mycobacterium* sp. strain ENV421.**

Gene	Amino acid residues	Molecular mass (kDa)	GC%	Functions
	Partial		63	Cationic transporter
<i>alkB</i>	412	45.7	63	Alkane hydroxylase
<i>alkF</i>	60	6.66	62	Rubredoxin
<i>alkG</i>	62	6.88	65	Rubredoxin
<i>alkU</i>	Partial		66	Transcriptional regulator

degenerate primers which were designed to bind these conserved sequences are expected to amplify various types of oxidoreductases.

A search was conducted for *alkT* homologs in several *Mycobacterium* genomes. Only the genomes that carry homologs of ENV421's *alkB* were used for this analysis. First, the blast program was used to search *P. putida*'s *alkT* homologue in their genome. In the genome sequence of *M. smegmatis*, it was found that the organism carries a number of oxidoreductases. A number of putative oxidoreductases were identified but none showed significant similarity to *P. putida*'s *alkT*. Also, none of these oxidoreductases had an *alkU* gene in close proximity.

Because of this low sequence similarity to *P. putida*'s *alkT*, and lack of further evidence that it is related to the *alkB* system, we could not determine whether any of these genes amplified by degenerate primers from ENV421 are rubredoxin reductase for alkane monooxygenase.

While examining the sequences of *alkT*, it was found that *alkT* has sequence similarity to reductases from cytochrome P450 monooxygenase. These two reductases do not form a separate clade, but rather they form one large clade (Figure 15). In contrast, reductases for soluble diiron monooxygenases form clusters distinct from these two enzymes. The hydroxylase subunit of *alkB* and cytochrome P450 do not show such a phylogenetic pattern. This indicates that a common ancestral reductase was recruited to different P450 and *alkB* families at separate points in the history of the enzyme's evolution.

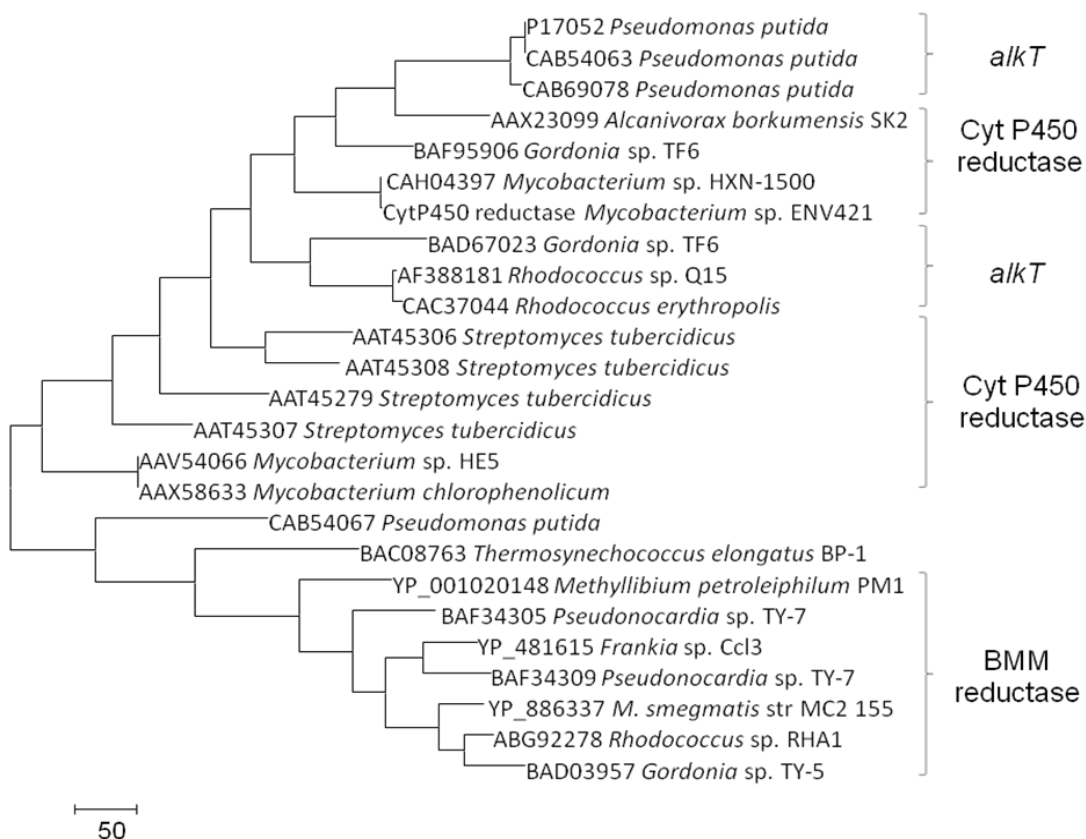


Figure 15. **Phylogenetic tree of oxidoreductases for soluble diiron monooxygenase, cytochrome P450 and alkane monooxygenases.** Abbreviation: reductase for soluble diiron monooxygenase (BMM reductase); reductase for bacterial cytochrome P450 (Cytochrome P450 reductase) and reductase for alkane monooxygenase (*alkT*).

3.2.2 Propane-mediated induction of the *alkB* gene in *Mycobacterium* sp. strain ENV421

Total RNA was extracted from cells grown on propane or on succinate. RT-PCR was performed using degenerate primers. Only RNA extracted from propane-grown cells yielded a product (Figure 16). Thus, expression of *alkB* is induced by propane and not by succinate.

3.2.3 Heterologous Expression of alkane monooxygenase of *Mycobacterium* sp. strain ENV421

Based on the hypothesis that cellular reductases produced by heterologous host cells can replace the missing AlkT activity, ENV421's *alkB* and *alkGF* alone were cloned into various expression vectors. The list of expression systems tested includes pET-30 (*E. coli*), pNV19 (*Rhodococcus*), and pCom8 (*Pseudomonas*). The hydroxylation of propane, 1,4-dioxane, and octane by each clone was examined by GC-MS. None of the clones showed hydroxylation activity for any of these compounds.

Since heterologous expression of only *alkB* and *alkFG* did not yield alkane nor 1,4-dioxane oxidation activity, it was concluded that co-expression of alkane monooxygenase specific *alkT* is important for reconstituting alkane oxidation activity in heterologous hosts. Due to the failure to identify *alkT* in strain ENV421, co-expression of a foreign *alkT* with ENV421's *alkBGF* was tested.

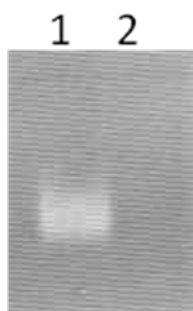


Figure 16. **RT-PCR analysis of *alkB* expression in *Mycobacterium* sp. ENV421 after growth on propane or succinate.** RT-PCR was performed to using RNA extracted from propane grown or succinate grown ENV421 (lane 1 and lane 2, respectively).

The expression of *alkB* with foreign *alkT* had yielded alkane oxidation activity in some cases but not in other cases. In our preliminary experiment, *alkB* from a gram positive *Gordonia* strain was expressed with *P. putida alkTGF*. The *E. coli* clone showed an unhealthy growth on the plate, implying a toxic effect of the construct. Since *alkB* is a membrane protein and known to form aggregates in the cell when it is not properly expressed, unsuccessful formation of an active monooxygenase complex might have lead to this toxic effect. The clone did not show alkane oxidation activity. On the other hand, co-expression of *alkB* from *Alkanivorax* with *P. putida's alkGFT* successfully showed the expected activity.

The determinant for successful co-expression of foreign *alkB*, *alkGF*, and *alkT* is not known. One possibility is whether the interacting surface of each subunit is conserved or not. There has been no study to determine residues responsible for these subunit interactions, nor residues involved in transferring of electrons from one subunit to another yet.

The determinant for successful expression of *alkT* with some *alkB* whose sequences have low sequence similarities may be due to the history of enzyme evolution as described above. Because *alkB* and *alkT* do not share the same evolutionary history, even if two organisms carry *alkB* with low sequence similarities, they may still have similar *alkT*. In these cases, the missing *alkT* may possibly be supplemented from another organism whose *alkB* sequences are very distinct.

alkB and *alkFG* from strain ENV421 were amplified with PCR and the products were cloned into pQE-30 (altered). *alkFGT* from *P. putida* was previously cloned into

pALTER_EX2 by Dr. Hung-Kuang Chang in Dr. Zylstra lab. Two plasmids were sequentially transferred into *E. coli* BL21 using chemical transformation.

The hydroxylase activity of the clone towards octane, propane, and 1,4- dioxane was examined by resting cell transformation and analyzed with GC-MS. The clone showed octane oxidation activity, which was determined by disappearance of 15% of provided octane in 2 hours (Figure 17). The clone did not exhibit propane nor 1,4-dioxane oxidation activity.

3.3 Identification and analysis of Cytochrome P450 (CYP153) in

Mycobacterium sp. strain ENV421

3.3.1 Sequence analysis and propane mediated induction of cytochrome P450 gene cluster in *Mycobacterium* sp. strain ENV421

The cytochrome P450 CYP153 family is known to oxidize alkanes ranging from C₅-C₁₃. It is found that alkane oxidizing bacteria lacking *alkB* often carry cytochrome P450 (van Beilen et al., 2006). Degenerate primers developed for assessing ecological distribution of cytochrome P450 in their study was used to examine whether strain ENV421 carries cytochrome P450.

The direct sequencing of PCR products showed multiple bases at some positions in the raw data indicating the presence of multiple cytochrome P450 genes in strain ENV421. This was also confirmed by Southern blot where multiple bands appeared when a PCR product was used as a probe (Figure 18). This result is probably due to the

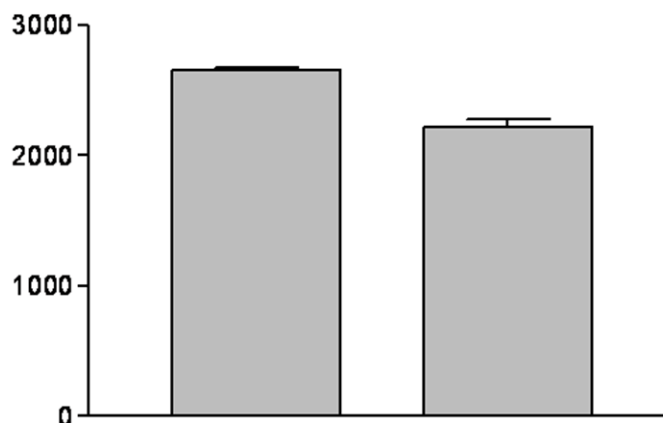


Figure 17. **The octane oxidation activity of *E.coli* BL21 recombinant clone expressing AlkBFG of ENV421 and AlkTFG of *Pseudomonas putida*.** 1) A recombinant clone expressing ENV421 alkBFG and *P. putida* AlkTFG and 2) a clone expressing only *P. putida* AlkTFG was used for this study. When the culture reached exponential phase, octane was added. After 2 hours of incubation, the amount of octane left in the culture was measured with gas chromatography.

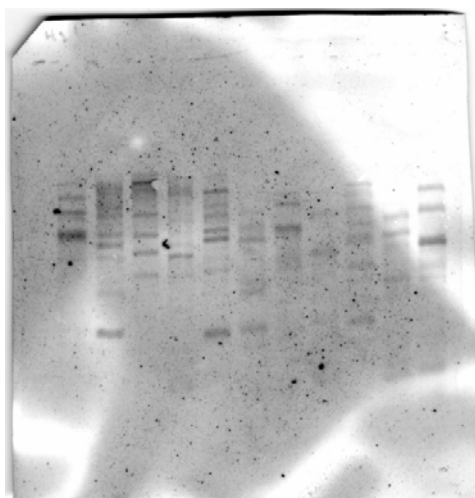


Figure 18. **Southern blot analysis of cytochrome P450 genes in *Mycobacterium* sp. strain ENV421.** The genomic DNA of ENV421 was digested by one or two restriction enzymes (lane 1: BamHI, lane 2: EcoRI, lane 3: kpnI, lane 4: SpeI, lane 5: XbaI, lane 5: PstI, lane 6: BamHI and EcoRI, lane 7: BamHI and KpnI, lane 8: BamHI and SpeI, lane 9: EcoRI and KpnI, lane 10: EcoRI and XbaI, and lane 11: EcoRI and PstI) and was separated by electrophoresis with 1% agarose gel. In order to make a DIG-labeled probe, PCR was performed using the degenerate primers designed to amplify cytochrome P450 CYP153. The genomic DNA was used for a template of a PCR reaction.

high sequence conservation at the primer binding site among different cytochrome P450 families and the presence of a large number of cytochrome P450 genes in this organism. Bacteria belonging to the *Corynebacterium* family can carry more than 20 cytochrome P450 genes (McLean et al., 2007).

In order to verify which cytochrome P450 is expressed in the propane grown cells and possibly important for propane and 1,4-dioxane oxidation, DNA sequence of RT-PCR product was determined. RT-PCR was performed using RNA extracted from propane grown cells and above mentioned degenerate primers. RT-PCR product was cloned into the pGEM-T vector. Several clones were sequenced. The RT-PCR yielded a product using RNA extracted from propane grown cells but not with RNA extracted from succinate-grown cells (Figure 19). All but one of the DNA sequences of the clones had high sequence similarity to the cytochrome P450 from *Mycobacterium* sp. HXN-1500 (CAH04396), which was experimentally shown to be involved in limonene and octane oxidation (van Beilen et al., 2006) (Figure 20). Another sequence showed similarity to the cytochrome P450 gene from *Mycobacterium* sp. MCS (YP_640381.1). The substrate range of this enzyme is unknown.

In order to obtain the sequence flanking the cytochrome P450 gene, inverse PCR was performed. Three ORFs in an operonic structure were identified: hydroxylase, rubredoxin reductase, and rubredoxin (Figure 21, Table 8). The gene order of cytochrome P450 operon in strain ENV421 and strain HXN-1500 is identical. The N-terminal sequence of the 42 kDa band, as mentioned above, matched the N-terminal sequence of deduced protein sequences of this cytochrome P450 gene.

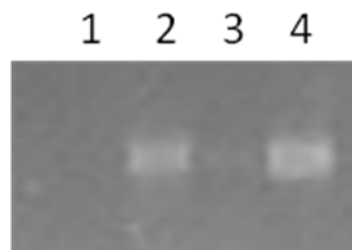


Figure 19. **Expression pattern of cytochrome P450 gene in *Mycobacterium* sp. strain ENV421 after growth on propane or succinate.** Total RNA was extracted from propane grown cells. RT-PCR was performed using degenerate primers for cytochrome P450 and 5ng of RNA. In order to confirm the absence of DNA contamination, two negative controls were run. First, standard PCR using RNA sample as a template was performed showing no band (lane 3). Another negative control was performed using RT-PCR reaction mix. Lanes 1 and 4 are identical reactions except that in lane 1 the initial 30 minute incubation at 50 °C was omitted, in lane 4 it was done. PCR reaction using Taq polymerase and genomic DNA template was performed as a positive control (lane 2).

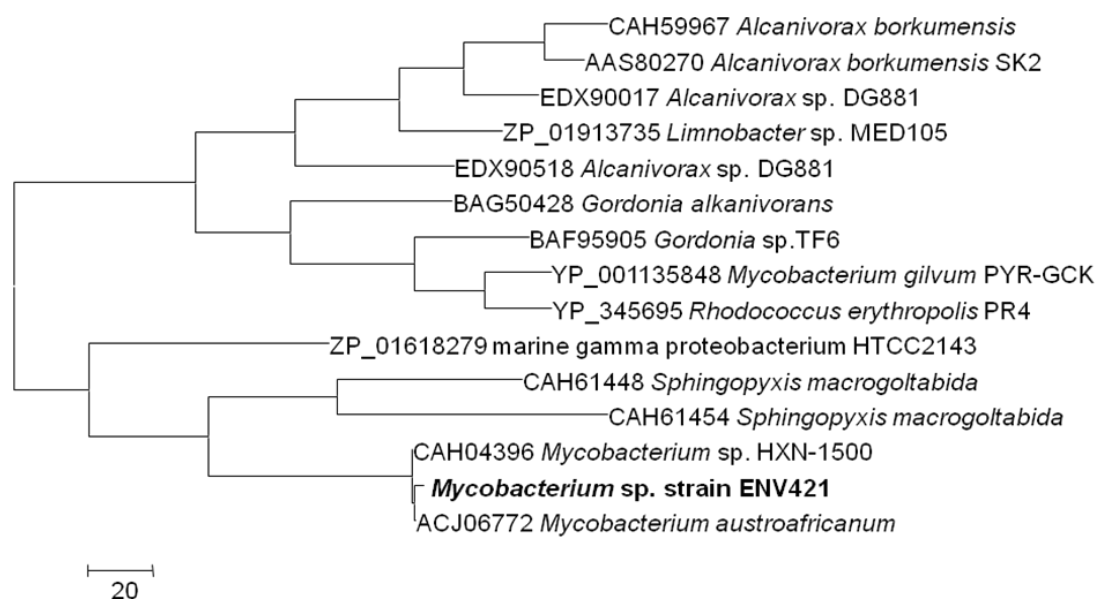


Figure 20. **Phylogenetic analysis of cytochrome P450 hydroxylase gene from *Mycobacterium* sp. strain ENV421.** The substrate ranges are known in only two cytochrome P450 homologs: octane in *Gordonia* sp. TF6 and limonene and C₆-C₁₂ alkanes in *Mycobacterium* sp. HXN-1500.

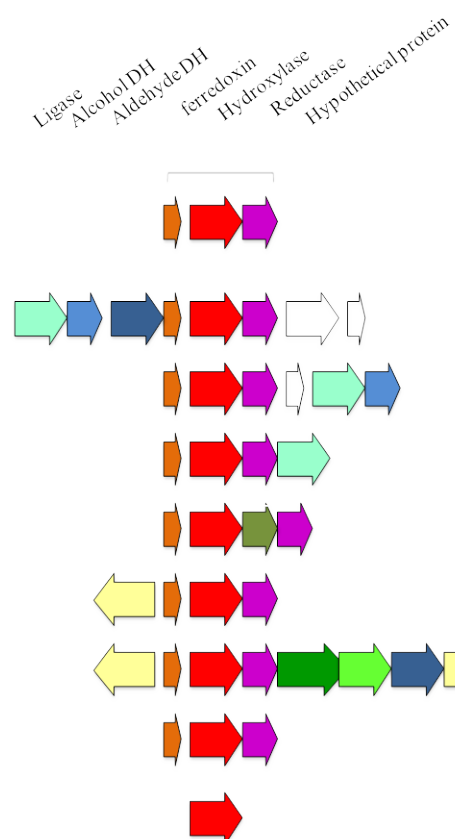


Figure 21. **Gene order and gene composition of cytochrome P450 gene cluster from *Mycobacterium* sp. strain ENV421.** The gene organization of the operons containing cytochrome P450 CYP153 are shown. Genes are abbreviated as Ligase: Ligase, Alcohol DH: alcohol dehydrogenase, Aldehyde DH: aldehyde dehydrogenase, ferredoxin: ferredoxin, hydroxylase :cytochrome P450 hydroxylase, reductase: ferredoxin reductase, alkJ: alcohol dehydrogenase for alkB system, XylM: homolog of xylene MO and AlkB.

Table 8. **Properties of *aphG*, *aphH*, and *aphI* gene products identified in *Mycobacterium* sp. strain ENV421**

Gene	Amino acid residues	Molecular mass (kDa)	GC%	Fuctions
<i>aphG</i>	420	47.7	59	Hydroxylase
<i>aphH</i>	424	45.4	64	Ferredoxin reductase
<i>aphI</i>	106	11.4	57	Ferredoxin

3.3.2 Heterologous expression of Cytochrome P450

The cytochrome P450 gene that had high sequence similarity to that of strain HXN-1500 was cloned into the *E. coli* expression vector pET-3a and expressed in *E. coli* BL21. After growth in LB medium, colonies exhibited blue and pink colors (Figure 22). The pigments were extracted from the cells by chloroform and separated on thin layer chromatography (TLC). One pink and one blue spot appeared as it was separated on the plate. The distance the blue pigment traveled was identical to that of an indigo standard (Figure 23). The pink pigment showed a resemblance to the TLC pattern of indirubin (Gilliam et al., 2000). Each pigment was extracted from the TLC plate and their light absorbance patterns were examined (Figure 24, 25). The highest absorbing peak was at 602 nm for the blue pigment and 536 nm for the pink pigment, which are identical to the indigo and indirubin standard, respectively (Figure 26). Thus, this clone is expressing active cytochrome P450 enzyme and it is capable of oxidizing indole to a mixture of indoxyl 3-oxindole and isatin, which were abiotically converted to indigo and indirubin (Figure 27).

The oxidation activity of this enzyme towards a variety of hydrocarbons, mainly alkanes and alkylbenzenes, was examined by biotransformation assay and analyzed by GC-MS. List of compounds tested are summarized in Table 9. Among the list of substrates tested, R-limonene, cymene, 4-ethyltoluene, propylbenzene, butylbenzene, pentylbenzene, hexylbenzene, heptylbenzene, octylbenzene and octane were oxidized by the cytochrome P450 enzyme from strain ENV421. When a standard for metabolites

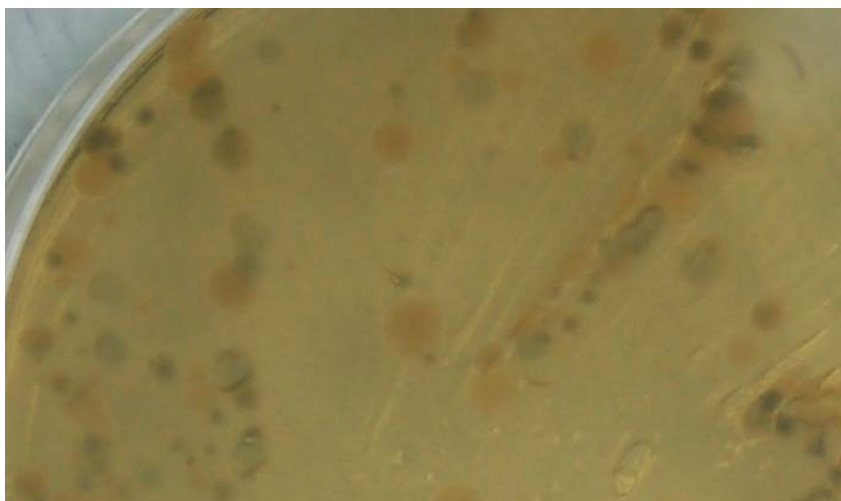


Figure 22. **Pigment formation by *E. coli* recombinant clone expression cytochrome P450 from *Mycobacterium* sp. strain ENV421.** The operon of propane-induced cytochrome P450 gene cluster was cloned into *E.coli* expression vector, pET-30. About two days after the clone was streaked on LB media with 50mg/l ampicillin, blue and pink color colonies appeared.

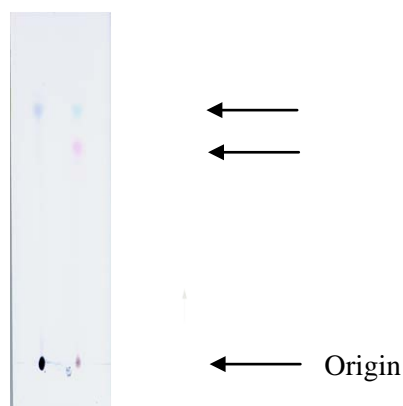


Figure 23. **The analysis of blue and pink pigments produced by *E. coli* recombinant clone expression cytochrome P450 from *Mycobacterium* sp. strain ENV421 using thin layer chromatography.** The pigments were extracted from the cells by chloroform and separated on polyester backed polyester-backed silica gel thin-layer chromatography plate with a solvent mixture of 50% toluene, 25% acetone, and 25% chloroform. Left: Indigo standard was dissolved in chloroform before applied onto TLC plate. Right: pigments extracted from *E. coli* expressing *Mycobacterium* sp. strain ENV4321 cytochrome P450.

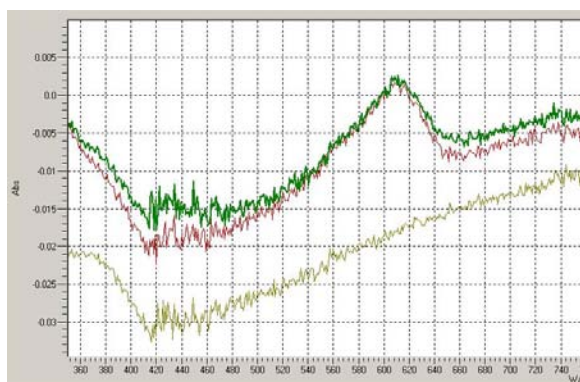


Figure 24. **UV-visible spectroscopy of blue pigment produced by recombinant *E.coli* clone expressing cytochrome P450 from *Mycobacterium* sp. strain ENV421 and indigo standard.** Pigments produced by *E.coli* clone expressing cytochrome P450 gene from ENV421 was extracted by chloroform and separated on TLC. Blue pigment which co-migrated with indigo standard was extracted and its absorbance pattern was examined. Each plot corresponds to: green line: blue pigment produced by a clone; red line: indigo standard; light green: chloroform only.

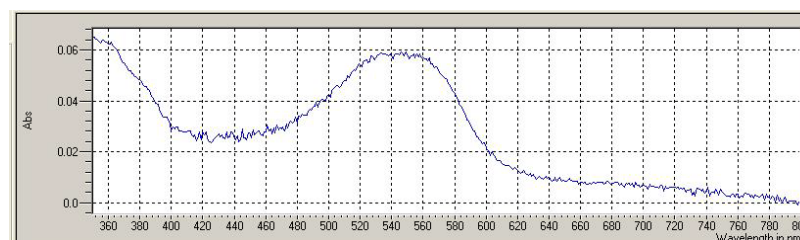


Figure 25. **UV-visible spectroscopy of pink pigment produced by recombinant *E.coli* clone expressing cytochrome P450 from *Mycobacterium* sp. strain ENV421.** Pigments produced by *E.coli* clone expressing cytochrome P450 gene from ENV421 were extracted by chloroform and separated on TLC. The pink pigment was extracted and its absorbance pattern was examined.

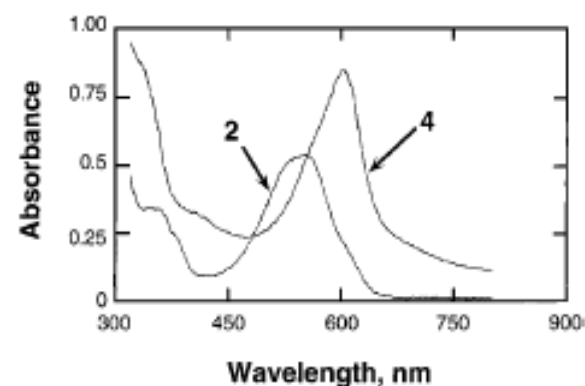


Figure 26. **UV-visible spectroscopy of indigo and indirubin.** The pigments were formed by recombinant P450 2A6 in *E.coli* cells and they were separated by TLC. Pigment 2 is indirubin and pigment 4 is indigo (Gilliam et al., 2000).

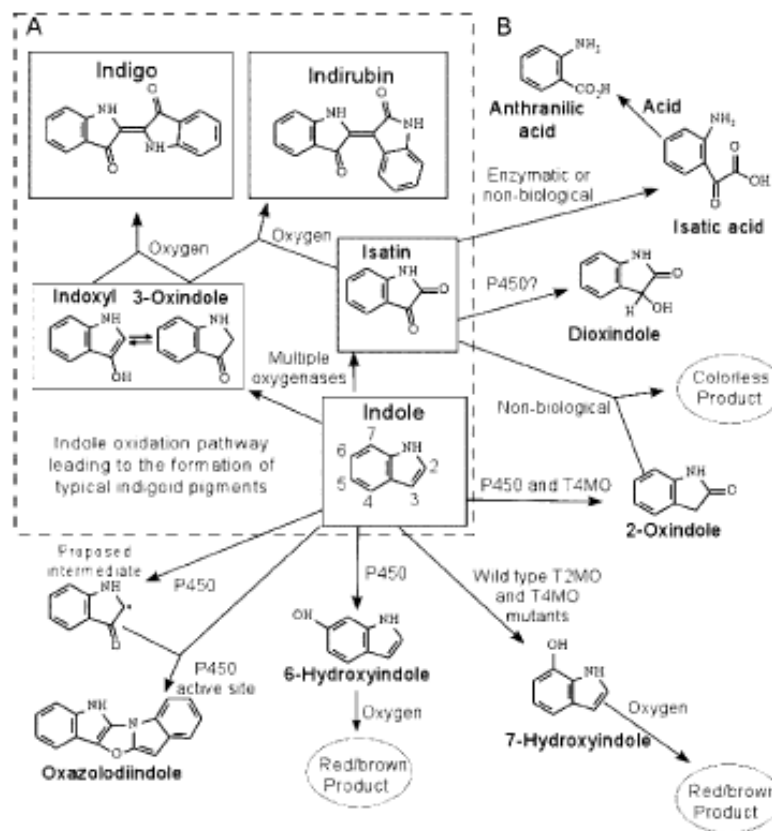


Figure 27. **Various indole oxidation products.** A) Oxidation of indole leading to the formation of indigo and indirubin B) Indole oxidation products not known to result in indigoid formation (Steffen et al., 1997).

Table 9. **List of substrates tested for oxidation by cytochrome P450 from *Mycobacterium* sp. strain ENV421**

Ethers	Alkanes	Cyclic and heterocyclic	Aromatics	
1,4-dioxane	Propane	Indole*	Cymene*	Ethylbenzene
Tetrahydrofuran	Octane	Indan	4-ethyltoluene*	Propylbenzene*
	Dodecane	Indene	<i>p</i> -xylene	<i>n</i> -Butylbenzene*
	Hexadecane	R-limonene*	<i>m</i> -xylene	Pentylbenzene*
	Cyclohexane	S-limonene	1,4-diisopropylbenzene	Hexylbenzene*
			<i>sec</i> -butylbenzene	Heptylbenzene*
			<i>n</i> -butylbenzene	Octylbenzene*
			<i>tert</i> -butylbenzene	Decylbenzene
			<i>iso</i> -butylbenzene	Decylcyclohexane
			Neopentylbenzene	diethylcyclohexane

*: Substrates that were oxidized by cytochrome P450 from *Mycobacterium* sp. strain ENV421

were commercially available, they were also analyzed by GC-MS. Their retention time and mass-spectrometry (MS) patterns were compared and identity of metabolites were verified. When it was not available, MS pattern of metabolites were compared to patterns available in MS library.

R-limonene was oxidized solely at the methyl side chain, forming perilla alcohol (Figure 28). S-limonene, however, could not be oxidized by this enzyme indicating the stereospecificity of this enzyme.

Two types of alkylbenzenes were oxidized by ENV421 cytochrome P450: 1) a benzene with two side chains (cymene and 4-ethyltoluene) and 2) a benzene substituted with a short to medium chain linear alkyl-group. A methyl side chain of cymene and 4-ethyltoluene was oxidized forming (4-isopropylphenyl)methanol and (4-ethylphenyl)methanol, respectively (Figure 29, 30). Both compounds carry a second side chain at *p*-position of methyl group. The oxidation of cymene and 4-ethyltoluene at this side chain could not be confirmed due to impurities in the substrates, which overlaps with the expected oxidized products. Other compounds with one or two short side chains, *m*-xylene, *p*-xylene, ethylbenzene, and 1,4-diisopropylbenzene could not be oxidized by this enzyme.

Benzene with a single side chain length of C₃-C₈ alkyl group was also oxidized by this enzyme (Figure 31-36). When the chain length is shorter (C₁-C₂), longer (C₁₀-longer), or branched, side chain could not be oxidized (Figure 38). Despite the propane inducible expression pattern of this gene, propane oxidation was not detected by this method. Interestingly, octane, a medium chain linear alkane, can be oxidized by this enzyme forming 1-octanol (Figure 37). Octane, however, cannot support a cell growth of

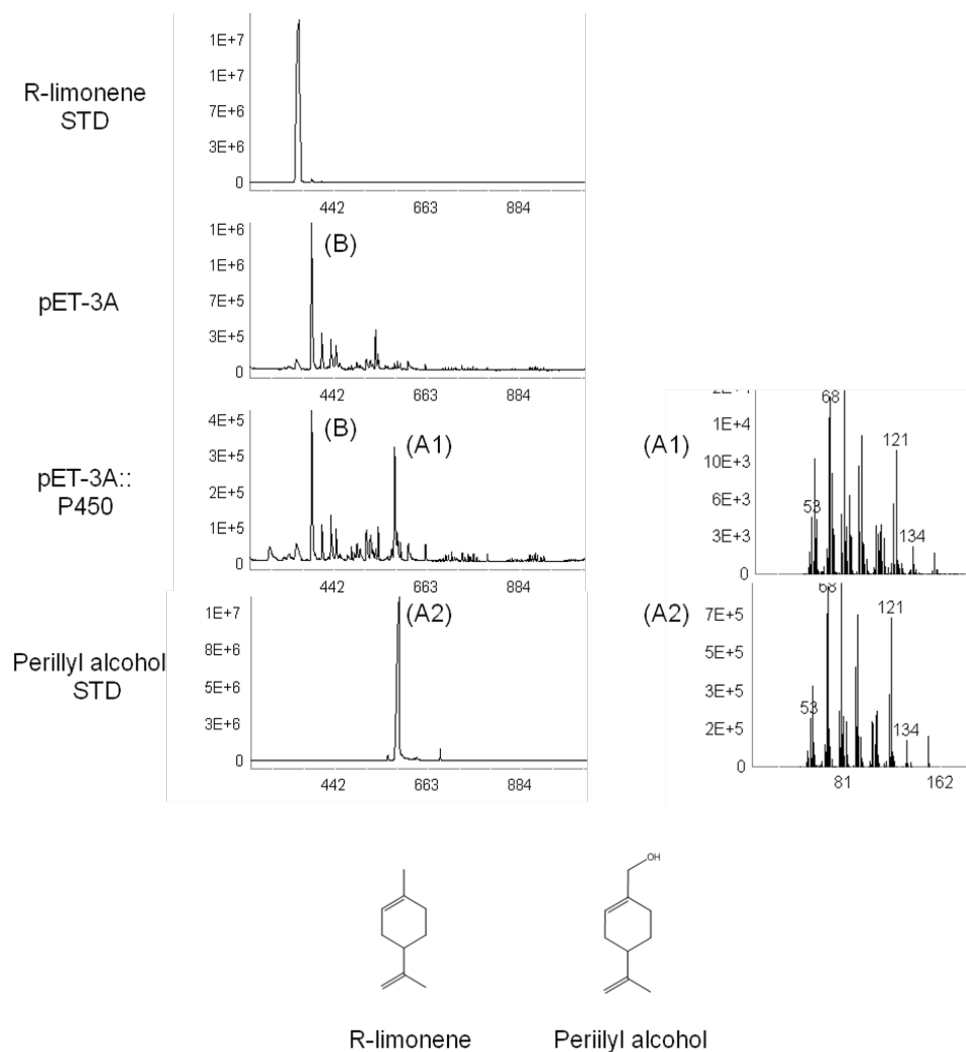


Figure 28. **The biotransformation of R- limonene to perillyl alcohol by cytochrome P450 from *Mycobacterium* sp. strain ENV421.**

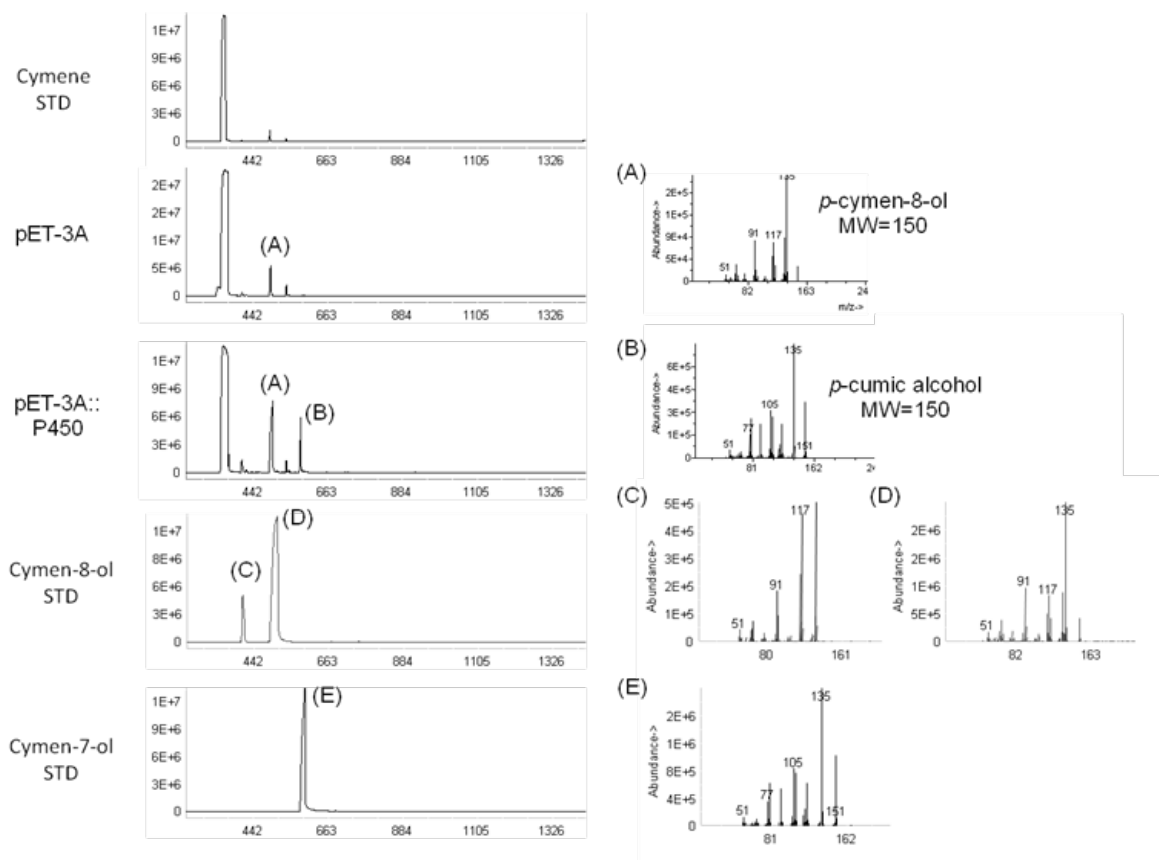


Figure 29. The biotransformation of cymene to *p*-cymen-7-ol by cytochrome P450 from *Mycobacterium* sp. strain ENV421.

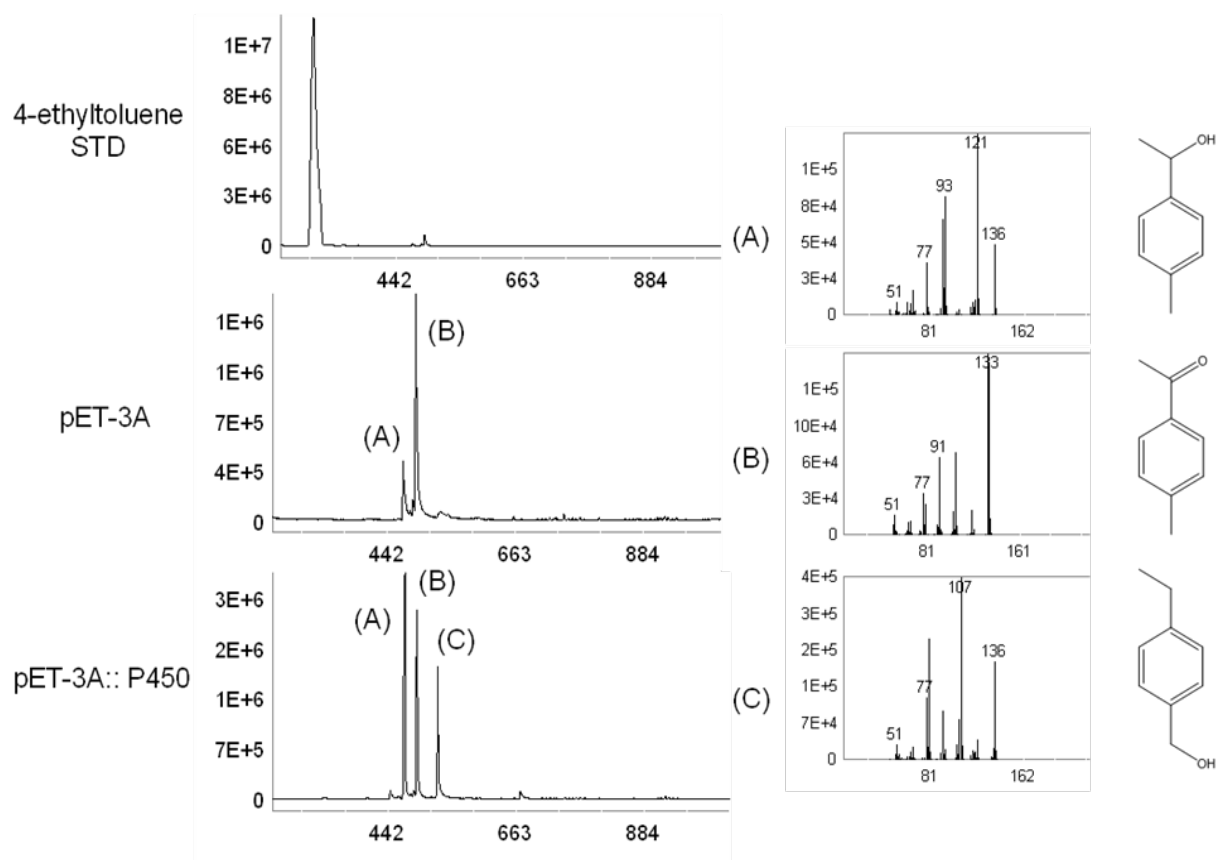


Figure 30. The biotransformation of 4-ethyltoluene to 4-(ethylphenyl)methanol by cytochrome P450 from *Mycobacterium* sp. strain ENV421.

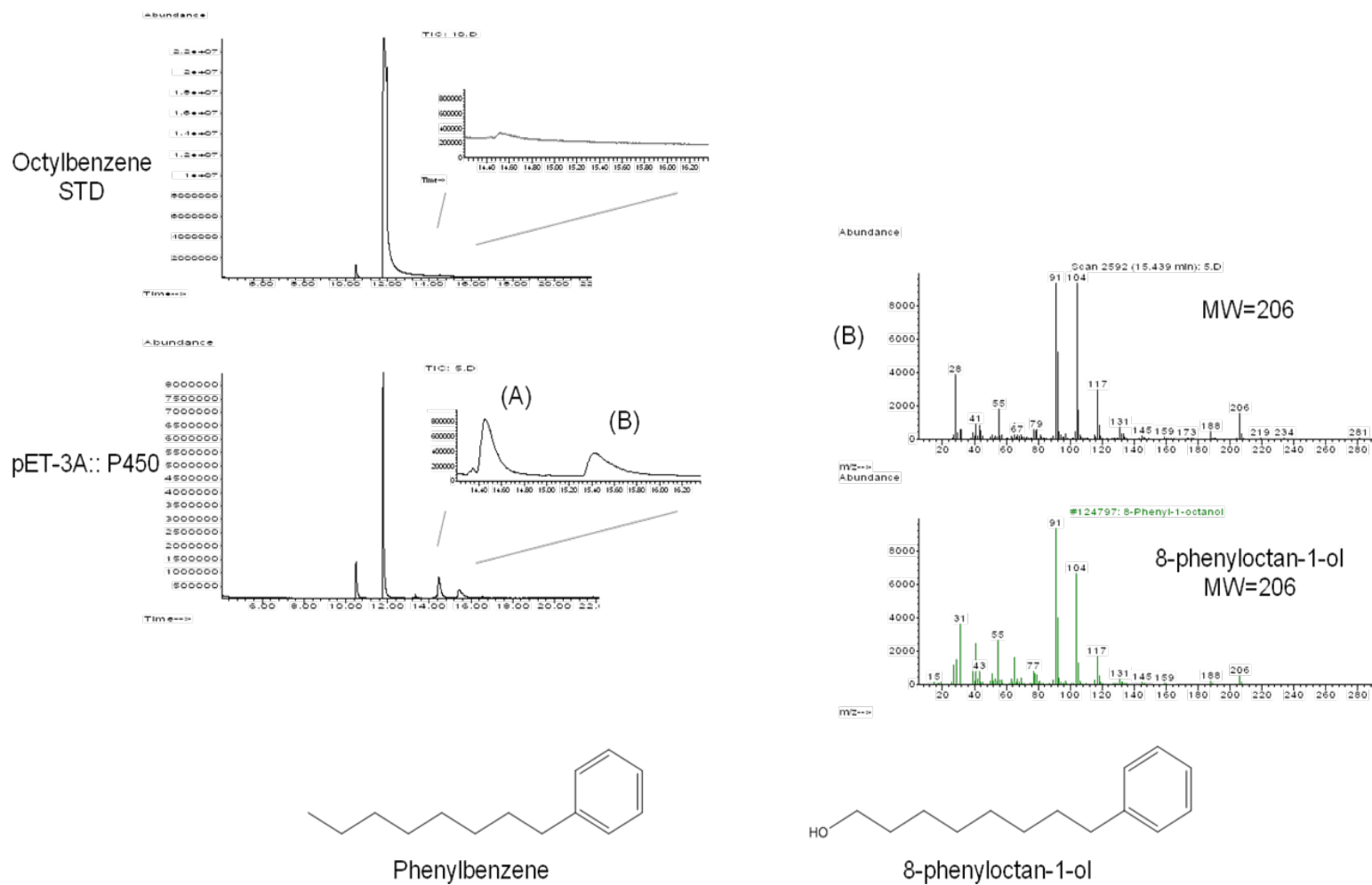


Figure 31. The biotransformation of octylbenzene by cytochrome P450 from *Mycobacterium* sp. strain ENV421.

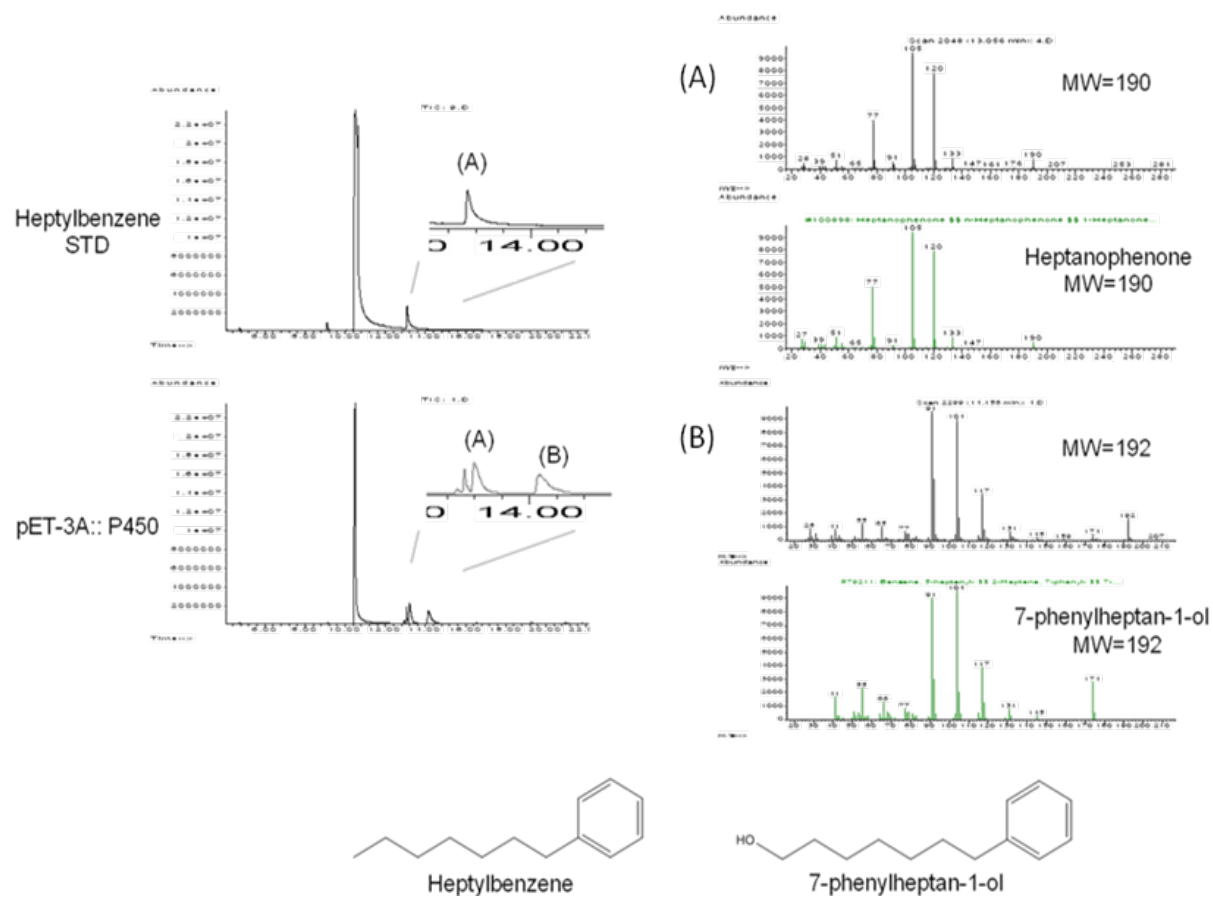


Figure 32. The biotransformation of heptylbenzene by cytochrome P450 from *Mycobacterium* sp. strain ENV421

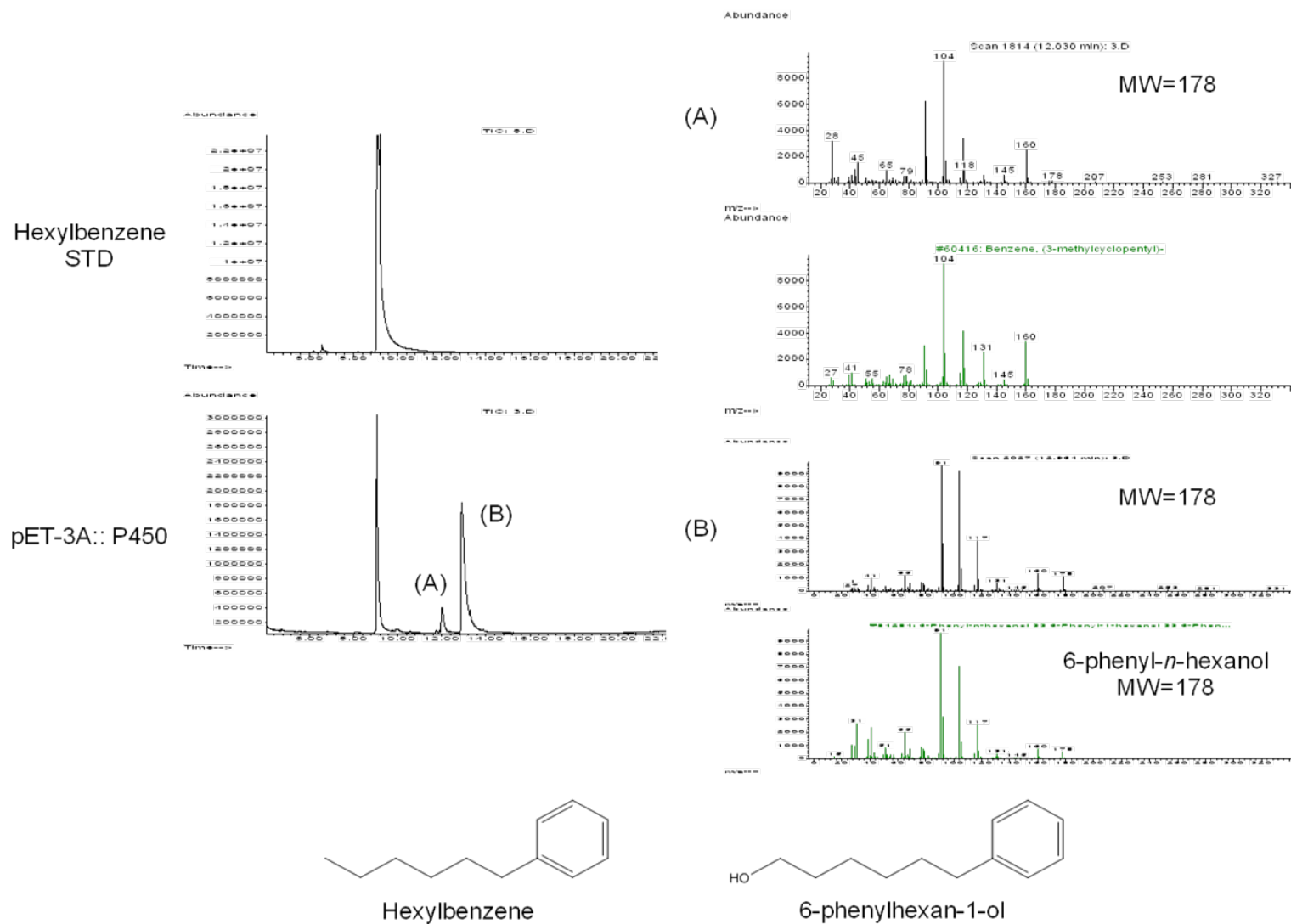


Figure 33. The biotransformation of hexylbenzene by cytochrome P450 from *Mycobacterium* sp. strain ENV421.

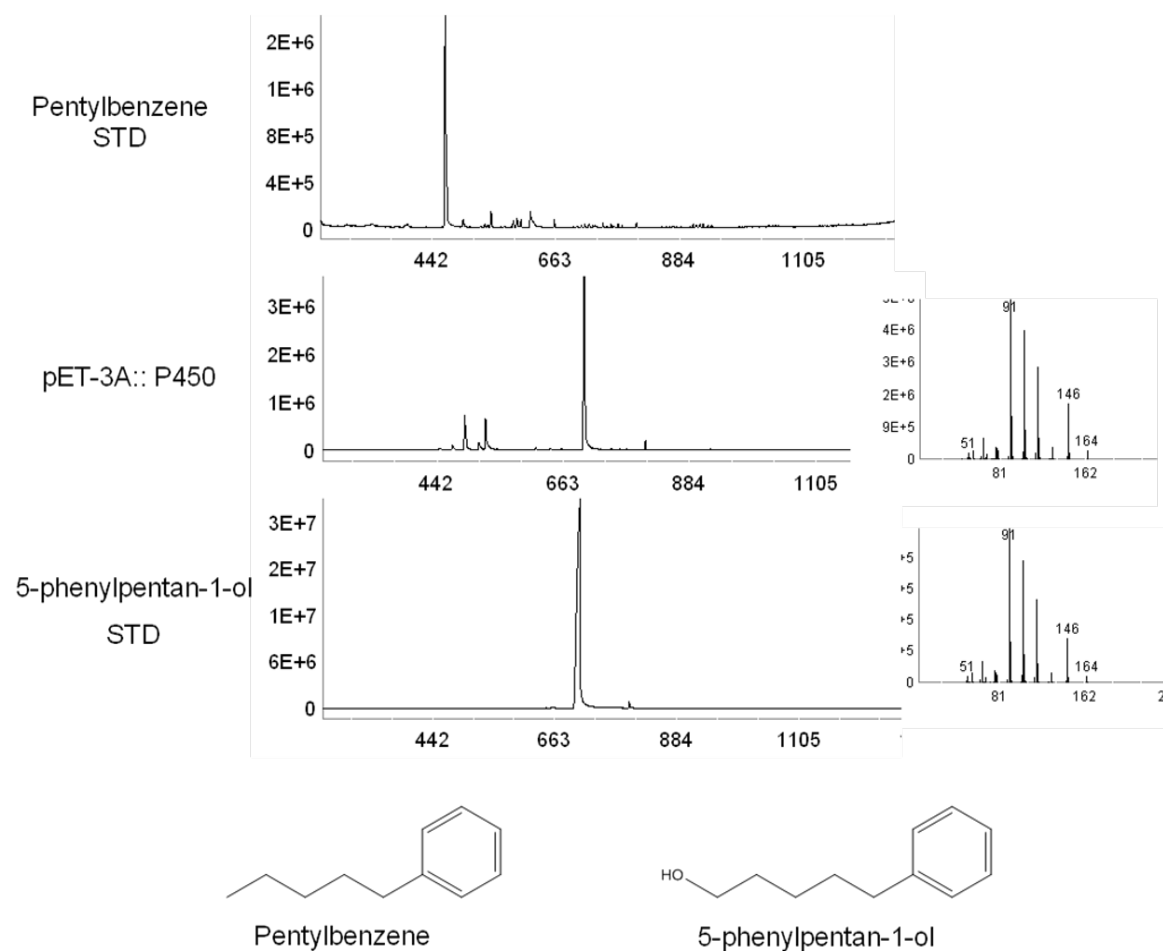


Figure 34. The biotransformation of pentylbenzene by cytochrome P450 from *Mycobacterium* sp. strain ENV421.

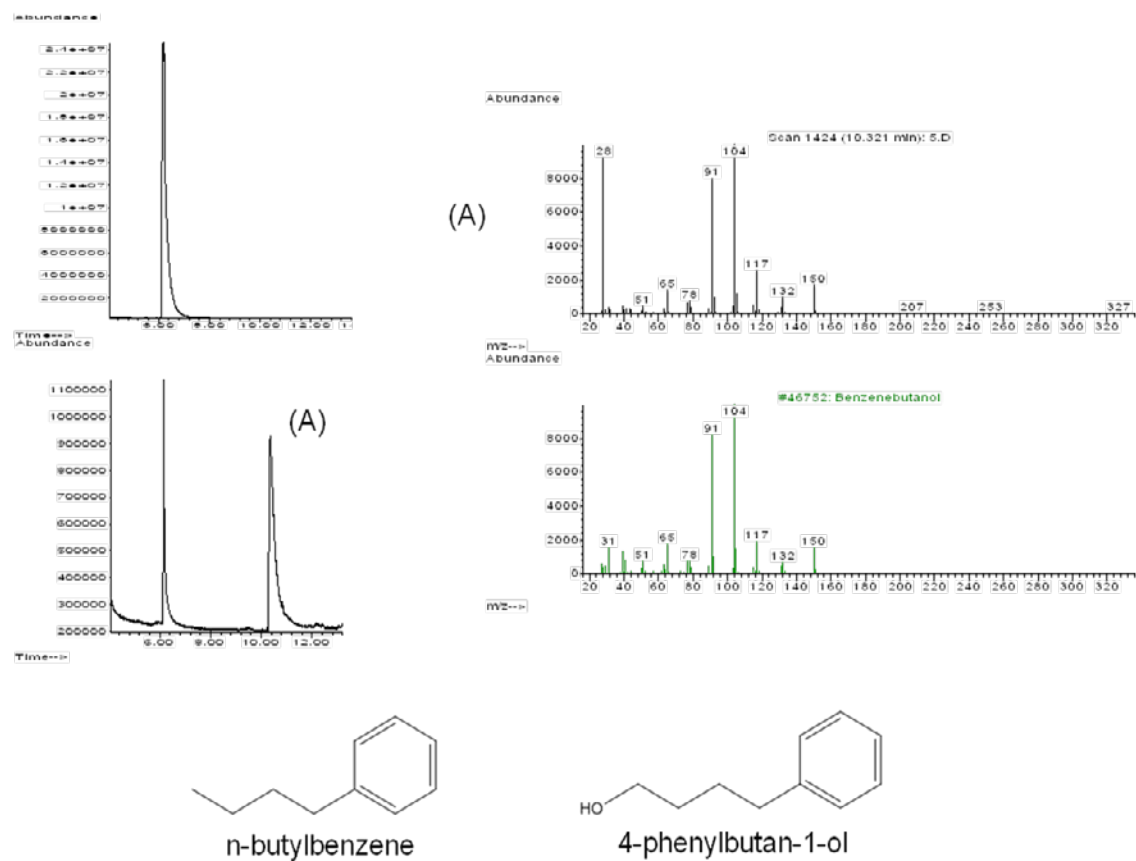


Figure 35. The biotransformation of n-butylbenzene by cytochrome P450 from *Mycobacterium* sp. strain ENV421.

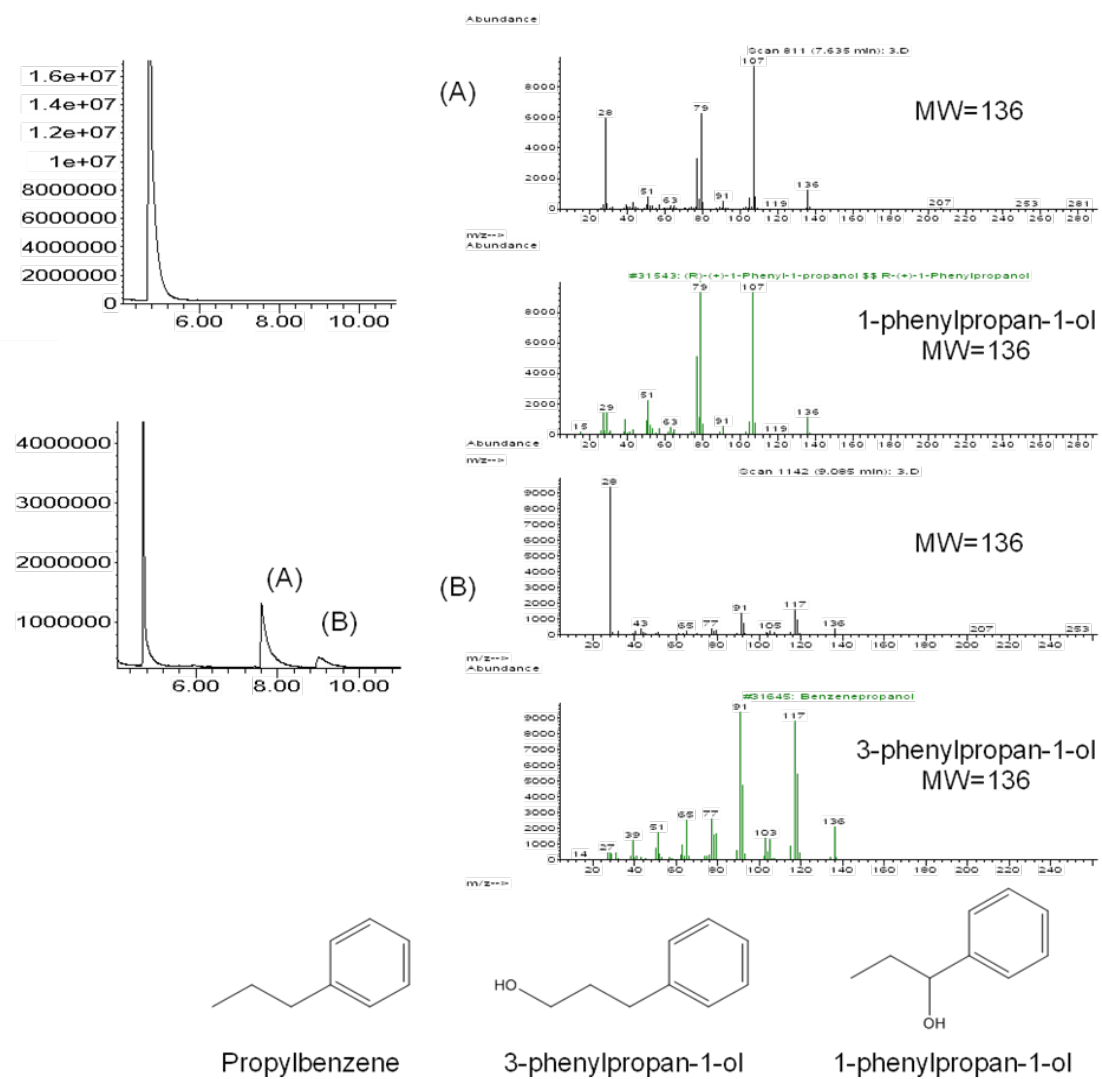


Figure 36. The biotransformation of propylbenzene by cytochrome P450 from *Mycobacterium* sp. strain ENV421.

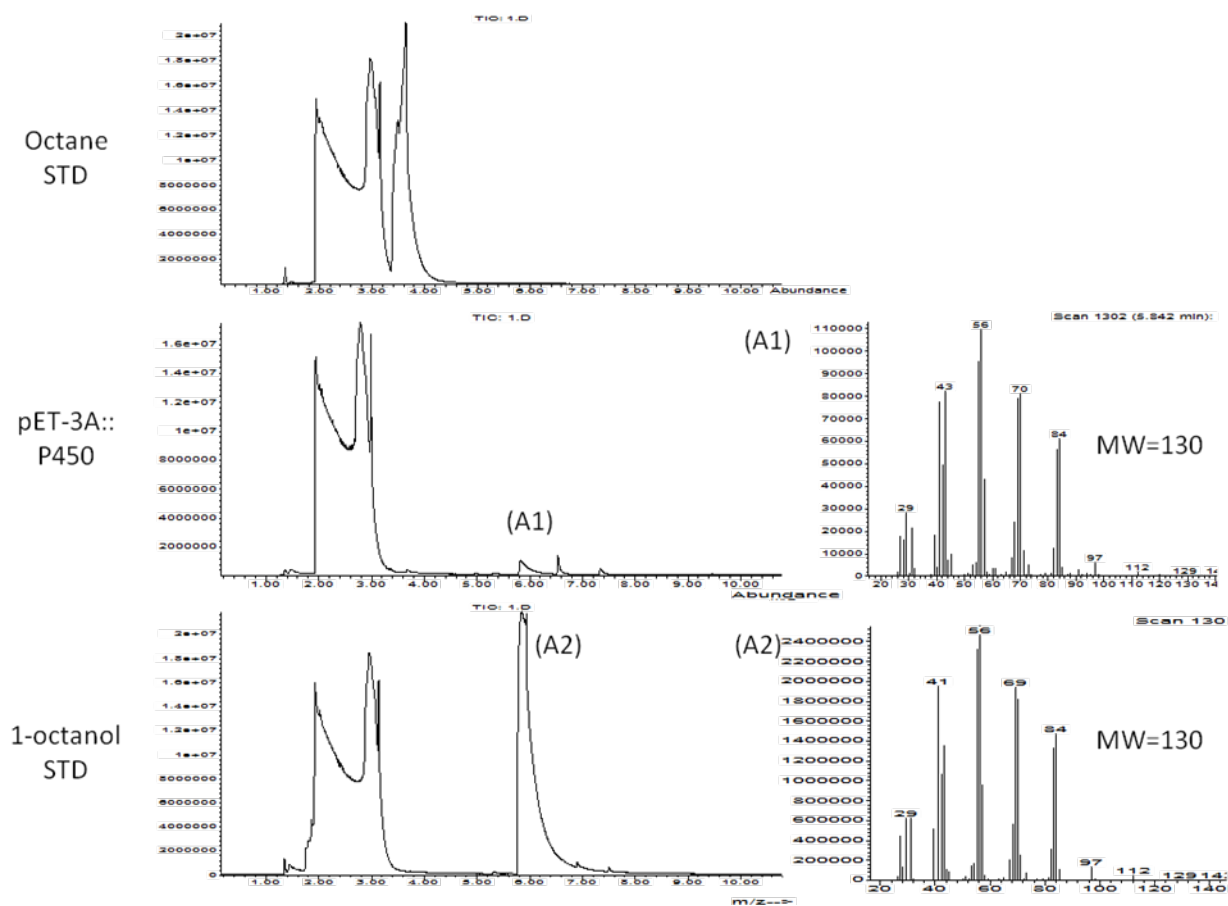


Figure 37. The biotransformation of octane to 1-octanol by cytochrome P450 from *Mycobacterium* sp. strain ENV421.

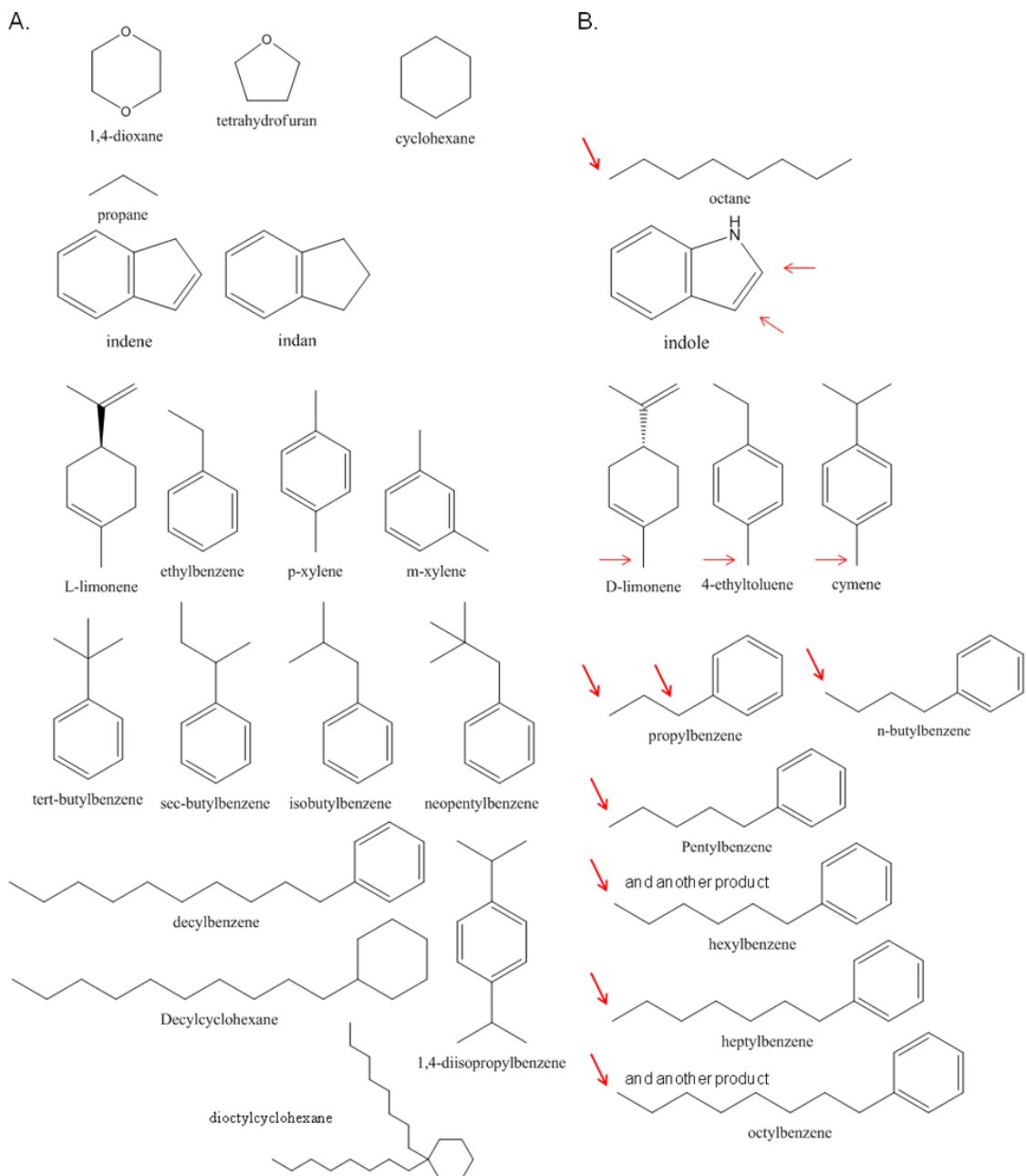


Figure 38. Summary of biotransformation assay of aliphatic compounds by cytochrome P450 from *Mycobacterium* sp. strain ENV421. A) compounds that were not oxidized and B) compounds that were oxidized by cytochrome P450 enzyme from strain ENV421. An arrow indicates the positions of the carbon that were hydroxylated by this enzyme.

strain ENV421. Oxidation of compounds whose chemical structures are similar to indole, indan and indene, was also examined using GC-MS. Neither of these substrates was oxidized by cytochrome P450 from strain ENV421.

Oxidation of 1,4-dioxane by this enzyme was examined by the same method. Products of 1,4-dioxane could not be detected by GC-MS. Disappearance of 1,4-dioxane after incubation with cells expressing cytochrome P450 enzyme was also monitored using GC-FID using Vocol column. There was no significant decrease in the amount of 1,4-dioxane in the medium containing cells expressing cytochrome P450 enzyme, in comparison to the abiotic control.

3.4 Identification and analysis of a soluble diiron monooxygenase (PMO) in

Mycobacterium sp. strain ENV421

3.4.1 Sequence analysis of propane monooxygenase gene cluster in

Mycobacterium sp. strain ENV421

Degenerate primers used in this study were designed based on conserved regions in di-iron monooxygenases including soluble methane monooxygenases, THF monooxygenase and propane monooxygenases. A 330 bp PCR fragment was PCR amplified and cloned into the pGEM-T vector. Out of 10 clones sequenced, 9 clones had identical sequences that have highest sequence similarity to a putative propane monooxygenase found in *Mycobacterium* sp. TY-6. Another clone contained part of a

methane monooxygenase gene most similar to soluble methane monooxygenase protein A in *Methylocystis* sp. WI14 (Figure 39, 40) .

The DNA sequence of the *prm* operon was partially completed by inverse PCR. The operon contains two of four propane monooxygenase subunits, *prmA* and *D* encoding the large subunit and small subunit, respectively. The deduced peptide sequence of the PCR product showed a high sequence similarity to propane monooxygenase from *Mycobacterium* sp. TY-6 (93%) (Kotani et al., 2006).

The presence of a coupling protein and a reductase subunit of a monooxygenase was examined using both a specific primer developed based on a sequence from strain TY-6 and degenerate primers developed based on conserved sites in aligned sequences. However, no product was observed with these PCR primers.

3.4.2 Propane-mediated induction of the propane monooxygenase in *Mycobacterium* sp. ENV421

The gene expression patterns of the α -subunit of PMO and sMMO in strain ENV421 were examined by RT-PCR. Total RNA was extracted from cells grown on propane or on succinate. RT-PCR was performed using the above mentioned degenerate primers. Only RNA extracted from propane grown cells yielded an RT-PCR product. The RT-PCR product was then sequenced to examine whether PMO and/or sMMO is expressed in propane grown cells. The RT-PCR product was cloned into the pGEM-T vector and DNA sequences of inserts in 10 random clones were determined. All 10

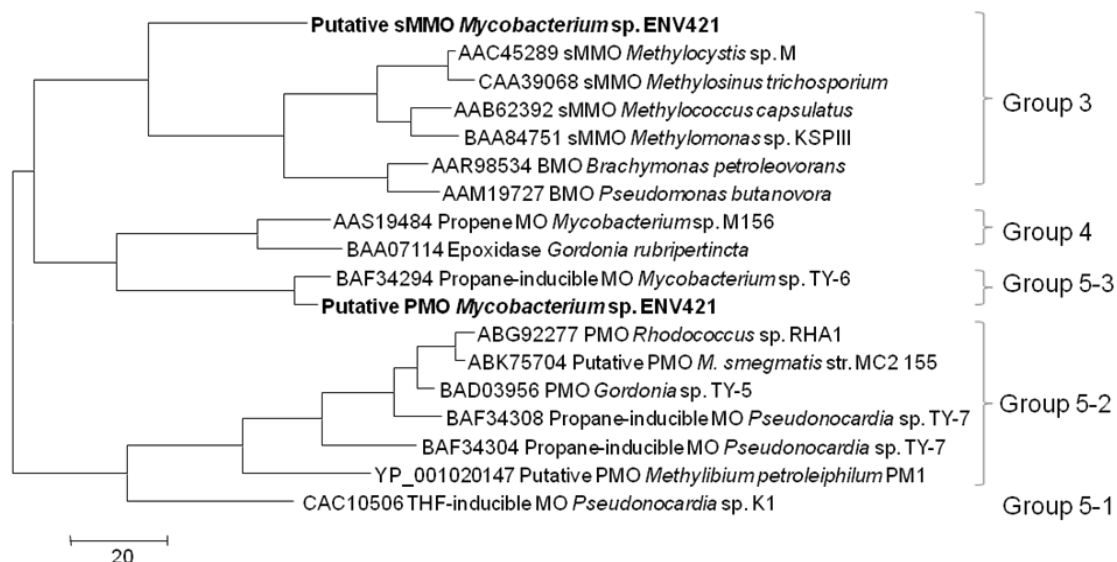


Figure 39. **Phylogenetic analysis of two soluble diiron monooxygenase genes identified in *Mycobacterium* sp. strain ENV421.** The sequences are labeled with each sub-groups of diiron monooxygenase family they belong to, as described in Figure 8 and 10.

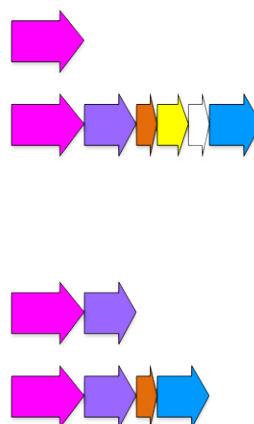


Figure 40. **Two soluble diiron monooxygenase genes identified in *Mycobacterium* sp. strain ENV421.** A) a hydroxylase gene, homologous to soluble methane monooxygenases from methanotrophic bacteria, such as *Methylocystis* sp. WI14 (Grosse et al., 1999). B) α and β subunit of hydroxylase whose protein sequence showed highest similarity to the propane-induced monooxygenase found in *Mycobacterium* sp. TY-6 (Kotani et al., 2006).

clones carried a fragment of PMO. Thus, despite the presence of two diiron monooxygenases, only PMO is expressed in propane-grown cells.

3.4.3 Heterologous gene expression of putative PMO

The two subunits of a putative propane monooxygenase found in ENV421 were amplified and cloned into the pET-30 vector. The clone did not show propane or 1,4-dioxane oxidation activity.

3.5 Alcohol dehydrogenases in *Mycobacterium* sp. strain ENV421

The N-terminal sequence of the propane-induced 42kDa protein matched zinc-containing alcohol dehydrogenases (Figure 41).

Based on the conserved sequences of these alcohol dehydrogenases, degenerate primers were constructed and PCR was performed with standard conditions. Only one type of dehydrogenase was amplified by this primer and its similar sequences on the database clustered in a different group from ones identified by N-terminal protein sequencing (Figure 42).

The presence of three alcohol dehydrogenases found in propane utilizing *Gordonia* sp. strain TY-5 was also examined. In strain ENV421, only *adh2* and *adh3* were identified through PCR using degenerate primers. Based on the result of RT-PCR, these two enzymes were not expressed in propane-grown cells.

ENV421	MKTRAAVLFEAGKPFVVEL
YP_756034.1	MKTRAAVAFEAGKPLEIVEV
AAP02982.1	MKTKAAVLLETGKPFEMEL
AAP02984.1	MKTKAAVLLEPGKPFEMEL
YP_702460.1	MKTKAAVLFEETHKPFIVEL
P81747	MKTKAAVLFEETHKPFIVEL
YP_710489.1	MKTKAAVLYEAGKPFIEEL
NP_217602	MKTTAAVLFEAGKPFELMEL
	*** *** * . **: *: * :

Figure 41. The multiple sequence alignment of N-terminal sequence of a propane induced 42kDa protein in strain ENV421 and zinc-alcohol dehydrogenases. The identity of sequences are shown in Figure 33.

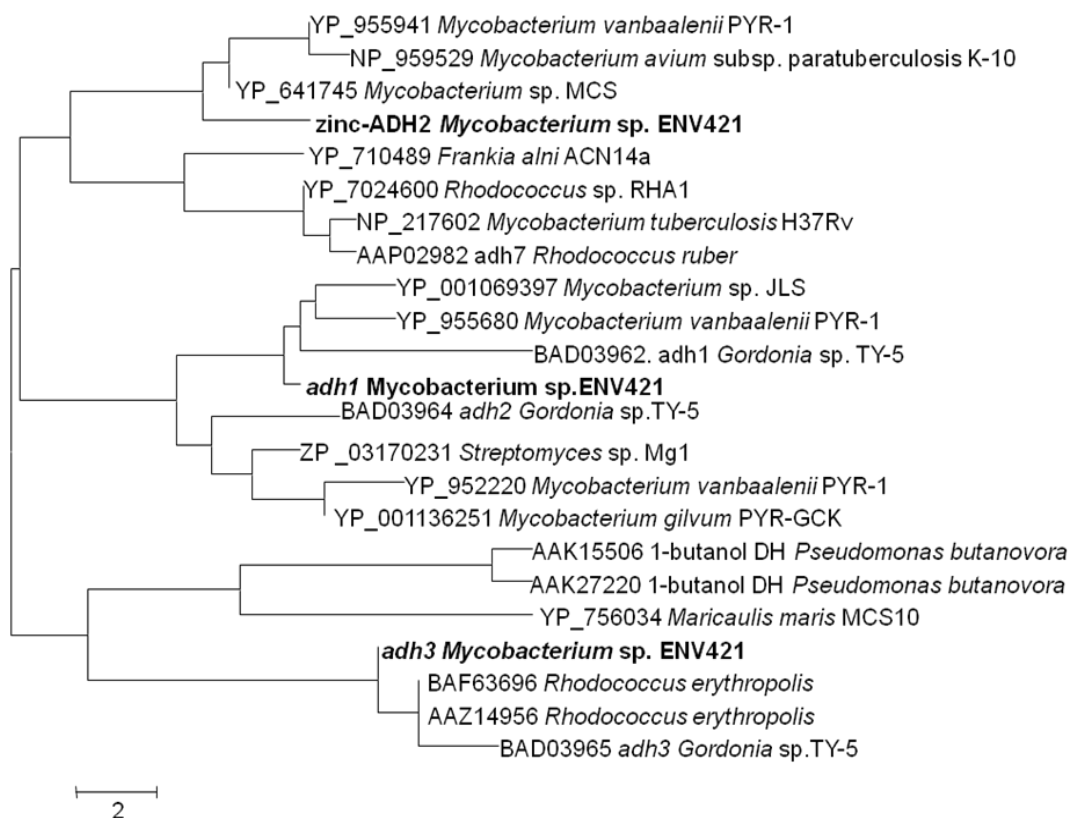


Figure 42. Phylogenetic analysis of alcohol dehydrogenases identified in *Mycobacterium* sp. strain ENV421. Four alcohol dehydrogenases were identified in strain ENV421. The complete or partial sequences of these genes were verified and their deduced protein sequence was used for analysis. The proteins labeled with * have N-terminal sequences that are highly homologous to N-terminal sequence of a propane inducible 42kDa protein in strain ENV421.

3.6 Genetic manipulation of *Mycobacterium* sp. ENV421

Several gram negative and gram positive shuttle vectors (pCom8, pSC-A, pJWB4N pBluescript, pET-3a, pGEM-3, pNV18, pSRK, pEM4, and pJAM2) were tested for their ability to replicate in *Mycobacterium* sp. ENV421. None of the vectors replicated in *Mycobacterium* sp. ENV421, prohibiting direct genetic manipulation of this organism.

3.7 Discussion

Transcription of *alkB* in strain ENV421 was upregulated by propane. When its *alkB* and *alkFG* were cloned alone, they did not yield any 1,4-dioxane or hydrocarbon oxidation activity. When they were coexpressed with rubredoxin reductase and rubredoxin genes (*alkT*, *alkFG*) from *P. putida* GPo1, the clone showed octane degradation activity. This apparent enzyme activity is low compared to the case when *P. putida alkBGFT* was expressed in *E. coli*. This clone converted the entire provided octane to octanol in 2 hours (data not shown). There are at least several possible reasons for this low apparent activity: 1) efficiency of translation is low due to high GC% content of the genes or due to codon bias, 2) the folding/ insertion of the enzyme into the membrane is not correct, or 3) native octane hydroxylation activity by this enzyme is low. 1,4-Dioxane or propane degradation by this clone was not observed.

Both the RT-PCR and proteomic analysis of ENV421 strain showed that a cytochrome P450 gene is expressed only in propane grown cells. It shares high sequence similarity to CYP153 from *Mycobacterium* sp. strain HXN-1500. It also shares a relatively high sequence similarity to octane-hydroxylating CYP153 in *Gordonia* sp. TF6 and *Acinetobacter* sp. OC4. The complete sequence of an operon containing cytochrome P450 CYP153 hydroxylase was obtained. The complete sets of genes encoding cytochrome P450 subunits were present in this operon: hydroxylase, ferredoxin, and ferredoxin reductase. The entire operon was cloned into an *E. coli* expression vector, pET-3A. The clone did not show oxidation activity towards 1,4-dioxane, propane or octane. This result is contrary to the observed alkane hydroxylation activity of cytochrome P450 from *Mycobacterium* sp. strain HXN-1500 (van Beilen et al., 2006). Based on the significantly high sequence identity between the two genes, it was expected that CYP153 in strain ENV421 would show at least an octane oxidation activity.

However, the clone exhibited hydroxylation activity towards various aliphatic organic compounds. Among various substrates tested, indole, limonene, and pentylbenzene were shown to be the substrates for this enzyme. The hydroxylation products of these substrates were analyzed with GC-MS. The substrates can be divided into three types: 1) heterocyclic, 2) aromatic structure with a methyl side chain and a C₂-C₃ side chain at its *para*-position, and 3) aromatic structure with a long linear side chain.

The production of indole and indirubin on LB plates indicated that indole could be oxidized at two positions on the 5-membered ring. The hydroxylation happened directly at the carbons within the ring structure. This indole oxidation activity was fairly low. When cells containing other indole hydroxylation enzymes were incubated on LB

media, the colonies formed dark colors at a relatively fast rate. The ENV421 clone, however, exhibited very faint color on LB media. The color developed after at least two days of incubation at room temperature. These observations imply that oxidation of carbons in the ring structure is not an optimal reaction for cytochrome P450 from strain ENV421. The structural analogues of indole, indan and indene, did not yield any products that can be detected by GC-MS. Thus, the presence of a nitrogen and a carbon-carbon double bond in the 5-membered ring seems to be an important factor for oxygenation. The enzymatic oxidation of indole has been observed in a variety of oxygenase families including soluble diiron monooxygenases, toluene 2-monooxygenase, toluene-4-monooxygenase, and phenol monooxygenase (McClay et al., 2005). There is only one known example of the cytochrome P450 family that can oxidize indole so far, which is a mutant of cytochrome P450_{CAM} (Li et al., 2000). The cytochrome P450 from ENV421 is the first native cytochrome P450 known to oxidize indole.

A second type of substrate is R-Limonene, cymene and 4-ethyltoluene. This substrate has two side chains, one of which is a methyl group and another is a short side chain at its *para*-position. There are several other studies of limonene oxidation by bacterial oxygenases, including CYP153 from *Mycobacterium* sp. strain HXN-1500 (van Beilen et al., 2005). Each oxygenase yielded a variety of mixtures of hydroxylated products (Figure 43, Table 10). CYP153 is unique among these enzymes in that it produces only perillyl alcohol from R-limonene. In addition to this position specificity, the reaction is also stereospecific. S-limonene could not be oxidized by this enzyme.

After an oxidation of a methyl side chain of R-limonene was observed, a variety of substrates with a methyl side chain were tested to see if they could also be oxidized by

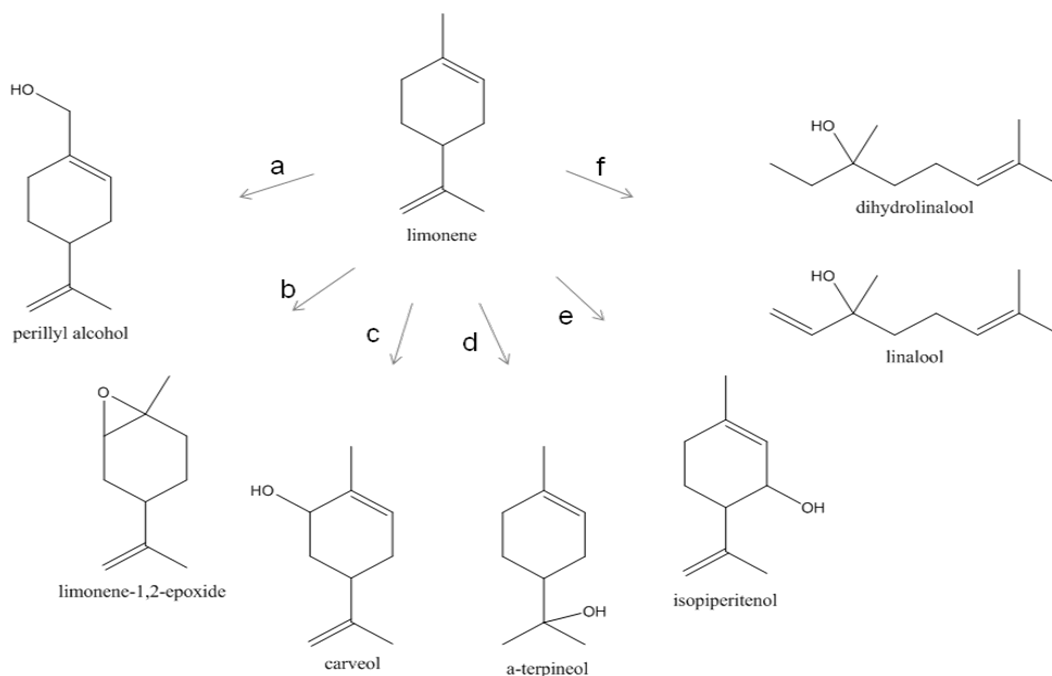


Figure 43. **Enzymatic oxidation product of limonene.** Limonene can be oxidized to a) peril alcohol b) Limonene 1,2 epoxide c) carveol d) α-terpineol e) isopiperitenol f) linalool and dihydro linalool. The list of enzymes known to oxidize each reaction is summarized in Table 10.

Table 10. **The list of known limonene hydroxylases.**

Organisms	Limonene oxidation products	References
Prokaryotes		
<i>Rhodococcus erythropolis</i> strain DCL14	Limonene 1,2-epoxide	Van der Werf et al., 1999
<i>Enterobacter cowanii</i>	Linalool, dihydrolinalool, perillyl alcohol, α-terpineol, γ-terpineol	Yang et al., 2007
<i>Pseudomonas gladioli</i>	(+)-α-terpineol and (+)-perillic acid	Cadwallader et al., 1989
<i>Bacillus stearothermophilus</i> BR388	Carveol, perillyl alcohol, α-terpineol	Cheong et al., 2000
Eukaryotes		
<i>Arxula adenivorans</i> and <i>Yarrowia lipolytica</i>	Perillic acid	Van Rensburg et al., 1997
<i>Trichosporon</i>	Isopiperitenone	Van Rensburg et al., 1997
<i>Mentha x piperita</i>	(-)-trans-isopiperitenol	Lupien et al., 1999
<i>Aspergillus cellulosa</i> M-77	(+)-isopiperitenone, (+)-limonene-1,2-trans-diol, (+)-ciscarveol and (+)-perillyl alcohol isopiperitenol and α-terpineol	Noma et al., 1992

ENV421 CYP153. Although the methyl group of the cymene and 4-ethyltoluene was oxidized, a methyl group of *p*- or *m*-xylene was not oxidized. The differences between substrates that can be oxidized and ones that cannot be oxidized are length of the side chain at the *p*-position, relative to the methyl group. Cymene has isopropyl group and 4-ethyltoluene have ethyl group at the *p*-position. *p*- and *o*-xylene have a methyl group as a second side chain. It is possible to conclude that methyl side chain can be oxidized when the molecule has another side chain whose length is longer than 2 carbon atoms.

The third type is benzene with a linear alkyl side chain. Propylbenzene, *n*-butylbenzene, pentylbenzene, hexylbenzene, heptylbenzene, and octylbenzene were oxidized by cytochrome P450 from strain ENV421. 5-benzylpentanol, benzene hydroxylated at the terminal carbon of pentyl side chain, was commercially available and run on GC-MS. Its retention time and fragmentation pattern of MS were identical to oxidation product of pentylbenzene formed by cytochrome P450 from strain ENV421. The same result was obtained with 4-benzylbutanol, and 3-benzylpropanol. The alcohol form of alkylbenzenes were not available for hexylbenzene, heptylbenzene, and octylbenzene, however, based on the result seen in propylbenzene, butylbenzene and pentylbenzene, oxidation of these alkylbenzenes must also happened at the terminal carbon of the side chains. The GC-MS pattern also implies this possibility. When the chain length is shorter (C₂: ethylbenzene), longer (C₁₀- longer: 1-phenyldecane), or branched (*sec*, *iso*, or *tert*-butylbenzene, neopentylbenzene), side chain could not be oxidized. The failure to oxidize these bulky, branched side chains is probably due to a steric hindrance.

Thus, CYP153 from strain ENV421 has a unique substrate range and specificity for hydroxylation. Surprisingly, despite its high expression in cells grown on propane, propane or 1,4-dioxane oxidation activity by this enzyme could not be detected by biotransformation assay. The data confirms that cytochrome P450 from strain ENV421 do not oxidize 1,4-dioxane when it is heterologously expressed in *E. coli*. Due to lack of genetic tools to construct knockout mutant of this enzyme, its involvement in 1,4-dioxane oxidation in strain ENV421 is not yet clear.

Two subunits of a 4-component diiron monooxygenase complex were identified and their sequences were resolved in strain ENV421. The protein sequence of the α -subunit showed a high similarity to that of putative propane monooxygenases. It showed highest similarity to propane induced monooxygenase in *Mycobacterium* sp. TY-6 (93% identity).

The two PMO whose propane oxidation capability was verified by gene knockout are from *Rhodococcus* sp. RHA1 and from *Gordonia* sp. strain TY-5. The PMO in ENV421 and TY-6 form a cluster distinct from these characterized propane monooxygenases, sharing only less than 30% sequence identity with the former two genes (Figure 39). Gene organization also differs between the two clusters. In strain ENV421 and TY-6, gene order is *prmADCB*, while in other species, it is *prmABCD* (*prm*, *A*, *B*, *C*, and *D*: large subunit, reductase, coupling protein and small subunit, respectively).

A reductase and a coupling protein of PMO could not be identified. The heterologous expression of two known subunits in *E. coli* did not yield 1,4-dioxane nor propane oxidation activity.

Four alcohol dehydrogenases were identified in strain ENV421. The 42 kDa band of propane induced proteins in SDS-PAGE (zinc-ADH1) matched N-terminal sequences of a family of zinc-containing alcohol dehydrogenases. The enzyme identified by degenerate primers based on sequences of these zinc-containing alcohol dehydrogenases identified another enzyme (zinc-ADH2) whose homologs form a separate cluster from zinc-ADH1 homologs (Figure 42).

The zinc-alcohol dehydrogenases in *Rhodococcus erythropolis* PR4, *Mycobacterium* sp. strain PYR-GCK, and *M. marinum* M, share 49% of their protein sequence with zinc-ADH2 and also are present in close proximity to cytochrome P450 CYP153 (Figure 21). Interestingly, these cytochrome P450's are similar to the cytochrome P450 identified in strain ENV421.

Two other alcohol dehydrogenases (Adh2, Adh3) are homologs of two 2-propanol dehydrogenases in another propane degrader, *Gordonia* sp. TY-5. In strain TY-5, propane is oxidized at the sub-terminal position, forming 2-propanol. Three propane inducible alcohol dehydrogenases were identified in this strain (*adh1*, *adh2*, and *adh3*). In strain TY-5, the *adh1* gene is located immediately downstream of the propane monooxygenase genes. *adh1* is the primary dehydrogenase for 2-propanol metabolism and is shown to be involved in growth on propane and 2-propanol. *adh2* and *adh3* are also possibly involved in 2-propanol oxidation. *adh2* and *adh3* are expressed in the cells during growth on 2-propanol.

In strain ENV421, only *adh2* and *adh3* were identified using primers that identified the three *adh* genes in strain TY-5. Neither *adh2* nor *adh3* were expressed in propane grown cells in ENV421. Our preliminary experiment showed that strain ENV421

can grow on 1-propanol but not on 2-propanol. The lack of expression of *adh2* and *adh3* may be a reason for its lack of ability to metabolize 2-propanol.

While propane monooxygenase in TY-5 transforms propane to 2-propanol, propane is likely transformed to 1-propanol in strain ENV421. The lack of *adh1* and two essential subunits of diiron monooxygenase type PMO may indicate the possibility of involvement of a different propane utilization system in strain ENV421. Thus, despite the high sequence similarity between alpha subunits of putative PMO in TY-5 and ENV421, PMO in ENV421 may not be important for propane utilization. Metabolism of 1-propanol in strain ENV421 is most likely catalyzed by one of the above mentioned zinc-type alcohol dehydrogenases.

Conclusion:

Strain ENV421 possesses all three oxygenases that we investigated. All of these enzymes are also expressed in propane grown cells. Since mutagenesis of these oxygenases using homologous recombination is not possible, involvement of these enzymes in propane and 1,4-dioxane oxidation was examined by heterologous expression in an *E. coli* host. Alkane monooxygenase and cytochrome P450 exhibited hydroxylation activity in *E. coli*. However, no 1,4-dioxane oxidation activity was observed.

Due to a different position specificity of propane oxidation in *Gordonia* sp. TY-5 and ENV421, it is proposed that the propane utilization system in ENV421 differs from the characterized system in strain TY-5. Hence it may utilize a novel enzyme for propane oxidation, which has not yet been characterized.

4.0 1,4-dioxane oxidation in *Pseudonocardia* sp. strain ENV478

Abstract:

Strain ENV478 oxidizes 1,4-dioxane after growth on THF. Degradation of 1,4-dioxane also occurs after growth on other substrates, such as lactate, sucrose and isopropanol, albeit at a low rate. Based on this observation, it is predicted that the enzyme responsible for 1,4-dioxane degradation is constitutively expressed at a low level and that THF induces its expression.

Because putative 1,4-dioxane oxygenase is constitutively expressed in strain ENV478, identification of the enzyme as a differentially expressed protein using SDS-PAGE was not applicable. Thus, we looked for candidate genes by PCR. The presence of *alkB*, cytochrome P450 and soluble diiron monooxygenase genes in strain ENV478 were screened by PCR using degenerate primers. The soluble diiron monooxygenase identified in ENV478 had high sequence similarity to THF-induced monooxygenase found in *Pseudonocardia* sp. strain K1. Thus, the focus of our project with this bacterium was on putative THF monooxygenase. The analysis of the transcription pattern showed that the gene cluster containing THF monooxygenase subunits (*thm* cluster) was constitutively expressed and its expression is up-regulated after growth on THF. Gene knockdown experiments provided direct evidence that the *thm* gene cluster is important for THF and 1,4-dioxane degradation in strain ENV478.

4.1 Sequence analysis of 16S rRNA gene in *Pseudonocardia* sp. strain ENV478

The 16S rRNA sequence of strain ENV478 showed that it belongs to the gram positive genus *Pseudonocardia* (Figure 2). It shares 97% sequence identity to the known THF degrading *Pseudonocardia* sp. strain K1. Both strains can grow on THF and cometabolically oxidize 1,4-dioxane, which lead to the hypothesis that the two organisms use the same sets of enzymes for THF and 1,4-dioxane oxidation.

4.2 Identification and analysis of putative tetrahydrofuran monooxygenase in *Pseudonocardia* sp. strain ENV478

4.2.1 Sequence analysis of tetrahydrofuran monooxygenase gene cluster in *Pseudonocardia* sp. strain ENV478

PCR reactions using degenerate primers to amplify a part of the α -subunit of soluble diiron monooxygenase yielded one PCR product. DNA sequencing revealed high similarity to the α -subunit of a putative tetrahydrofuran monooxygenase found in *Pseudonocardia* sp. strain K1. Because of this high sequence similarity, multiple specific primer sets for the entire operon were designed based on the sequence of strain K1. Combined with inverse PCR, a DNA sequence of an approximately 10 kb region was obtained.

The set of genes that are present in the 10 kb fragment is summarized in Table 11 and Figure 44. In summary, *ORFy* is a short open reading frame with unknown

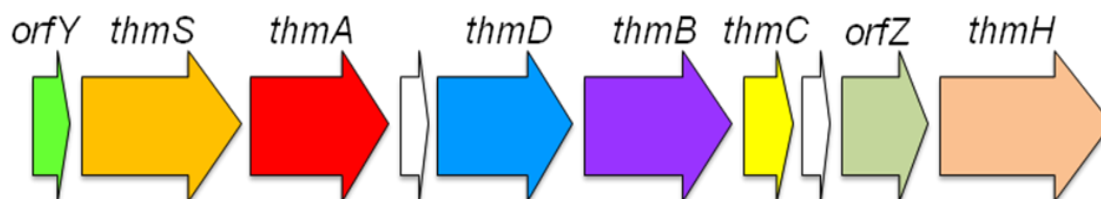


Figure 44. **Gene composition and gene organization of an operon containing putative THF monooxygenase and dehydrogenases in *Pseudonocardia* sp. strain ENV478.**

The list of genes present in this cluster is summarized in Table 11.

Table 11. **List of genes identified in *thm* gene cluster and their predicted functions.**

Gene	Amino acid residues	Molecular mass (kDa)	GC%	Predicted functions
<i>orfY</i>	107	11.8	59	Unknown
<i>sad</i>	500	53.5	61	Succinate semialdehyde
<i>thmA</i>	545	62.5	63	THF mO- α subunit
<i>thmD</i>	360	39.9	56	THF MO oxidoreductase
<i>thmB</i>	346	39.3	61	THF MO- β subunit
<i>thmC</i>	117	12.5	59	THF coupling protein
<i>orfZ</i>	221	22.3	58	Unknown
<i>aldH</i>	479	51.5	59	Putative 4-hydroxybutyrate dehydrogenase

function. No homologues are found in other operons containing diiron monooxygenases. *Thm ORFy* homologues are found in the operon for ethyl tert-butyl ether (ETBE) oxidation pathways in *Ralstonia eutropha* JMP134 (Chauvaux et al., 2001). In the ETBE operon, the hydroxylase is cytochrome P450. Although its function is unknown, *EthD* is essential for ETBE hydroxylation. Another homologue is found in *Rhodococcus* sp. strain RHA-1, neighboring cytochrome P450 CYP116 also. Despite the differences in type of oxygenase (THF: diiron monooxygenase, ETBE pathway: P450), this gene may be important in THF hydroxylase activity also. *thmS* encodes succinate semialdehyde dehydrogenase, which is most likely involved in one of the downstream steps in the THF degradation pathway. *thmADBC* encode components of the monooxygenase complex, α -subunit, reductase, β -subunit, and coupling protein, respectively. *ORFz* is a putative membrane protein with unknown function. ThmH is a putative aldehyde dehydrogenase possibly oxidizing another substrate feeding into the THF degradation pathway, 4-hydroxybutyraldehyde.

The gene order of *thm* gene cluster in strain K1 and strain ENV478 are identical, and sequences are on average 98% identical.

4.2.2 THF-mediated induction of the THF monooxygenase gene in *Pseudonocardia* sp. ENV478

The expression pattern of putative THF monooxygenase in THF or succinate-grown cells was examined by RT-PCR and quantitative RT-PCR (Q-RT-PCR). The specific primers were designed to amplify approximately 800 and 150 bp fragments

within the β -subunit for RT-PCR and for Q-RT-PCR, respectively. The product length was the optimal length for each technique. The RT-PCR reaction showed that the gene was expressed not only in THF-grown cells but also in succinate-grown cells (Figure 45). Quantitative real time PCR was used to assess the quantitative difference in its transcript level in cells grown in THF, succinate, or glucose. Comparison of the relative transcript level in each sample was conducted by the method described in the paper by Liu et al. with some modifications (Liu et al., 2002).

The real-time PCR efficiencies of the reference gene (16S rRNA gene) and target gene (*thmB*) were calculated by first constructing a standard curve using a serial dilution of a DNA template. The plasmids containing 16S rRNA or *thmADBC* were used as a template. The fluorescence signal baseline and threshold were set automatically by the 7300 Real-Time PCR System (Applied Biosystems, Foster City, CA). The “Absolute expression” method was used to generate a Ct value for each sample. Ct cycles versus DNA input concentration were plotted to calculate the slope. The range of 1 to 2×10^4 copies of DNA template was used for constructing standard curve. Each graph exhibited a high linearity (Pearson correlation coefficient $r > 0.95$). The equation for the fitted lines for 16S rRNA and *thmB* primers are shown in Table 12. The corresponding real-time PCR efficiencies were calculated according to the equation:

$$E = 10^{[-1/\text{slope}]} \quad \dots \text{(equation 1)}$$

Although the amount of cDNA produced by the RT-PCR reaction should be proportional to the amount of mRNA present, the exact amount of cDNA transcribed from mRNA in the sample cannot be quantitatively determined. However, if it is possible to assume that the efficiency of the reverse transcriptase reaction is constant in each

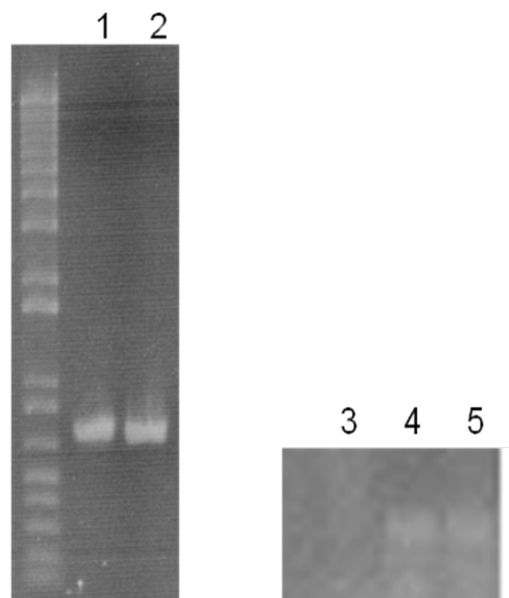


Figure 45. **RT-PCR analysis of *thmB* gene expression in THF or succinate grown ENV478.** Cells were grown on MSB media with THF (lane 1) or succinate (lane 2-5) as a sole carbon source. When cell density reached OD₆₀₀ 0.3, RNA was extracted and quantified. 5ng of RNA was used in each RT-PCR reaction. The DNA contamination in RNA extracted from succinate-grown cells was closely examined as following. Genomic DNA was used as a positive control (lane 4). While RT-PCR was performed completely ((1) 50°C for 30 min, (2) 30 cycles of 94°C for 30 sec, 55°C for 30 sec, 72°C for 30 sec and (3) 72°C for 5 min), it yielded a product (lane 5), but omitting a initial reverse transcriptase step (50°C for 30min), no RT-PCR product was produced.

Table 12. **Efficiency of primers for amplifying *thmB* or 16S rRNA gene in Quantitative RT-PCR reactions.**

Gene	Standard curve [*]	R value	E value ^{**}
<i>thmB</i>	$F(x) = -3.426668x + 36.330097$	R2=0.999840	1.958072
16S rRNA	$F(x) = -3.031619x + 30.455404$	R2=0.998729	2.137257

^{*}F(x) is a Ct value, x is a log [cDNA]

^{**}E value was calculated by an equation 1 : $E = 10^{[-1/\text{slope}]}$

sample, we can assume that the ratio of mRNA and resultant cDNA between two samples is the same.

Relative quantification of a target gene (*thmB*) in comparison to a reference gene (16S rRNA) was performed using the following equation explained by Liu and Saint, 2002 and Pfaffl et al., 2001.

$$\text{Ratio} = \frac{E_{\text{target}}^{\Delta C_{\text{target}}(\text{sample1} - \text{sample2})}}{E_{\text{ref}}^{\Delta C_{\text{ref}}(\text{sample1} - \text{sample2})}} \quad \dots \text{ (equation 2)}$$

This equation shows a mathematical model of a relative expression ratio in real-time PCR. E_{target} is the real-time PCR efficiency of the target gene transcript; E_{ref} is the real-time PCR efficiency of a reference gene transcript; ΔC_{target} is the Ct deviation of sample1 to sample2 of the target gene transcript; ΔC_{ref} is the Ct deviation of sample1 to sample2 of the reference gene transcript. The reference gene is a stable and secure unregulated house-keeping gene.

In our case, this equation can be written as:

$$\text{Ratio} = \frac{E_{\text{thmB}}^{\Delta C_{\text{thmB}}(\text{succinate or glucose} - \text{THF})}}{E_{16S}^{\Delta C_{16S}(\text{succinate or glucose} - \text{THF})}} \quad \dots \text{ (equation 3)}$$

The relative expression ratio of a *thmB* gene in each sample was calculated based on E and the Ct deviation of THF grown sample versus succinate or glucose sample, in comparison to a reference gene (16S rRNA). The result is summarized in Table 13. Using the equation, it was concluded that in THF-grown cells, the *thm* operon is up-regulated about 700 fold compared to glucose or succinate grown cells.

The molecular basis for up-regulation of the *thm* genes in THF grown cells was examined next. The transcriptional level of bacterial genes involved in carbon utilization

Table 13. ΔC_t values and relative amounts of *thmB* mRNA in *Pseudonocardia* sp. strain ENV478 cells grown on different carbon sources.

Growth substrate	$\Delta C_{t\text{target}}(\text{sample1} - \text{sample2})$ ^{*1}	$\Delta C_{t\text{thmB}}$ ^{*2}	$\Delta C_{t\text{16S}}$ ^{*3}	Ratio ^{*4}	Relative amount of <i>thmB</i> mRNA ^{*5}
THF				NA	730
Succinate	$\Delta C_t (\text{succinate} - \text{THF})$	5.86		201*	3.62*
Glucose	$\Delta C_t (\text{glucose} - \text{THF})$	5.98 ± 1.16	-1.27	602	1.21
THF + succinate	$\Delta C_t (\text{THF+succinate} - \text{THF})$	3.41 ± 0.679	-0.55	730	30.0
THF + glucose	$\Delta C_t (\text{THF+glucose} - \text{THF})$	6.71 ± 0.763	-1.1	24.3	1

^{*1} $\Delta C_{t\text{target}}$ is the C_t deviation of sample1 to sample2 of the target gene transcript; i.e. $\Delta C_t (\text{succinate} - \text{THF})$ is C_t value of real time RT-PCR reaction using RNA extracted from succinate grown cells minus C_t value of real time RT-PCR reaction using RNA extracted from THF grown cells.

^{*2} $\Delta C_{t\text{thmB}}$ is a C_t deviation of sample1 to sample2 of *thmB* gene transcript.

^{*3} $\Delta C_{t\text{16S}}$ is a C_t deviation of sample1 to sample2 of 16S rRNA transcript.

^{*4} Ratio = $E_{\text{thmB}}^{\Delta C_{t\text{thmB}}(\text{sample1-sample2})} / E_{\text{16S}}^{\Delta C_{t\text{16S}}(\text{sample1-sample2})}$: equation 2.

^{*5} Ratio^{*4} was standardized in relative to the value for THF + glucose.

can be controlled via catabolic repression or by induction. The quantitative PCR using a combination of substrates was used to directly assess the effect of different substrates on *thm* transcription. The cells were grown either solely on THF, succinate or glucose or on combination of THF + succinate or THF + glucose. The result is shown in Table 13. The amount of *thmB* transcripts in succinate, glucose or THF+ glucose grown cells were almost identical. While THF + glucose grown cells have almost the identical transcription level as cells grown on glucose only, THF + succinate grown cells have about 30 fold higher expression than cells grown on succinate only.

4.2.3 Transcript analysis of THF monooxygenase gene in *Pseudonocardia* sp. ENV478

In order to examine whether putative *thm* genes are transcribed in an operonic form, RT-PCR was performed using a primer set amplifying intergenic regions (Figure 46). The result showed that there were at least two polycistronic transcripts: one containing *ORFy* and *thmSADBC*, and another containing *ORFz* and *thmH*. Both transcripts are expressed in the presence of THF.

The RT-PCR reactions amplifying intergenic regions showed different intensities of bands. Lane 3 and lane 8 in figure Figure 46 are particularly fainter than bands in other lanes. PCR reactions using genomic DNA as a template showed high intensity bands for all of the reactions, assuring the quality of all of the primers used (data not shown). The low intensity in some RT-PCR reactions indicated the possibility that there are partial breaks in transcripts at these sites.

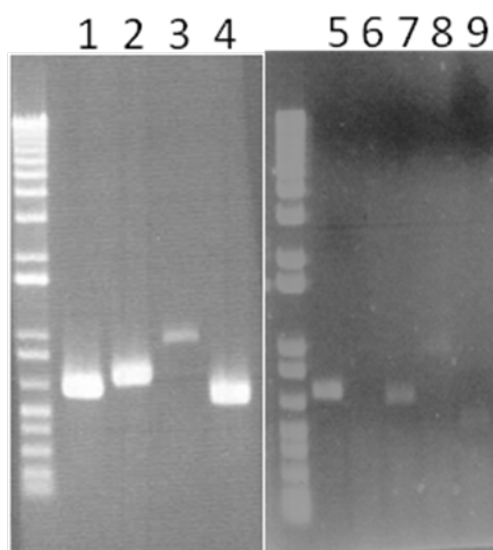
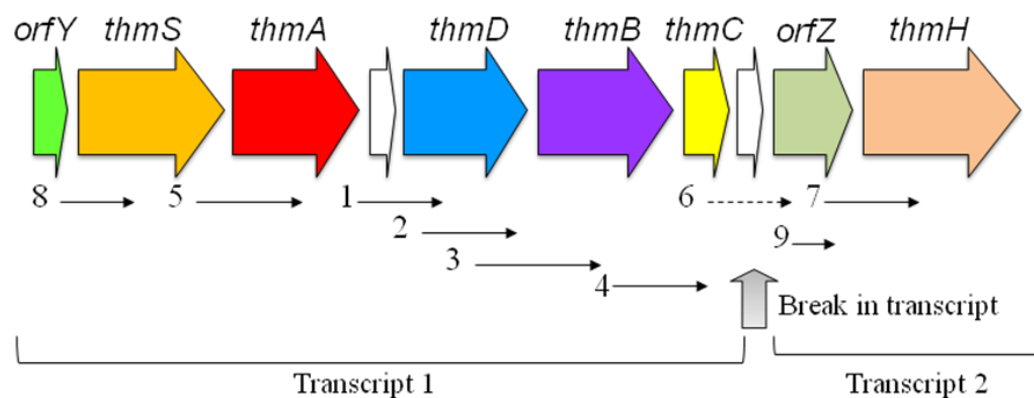


Figure 46. **RT-PCR analysis of THF-induced *thm* genes.** The RNA was extracted from THF-grown cells as described in Figure 36. The sets of primers were designed so that they will amplify the fragment spanning two neighboring genes. The products of PCR using each primer sets amplified: 1: *thmA-thmD*; 2: *thmA*; 3: *thmD-thmB*; 4: *thmB-thmC*; 5: *thmS-thmA*; 6: *thmC-orfZ*; 7: *orfZ-thmH*; 8: *orfY-thmS*; 9: *orfZ*. Although the PCR using genomic DNA as a template yielded products with high efficiency in all reactions (data not published), RT-PCR yielded high level (lane 1,2,4,5, and 7), low level (lane 3, 8 and 9) or no product (lane 6).

In order to examine whether there is a break in the transcript and also to verify the sequence of 5' end of each short transcript, 5' RACE assay was performed. The presence of 5' ends of mRNA in front of *ORFy*, *thmS*, *thmA* and *thmB* were tested with RNA extracted from THF-grown cells, and it was found that all four genes have 5' end of transcripts at about 100-150 base pairs upstream of the translational start site (Figure 47). Because each reaction did not yield multiple products, these ends are not likely to be a result of random RNA degradation during the extraction. Thus, the 5' end of transcripts identified at these positions is indicative of the presence of multiple transcripts with varying length and beginning. The sequences upstream of translation start site of *ORFy*, *thmS*, *thmA* and *thmB* were compared using BLAST2 program (Tatusova et al. 1999). The DNA sequences between -10 to -35 position of *orfY* and *thmS* transcripts exhibited high sequence similarity to each other (Figure 48). The DNA sequences of region from 40 to 70 bases upstream of *thmA* and *thmB* translational start site also shared similarity to one another. The biological roles of these conserved sequences are unknown.

The presence of hairpin structure immediately downstream of the *thm* cluster was identified by RNA secondary structure prediction program (Figure 49) (Brodsky et al., 1992). Interestingly, similar structure was also present immediately following *thmA*. These structures might have given rise to the partial termination of transcription at these sites. Conclusions on 5' RACE assay and inverted repeat analysis are summarized in Figure 50.

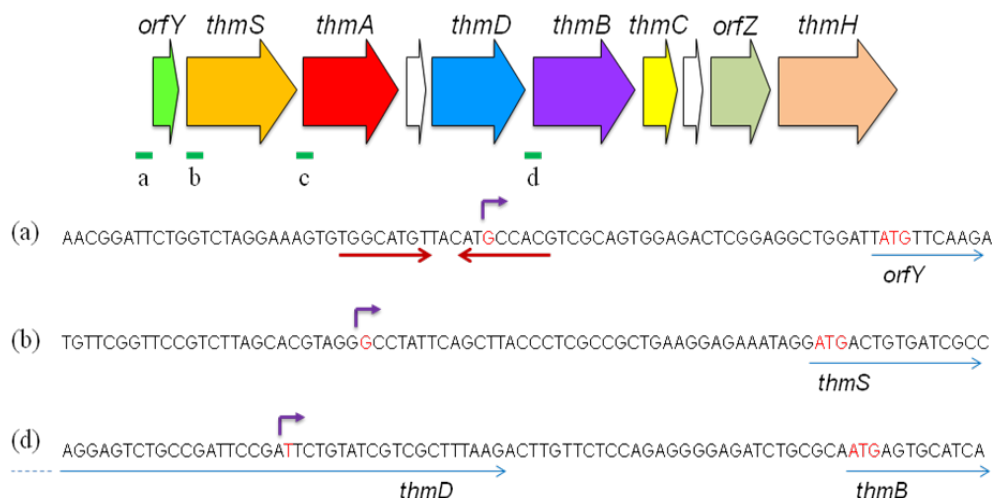


Figure 47. **The positions of 5' ends of mRNA identified by 5' RACE Assay.** The 5' RACE assay was performed using RNA extracted from THF-grown cells. Reverse primers were designed to bind sequences at 250bp downstream of the start codon for A) *orfY*, B) *thmS*, C) *thmA*, and D) *thmB*. RT-PCR with expected size was obtained for all positions. The sequence was successfully determined for reaction A, B and D. The ends of transcripts are labeled with gray arrows and translation start sites are labeled with blue arrows. The inverted repeat overlapping putative transcription start site of *orfY* is labeled with red arrows.

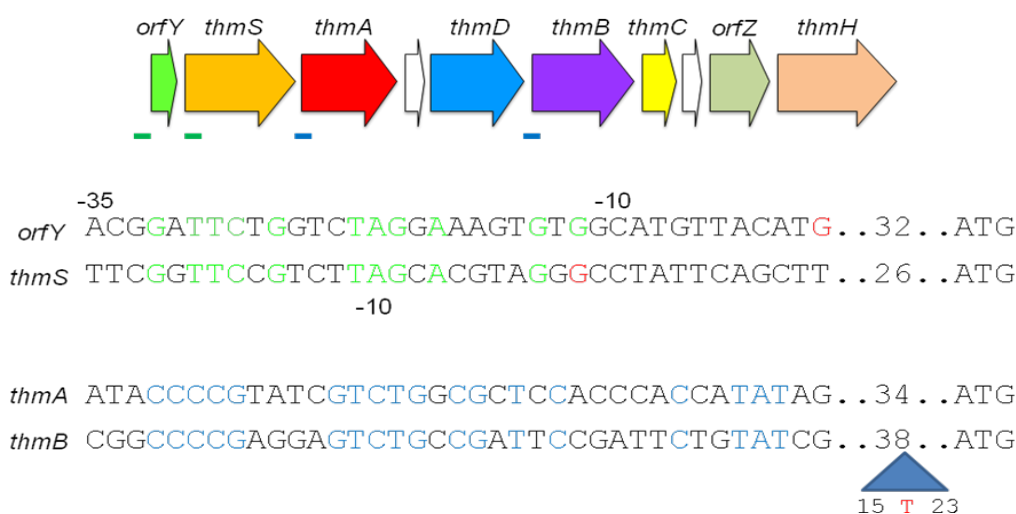


Figure 48. **Alignment of sequences upstream of *thm* genes in *Pseudonocardia* sp. strain ENV478.** The sequences upstream of *orfY*, *thmS*, *thmA*, and *thmB* translational start sites were aligned using BLAST2 program. The 5' ends of mRNA identified by 5' RACE assay were labeled in red. Bases conserved between two sequences were labeled in green (*orfY* and *thmS*) or blue (*thmA* and *thmB*).

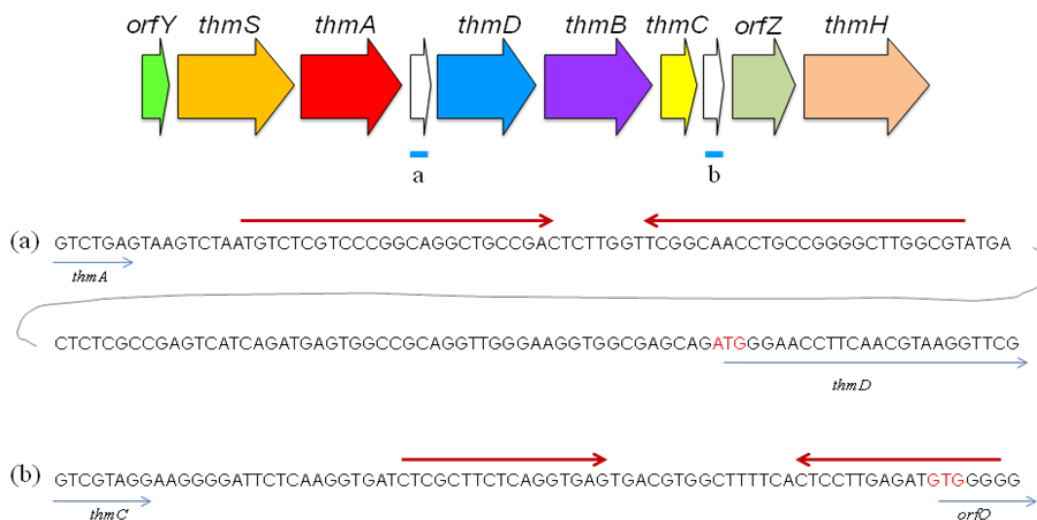


Figure 49. **The inverted repeats at downstream of *thmA* and *thmC* in *Pseudonocardia* sp. strain ENV478.** The translation start sites are labeled with blue arrows. The inverted repeats are labeled with red arrows.

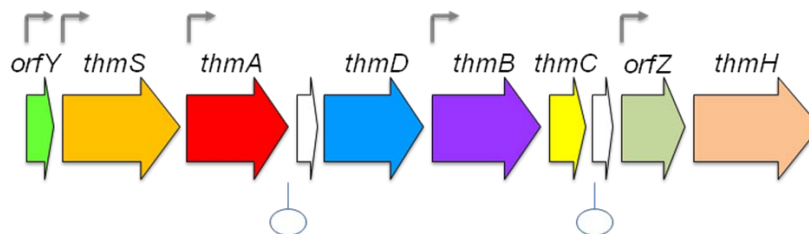


Figure 50. **Transcription pattern of *thm* gene clusters in *Pseudonocardia* sp. strain ENV478.** RT-PCR and Q-RT-PCR identified breaks in transcripts in front of *orfY*, *thmS*, *thmA*, *thmB* and *orfZ* (gray arrow). Two putative rho-independent transcription termination sites are present immediately downstream of *thmA* and *thmC*.

4.2.4 Analysis of the origin of multiple *thm* transcripts in

Pseudonocardia sp. strain ENV478

Next, we wanted to understand the controversy between operonic structure of transcripts found by intergenic RT-PCR and multiple 5' ends identified by 5'RACE assay. The first assay showed that mRNA transcribing ORFy, *thmS*, *thmA*, *thmD*, *thmB*, and *thmC* are transcribed from one cis-transcript. On the other hand, 5' RACE assay showed that there were 5' ends of mRNA in front of *ORFy*, *thmS*, *thmA* and *thmB*.

In bacteria, RNA degradation is carried out by 3'→5' exonuclease. The involvement of neither 5'→3' exonuclease nor endonuclease in RNA degradation in bacteria has been shown. Thus, the 5' end of a transcript cannot be a product/intermediate of the RNA turn over process. Rather, it must be made by a specific process and possible mechanisms that have yielded these 5'ends were examined next.

There are at least two possibilities of why there are multiple 5' ends of transcripts in the middle of the operonic transcript.

The first possibility is that there are multiple promoters starting at each 5'end. The operonic transcription pattern identified by RT-PCR reaction is thus a few run-off products of transcription from upstream. This possibility was examined first by sequence alignment. When upstream sequences of *orfY*, *thmS*, *thmA*, *thmB* and *orfZ* were aligned, no significant match was found. Next, various promoter prediction programs were used to examine whether there was any predicted transcription start site in these positions (<http://linux1.softberry.com/berry.phtml>). The transcription regulatory site was also

analyzed with program available online. Neither analysis predicted any of these sites in this operon.

Another possibility is that two long nascent transcripts are processed into smaller transcripts by RNaseE. mRNA maturation is a well known phenomenon in bacteria and it is one tactic to control gene expression from operonic transcripts (Allenby et al., 2004; Condon, 2003). In these cases, different stoichiometric amounts of each gene product from the operon are required. Bacteria can control the level of each gene by changing the amount of each transcript. First, nascent transcript is processed into smaller transcripts containing one or more genes by RNaseE. Then, a transcript whose gene product is not required at high level will be preferentially degraded, allowing it to be expressed at a lower level than the rest of the genes. Since the consensus sequence for RNaseE recognition site has not been identified, bioinformatic tools to locate the critical bases are not yet available. Thus, the following experimental approach was taken to distinguish the two possibilities.

Traditionally, RNA maturation is studied using Northern blot analysis. RNA maturation can be examined by monitoring the appearance of processed transcripts over time after transcription has been halted by antibiotics, such as rifampicin. The addition of rifampicin does not interfere with any cellular processes other than transcription, enabling us to examine the RNA processing without additional transcripts being produced. Recently, analysis of transcripts by quantitative RT-PCR has been attempted. In our study, a procedure done by Sowers (2006) was modified to add more accuracy.

First, cells were grown on THF as the sole carbon source and the transcription of mRNA in actively growing cells was stopped by addition of rifampicin. Total RNA was extracted from cells at 0, 2, 6 min after the addition of rifampicin.

RT-PCR was performed using sets of primers designed to amplify specific parts of *thm* transcripts as described in Figure 51. The positions of three target sites for RT-PCR are shown in Figure 52. Each set of primers amplify about 150 bp by PCR. The primers for *thmA* and *thmB* RT-PCR2 were constructed so that the forward primer binds upstream of the 5' end that was identified by the RACE assay, and the reverse primer binds downstream of the site. In an RT-PCR reaction, this primer set will yield a product with a long (nascent) transcript spanning the gene of interest and its upstream gene. The short transcripts, either digestion products or mRNA whose transcription started at the site, will not yield RT-PCR products (Figure 53). Thus, it can be said that a decrease in RT-PCR product is due to the disappearance of long nascent mRNA through RNA processing.

The primer set for *thmB* RT-PCR1 amplifies the middle of the *thmB* gene within which no putative promoters or RNA processing sites exist. A decrease in the number of RT-PCR product should have simply depended on non-specific cellular digestion of RNA. 16S rRNA was used as a control to standardize the amount of total RNA in each sample. It also served as another control for the rate of random RNA degradation.

In the first case, after transcription is halted, the amount of both long and short transcripts will decrease due to non-specific RNA degradation, but the ratio should stay relatively the same. With our RT-PCR reaction, it is expected that the ratio of RT-PCR-1 to RT-PCR-2 should remain almost constant.

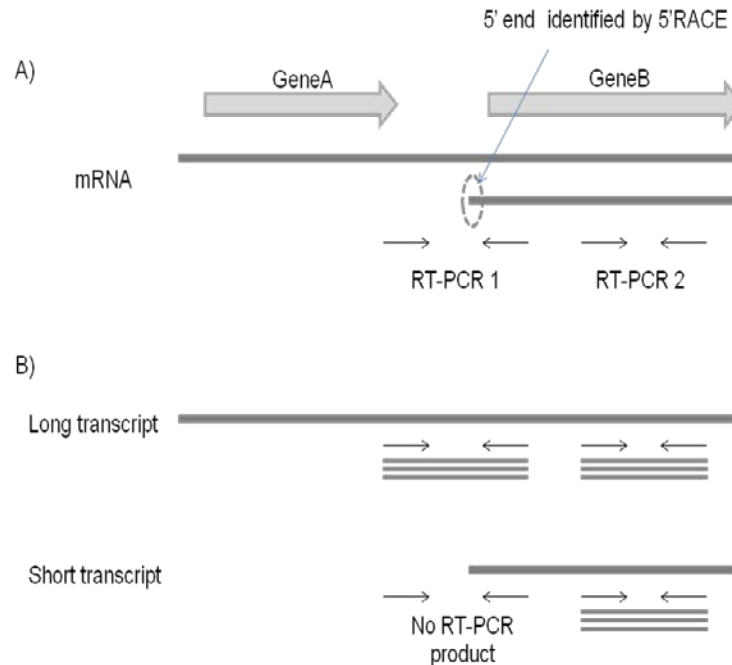


Figure 51. **The primer design for *thm* transcript analysis in *Pseudonocardia* sp. strain ENV478.** A) The positions for primers were chosen based on 5' ends of transcripts identified by 5' RACE assay. PCR1: The forward primer was designed for the sequence upstream of 5' end of transcript. The reverse primer was designed for the sequence downstream of 5' end. PCR2: Primers were designed to amplify an internal fragment of a gene. Each primer was designed to amplify approximately 300bp PCR product. B) The predicted RT-PCR products by the two primer sets using long transcript (as identified by RT-PCR experiment) or short transcript (as identified by 5' RACE assay). Primer set 1 can amplify product using long transcript but not with short transcript. Primer set 2 amplifies RT-PCR product with both type of transcript.

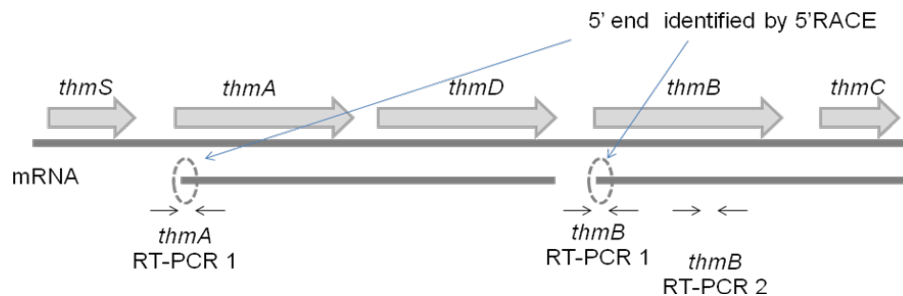


Figure 52. **The primers for *thm* transcript analysis of RNA fragmentation in *Pseudonocardia* sp. strain ENV478.**

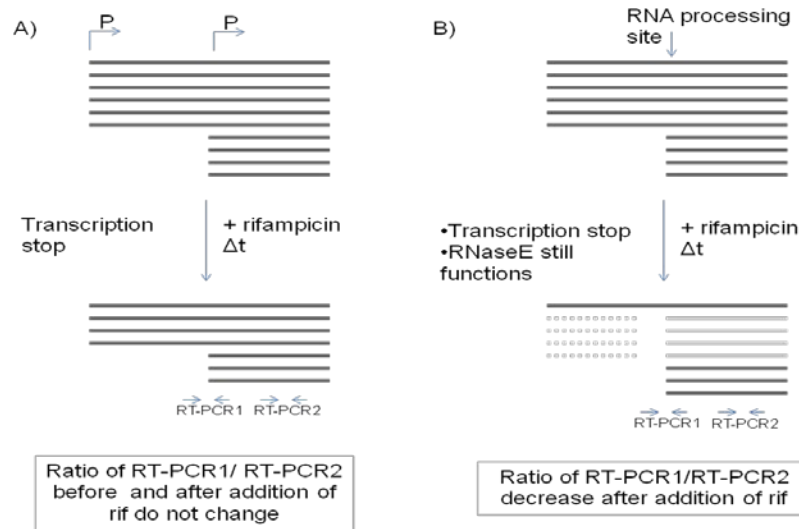


Figure 53. **The predicted result of RT- PCR reaction in two different scenario for the origin of multiple *thm* transcripts.** A) Scenario 1: The 5' end is a result of a transcription started at the promoter immediately upstream of a gene. After transcription is stopped by an addition of rifampicin, all of the transcription is stopped. The amount of long, operonic transcript relative to the shorter transcript with identified 5' end do not change before and after the addition of rifampicin. The reduction in absolute amount of each type of transcript should only depend on random RNA degradation. B) Scenario 2: The 5' end is created as a result of RNA processing by RNaseE. After the addition of rifampicin, RNaseE is still functional and RNA processing will still progress. The relative amount of shorter transcript having defined 5' end will increase compared to long, operonic transcript. Since primer set 1 do not yield a RT-PCR with short transcript as a template, RT-PCR product of PCR1 compared to PCR2 decrease over time after rifampicin addition.

Table 14. **Efficiency of primers for amplifying 16S rRNA and intragenic or intergenic fragment of *thm* genes in Quantitative RT-PCR reactions.**

Target	Standard curve	R ²	E value
16S rRNA	$F(x) = -3.032x + 30.46$	0.9987	2.04
<i>thmB</i> RT-PCR2	$F(x) = -3.426x + 36.33$	0.999840	1.96
<i>thmB</i> RT-PCR1	$F(x) = -3.412x + 45.11$	0.999	1.96
<i>thmA</i> RT-PCR1	$F(x) = -1.702x + 31.04$	1	3.87

*F(x) is a Ct value, x is a log [cDNA]

**E value was calculated by an equation 1 : $E=10^{[-1/\text{slope}]}$

For the second scenario, the long transcripts will be digested to smaller transcripts by RNaseE, the ratio of shorter transcripts compared to long transcripts will increase. In our RT-PCR experiment, the amount of RT-PCR-2 is expected to remain the same but the RT-PCR-1 should decrease since RT-PCR-1 cannot yield a product from short transcripts. Thus the ratio of RT-PCR-1 to RT-PCR-2 is expected to decrease over time.

The standard curve for Ct value vs template concentration for each primer set was constructed. The E value was calculated as described in equation 1 (Table 14).

Relative quantification of a t_0 sample versus t_2 or t_6 samples were performed using equation 4.

$$\text{Ratio} = \frac{E_{\text{thmB}}^{\Delta Ct_{\text{thmB}}(t_0 - t_m)}}{E_{16S}^{\Delta Ct_{16S}(t_0 - t_m)}} \dots (\text{equation 4})$$

The relative expression ratio of a target gene is calculated based on E and the Ct deviation of sample (t_2 or t_6 sample) versus control (t_0 sample), relative to that of a reference gene (16S rRNA).

E_{thmB} is the real-time PCR efficiency of the target gene (*thmB*) transcript; E_{16S} is the real-time PCR efficiency of a reference gene (16S rRNA) transcript; ΔCt_{thmB} is the Ct deviation of t_0 to t_2 or t_6 samples of the *thmB* gene transcript; ΔCt_{16S} is the Ct deviation of t_0 to t_2 or t_6 samples of the 16S rRNA gene transcript.

The rate of decrease in intergenic RT-PCR product (RT-PCR-1) in comparison to intragenic RT-PCR (RT-PCR-2) can be seen in Figure 54-A. While the absolute amount of intragenic RT-PCR-1 decreased to only 89% at 6 min after ceasing transcription, intergenic RT-PCR2 amplifying upstream of *thmB* and *thmA* decreased to 21% and 49% of the t_0 sample, respectively. The ratio of RT-PCR-1 to RT-PCR-2 becomes smaller over

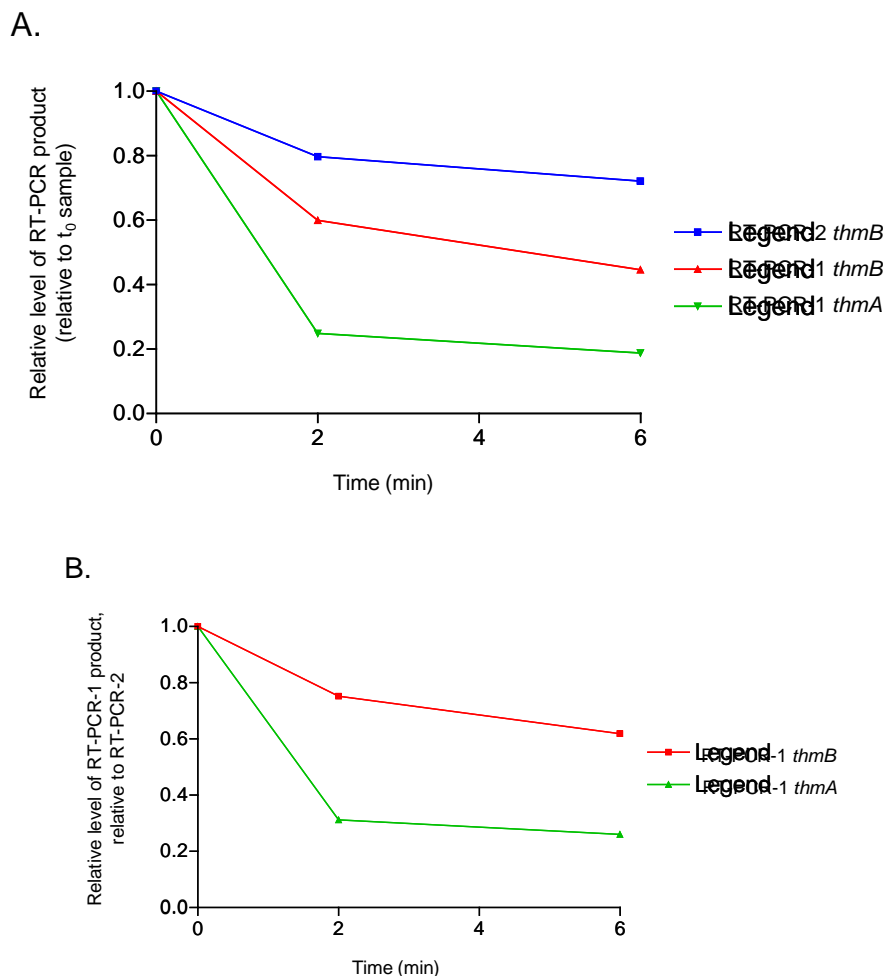


Figure 54. **Relative level of *thmA* and *thmB* intergenic region and *thmB* intragenic region 0,2,and 6 min after halting transcription by an addition of rifampicin.** A) The relative amount of RT-PCR-1 for intergenic region upstream of *thmA* (pink) and *thmB* (green), and RT-PCR-2 for intragenic region of *thmB* (dark blue). Amount of each RT-PCR product was normalized to its own t_0 sample. B) The ratio of RT-PCR-1 for *thmA* (red) or *thmB* (blue) to RT-PCR-2. The relative amount of each RT-PCR-1 product in graph-A was divided by RT-PCR-2 value of the sample from the same time point.

time in both genes, indicating that the difference between short transcripts and long transcripts becomes bigger over time (Figure 54-B). This result matches our second hypothesis that shorter transcripts are made by RNA processing of long transcripts by RNaseE. The above mentioned conserved sequences upstream of *orfY*, *thmS*, *thmA* and *thmB* may be involved in the processing.

4.2.5 Genetic manipulation of *Pseudonocardia* sp. ENV478

Several gram negative and gram positive shuttle vectors were tested for their ability to replicate in strain ENV478. Among the many plasmids tested, only *Rhodococcus* shuttle vector pNV18 can replicate in strain ENV478. The transformation efficiency was low (approximately 1 transformant per 1 µg plasmid) when standard transformation protocols were followed. Several different transformation conditions were attempted to increase the efficiency. The efficiency was highest when cells were grown on rich media and electroporation was carried out at room temperature, rather than 4°C. At this condition, the transformation efficiency became as high as 200 transformant per 1 µg plasmid DNA. Cells were incubated at 30°C without shaking for 3 hours before being plated on TSA with 50 mg/l kanamycin.

4.2.6 Gene knockdown of *thmB* in *Pseudonocardia* sp. strain ENV478

The knockdown of gene expression using antisense technology is widely used in *C. elegans*. The effective mRNA concentration is reduced by synthetic RNA introduced

into the organisms where synthetic RNA is designed to be complementary to target mRNA. mRNA and synthetic RNA will form double stranded RNA (dsRNA) which will be degraded, thus the effective concentration of mRNA is reduced to almost zero, essentially knocking out the gene of interest.

The reduction of mRNA level by introduction of complementary RNA has also been observed in bacteria. The usage of antisense RNA technology to knockdown gene expression has recently started to be used for studies of bacteria in which no other genetic tools are available or when the gene of interest is essential.

In this project, a PCR fragment spanning -50 to +200 of the α and β subunit of THF monooxygenase was amplified. It was cloned so that it will be transcribed in the direction opposite to the mRNA. The promoter of kanamycin gene in pNV19 was used to express the antisense RNA.

First, the effect of knockdown of *thmB* gene expression on ENV478's growth on THF was examined. Cells were grown on succinate overnight and then transferred to fresh medium containing only THF as a carbon source. The growth curve is shown in Figure 55. A wild-type strain of ENV478 (WT) and a strain carrying pNV19 vector (vector control) started to grow immediately after they were transferred to fresh medium. Their initial growth pattern was exponential without a lag. *thmA* and *thmB* knockdown mutants showed no growth for the first 40 hours. This is at this point when wildtype and vector control strains began the stationary phase growth.

Then the effect of *thmA* gene knockdown on 1,4-dioxane degradation was analyzed. Vector control and mutant strains were incubated with a mixture of THF and 1,4-dioxane in phosphate buffer. The amount of 1,4-dioxane and THF left in the buffer

was measured by GC-FID. THF and 1,4-dioxane were utilized completely by vector control strain within 108 and 156 hour, respectively (Figure 56). Incubation of THF and 1,4-dioxane with *thmA* knockdown strain left 40% and 32% of provided substrates non-degraded even after 204 hour of incubation. The low but significant level of THF and 1,4-dioxane degradation by *thmA* knockdown strain is possibly due to incomplete inhibition of *thmA* translation.

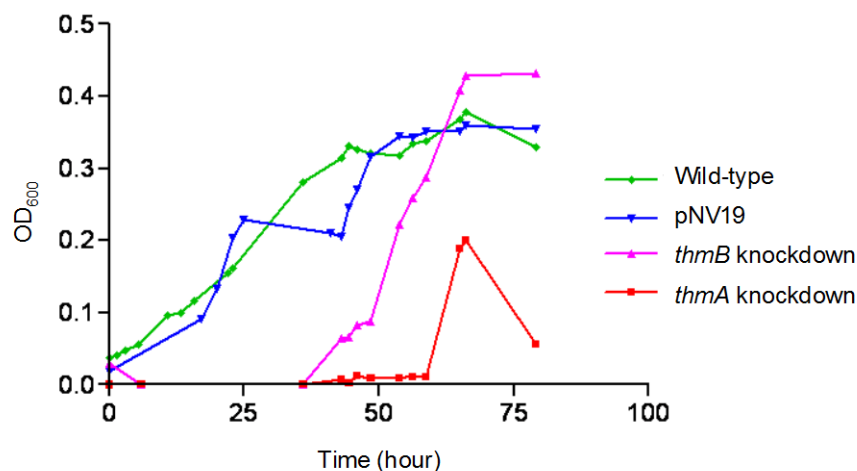


Figure 55. **The growth curve of wild-type and *thmA* and *thmB* knockdown mutant strains of *Pseudonocardia* sp. strain ENV478 on THF.** Cells were grown on MSB with 10mM succinate as a sole carbon source until it reached exponential phase. Cells were harvested and washed before added to fresh media containing 10mM THF as a sole carbon source. The cell density (OD₆₀₀) was observed for over 3 days. Four strains of bacteria was tested : a wildtype strain (blue), wildtype strain with pNV19 (green line), *thmA* knockdown mutant (red), and *thmB* knockdown mutant (pink).

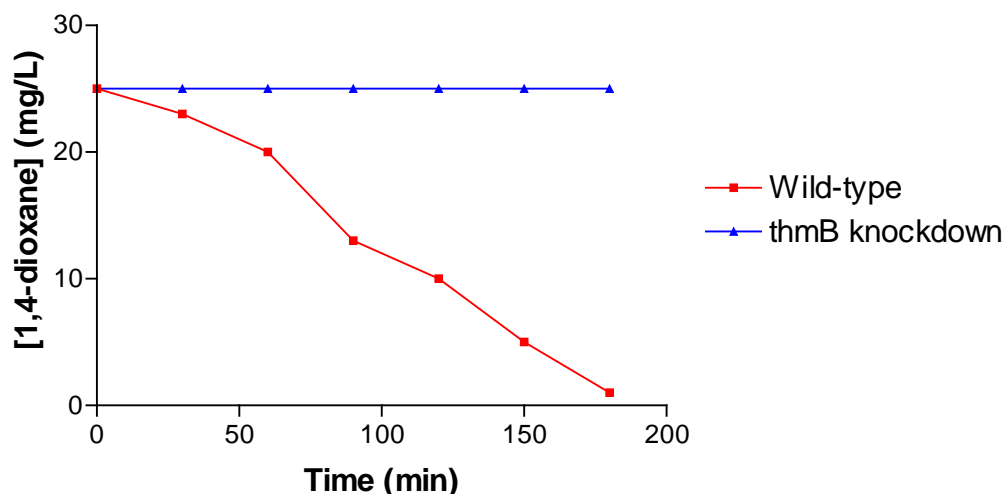


Figure 56. **1,4-dioxane degradation by wild-type and *thmB* knockdown mutant strain of *Pseudonocardia* sp. strain ENV478.** The cells were grown on MSB media with 10mM succinate until it reached OD₆₀₀ 0.5. THF was added to induce the *thm* genes and cells were incubated until OD₆₀₀ 1.0. The disappearance of 1,4-dioxane was monitored by gas chromatography. Two strains of bacteria was tested: wild-type strain and *thmB* knockdown mutant strain of *Pseudonocardia* sp. strain ENV478.

4.3 Alkane monooxygenase (AlkB) gene cluster in *Pseudonocardia* sp. strain

ENV478

The primer developed for amplifying the 550 bp internal fragment of *alkB* were used to examine whether ENV478 carries *alkB*. It did not yield a PCR product.

4.4 Identification and analysis of cytochrome P450 gene cluster in

Pseudonocardia sp. strain ENV478

.

The degenerate primers for cytochrome P450 amplified a PCR product. The direct sequencing of the PCR product yielded multiple peaks at various positions, indicating the presence of multiple cytochrome P450 genes in strain ENV478.

The RT-PCR reaction using RNA extracted from THF-grown strain ENV478 showed that cytochrome P450 was expressed, although the intensity of the band on agarose electrophoresis was low (data not shown). The RT-PCR product was cloned into the pGEM-T vector, and several of these clones were sequenced. Several showed highest similarity to a cytochrome P450 from *Mycobacterium smegmatis* strain MC2 155 (ABK70288) and another set of sequences were most similar to RubU of *Streptomyces collinus* (AAM97370). Neither of these strains are known to oxidize THF, 1,4-dioxane, or any other hydrocarbon.

4.5 Discussion

Strain ENV478 utilizes THF as a sole carbon source and oxidizes 1,4-dioxane through a cometabolic process. A monooxygenase whose gene expression pattern differs in the presence or absence of THF was identified. The DNA sequence of a 10 kb fragment containing genes possibly involved in the THF degradation pathway was verified. The gene order and DNA sequence showed high homology to a THF-induced monooxygenase found in *Pseudonocardia* sp. strain K1.

The operonic transcription pattern of the 10 kb fragment was examined by RT-PCR. It showed that the genes are transcribed in two cistrons. Both of these operons are expressed in THF-grown cells. This is different from what was observed in strain K1, where the second operon, containing *thmH*, was not expressed in THF-grown cells. In strain K1, *thmH* gene was expressed only after the growth on 1, 4-butanediol. 1,4-butanediol is proposed to be oxidized by ThmH and its oxidized product is metabolized through the second half of THF degradation pathway.

The *thmB* transcripts are also expressed in cells grown on carbon sources other than THF. The quantitative differences of *thmB* transcripts in THF grown cells and in succinate grown cells were examined with Q-RT-PCR. There is about a 700 fold higher level of *thmB* transcript in THF-grown cells than in succinate-grown cells.

Both RT-PCR and quantitative RT-PCR experiments indicated that the *thm* operon is transcribed constitutively at a low rate in cells grown on carbon sources other than THF. This result is consistent with our earlier observation from the whole cell 1,4-dioxane oxidation assay. In the assay, 1,4-dioxane can be degraded at a low rate after growth on non-THF carbon sources. The transcription level of the *thm* genes in this

condition is low. On the other hand, the rate of degradation is faster after the growth on THF, and in the same condition, the level of transcription of the *thm* operon is high.

This result is different from what was observed in *Pseudonocardia* strain K1, where *thmB* and other monooxygenase components were expressed only after growth on THF (Thierner et al., 2003). The transcription of these genes was strictly turned off in succinate-grown cells. The molecular basis for this different transcription pattern is not known.

Promoter sequence analysis using bioinformatic tools did not show that *thm* operon contain a standard operator sequence. This is probably because of high sequence divergence of ENV478 promoters from that of *E. coli* and other bacterial promoters. Thus, promoter assay using promoter-less vector in *E. coli* was not attempted. Instead, quantitative PCR using a combination of substrates was used to directly assess the effect of different substrates on *thm* transcription.

The Q-RT-PCR experiments using combination of substrates showed interesting patterns. Cells grow on glucose only or grow on THF and glucose showed the same transcription level of *thmB*. The addition of THF to glucose media did not have any effect on the transcription level of *thmB* implies the catabolic repression of *thmB* transcription by glucose. On the other hand, additions of THF to succinate media increase the *thmB* transcription level at 30 fold. This result implies the induction of *thmB* transcription by THF in succinate grown cells. However, it did not completely restore the induction level observed in cells grown on THF only, implying the repression of *thmB* transcription by succinate. Succinate, however, does not seem to repress the *thmB* transcription as

effectively as glucose. Thus there seems to be a complex mechanism for *thm* gene regulation.

In strain ENV478, RT-PCR products spanning some intergenic sites appeared low intensity in comparison to other products in gel electrophoresis (Figure 46). 5' RACE assay identified 5' ends of transcripts in front of *ORFy*, *thmS*, *thmA* and *thmB*. In *Pseudonocardia* sp. K1, the transcription pattern of *thm* operons were examined by Northern blot (Figure 57). The result showed that the first *thm* operon was also encoded by multiple transcripts with different length, starting in front of *ORFy*, *thmS*, *thmA* and *thmB*. Based on our 5' RACE assay and K1's Northern blot, the collection of transcripts that might be present in strain ENV478 was proposed as shown in Figure 58.

Next, the mechanism of producing various transcripts was examined using Q-RT-PCR. Using different sets of primers, changes in the amount of long (unprocessed) transcripts and short (possibly processed) transcripts were examined in cells whose transcription is halted. While the amount of long transcripts did not change drastically, the amount of short transcripts increased significantly. Because this increase cannot be due to the newly synthesized transcription, it is due to maturation of nascent RNA by RNaseE.

Although this experiment cannot completely eliminate the possibility that there are other mechanisms that produced multiple transcripts, it can be said that maturation is certainly taking place.

This result implied that possibly non-stoichiometric amounts of each gene product are required to form the enzyme complex. The biochemical analysis of this enzyme complex has not been performed, but based on the information of known soluble diiron

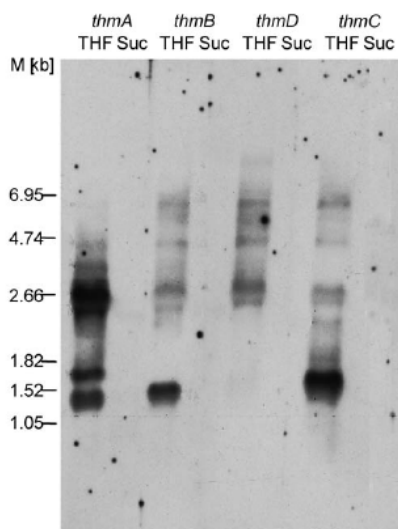


Figure 57. Transcription pattern of *thm* gene clusters in *Pseudonocardia* sp. strain K1 (Thierner et al., 2003). Multiple THF-induced transcripts containing the *thm* genes were identified by northern blot analysis.

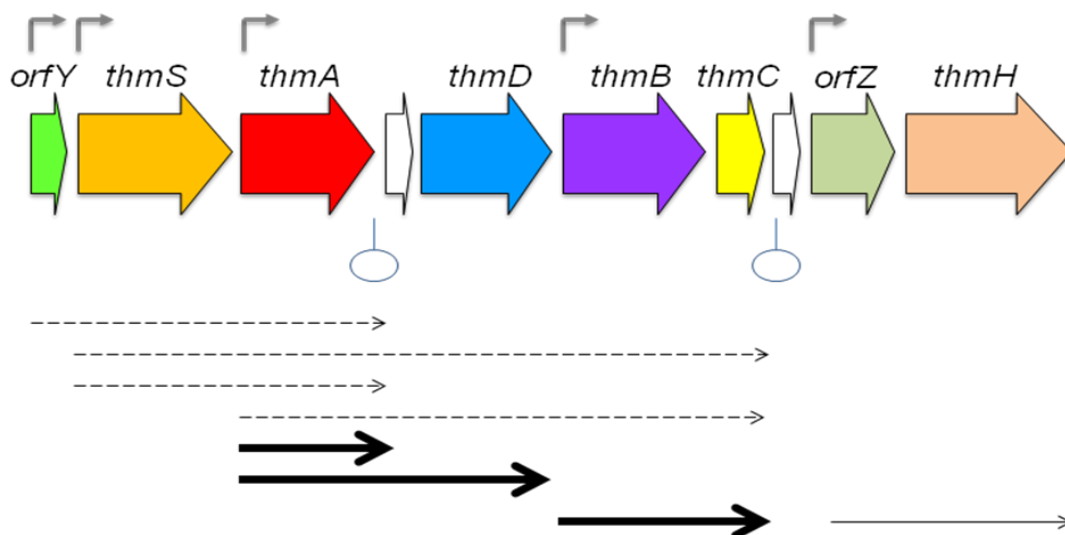


Figure 58. The predicted combination of *thm* transcripts in *Pseudonocardia* sp. strain ENV478. The 5' end of multiple mRNA was identified by primer extension and they are indicated with arrows. The putative terminator after *thmA* and *thmC* is indicated as with blue circle. Based on the size and intensity of *thm* mRNA identified by Northern blot analysis in *Pseudonocardia* sp. strain K, more abundant mRNA was labeled with thicker arrows.

oxygenases that is similar to *thm* monooxygenase, it may form a hexamer of α , β , and γ subunits as $(\alpha\beta\gamma)_2$ with an unknown stoichiometric amount of reductase.

Our cloning studies showed that heterologous expression of any of the *thm* subunits by themselves are toxic to cells (data not shown). While the same amount of α and β subunits may be required, probably much more or less reductase is required for proper expression. Since the *thm* operon in ENV478 has a reductase gene between the α and β genes, to keep proper ratios of α , β and γ vs reductase, RNA processing may be required.

The knockdown mutants of *thmA* and *thmB* lost their ability to grow on THF. The growth after 40 hours in incubation is most likely because mutants, which have lost the antisense construct, took over the population. The 1,4-dioxane degradation activity in wild-type and *thmB* knockdown mutant strains were examined with gas chromatography. While the vector control strain can oxidize 15 μ M 1,4-dioxane in 152 hours, *thmA* knockdown strain left 32% of provided 1,4-dioxane non-degraded even after 204 hour of incubation. Thus, this putative THF monooxygenase, which belongs to the soluble diiron monooxygenase family, is responsible for 1,4-dioxane oxidation in *Pseudonocardia* sp. strain K1.

It was hypothesized that the putative THF monooxygenase oxidizes cyclic ethers at the carbon next to the oxygen. In the case of THF, 2-hydroxytetrahydrofuran is the oxidation product of THF. The ring is spontaneously cleaved and further oxidations will form 4-hydroxybutyrate, which can be easily metabolized through the central metabolic system. In the case of 1,4-dioxane, initial oxidation yields 2-dioxane-ol. The spontaneous scission of one ether bond will allow the formation of β -hydroxyethoxyacetic acid (β -

HEAA), which still contains another ether bond. The lack of enzymes capable of metabolizing β -HEAA is possibly the reason why strain ENV478 cannot grow on 1,4-dioxane as a sole carbon source.

In THF-grown ENV478, two cytochrome P450 genes were shown to be expressed. In Eukaryotes, it was discovered that the gene expression of multiple copies of cytochrome P450 were upregulated when xenobiotics were present (Quiros et al., 2007, Danison et al., 1995). These cytochrome P450s were not involved in substrate oxidation per se, but rather were involved in cellular response to stress. Therefore, it is possible that cytochrome P450s that were identified by RT-PCR were expressed in response to the toxic effect of THF, and were not actually involved in its catalysis.

5.0 1,4-dioxane oxidation in *Rhodococcus* sp. strain ENV425

Abstract:

Rhodococcus sp. ENV425 is another bacterium which oxidizes 1,4-dioxane during growth on propane. The presence of three types of oxygenases that are present in strain ENV421 was also screened using degenerate primers in strain ENV425. All of them were identified, however, only genes for a soluble diiron monooxygenase was expressed in propane grown cells. An entire set of genes encoding oxygenase subunits were identified. The heterologous expression of these subunits in *E. coli* did not yield propane nor 1,4-dioxane oxidation activity.

5.1 Identification and analysis of propane monooxygenase in *Rhodococcus* sp. ENV425

5.1.1 Sequence analysis of propane monooxygenase gene cluster in *Rhodococcus* sp. strain ENV425

The degenerate primers designed to amplify PMO amplified a gene highly similar to PMO from *Rhodococcus* sp. strain RHA-1 and other gram positive strains (Figure 59). Inverse PCR was performed to obtain its upstream and downstream sequences. The DNA sequence of 8 kb was obtained with this method, and 8 genes that are transcribed in the same orientation were identified (Table 15, Figure 60). The list of genes found is: *prmABCD*, amido hydrolase, a hypothetical protein, alcohol dehydrogenase, and

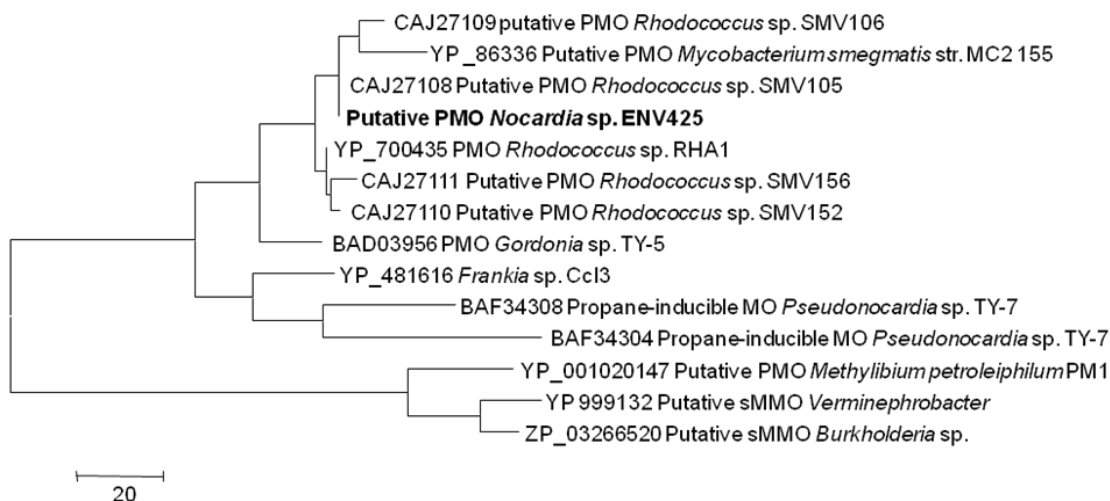


Figure 59. **Phylogenetic analysis of soluble diiron monooxygenase α -subunit from *Nocardia* sp. strain ENV425.**

Table 15. **List of genes identified in *prm* gene cluster and their predicted functions.**

Gene	Amino acid residues	Molecular mass (kDa)	GC%	Predicted functions
<i>prmA</i>	544	63.2	65	Soluble diiron MO α -subunit
<i>prmD</i>	370	41.0	64	Soluble diiron MO reductase
<i>prmB</i>	368	41.7	67	Soluble diiron MO β -subunit
<i>prmC</i>	113	12.5	63	Soluble diiron MO coupling protein
	348	40.1	64	Amidohydrolase
	247	26.8	71	Hypothetical
	341	35.8	72	Alcohol dehydrogenase
	549	58.1	68	Chaperonin GroEL

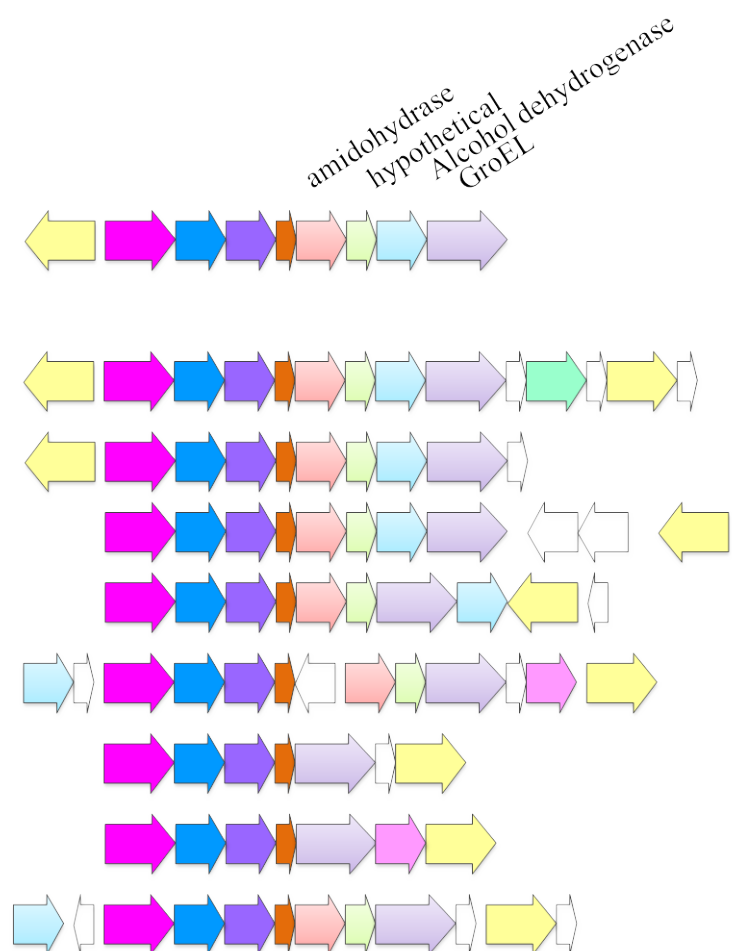


Figure 60. **Gene organization of propane monooxygenase gene cluster in *Nocardia* sp. strain ENV425** . Properties of each gene are summarized in Table 15.

molecular chaperonin (GroEL). Both the DNA sequence and the gene order are highly similar to putative PMO in *Rhodococcus* sp. RHA-1.

5.1.2 Propane and NDMA (N -Nitrosodimethylamine) mediated induction of propane monooxygenase gene cluster in *Rhodococcus* sp. strain ENV425

RT-PCR reaction using RNA from propane-grown strain ENV425 showed that PMO is expressed in propane grown cells (Figure 61).

The expression pattern of this gene in response to the presence of NDMA was also examined. The cells were grown either on glucose only or on glucose and NDMA (Figure 62). RT-PCR reaction yielded a product only in the presence of NDMA. The non-quantitative comparison of RT-PCR products yielded using RNA extracted from glucose and NDMA grown cells and RNA extracted from propane grown cells indicated that the induction of expression was much higher in propane grown cells.

5.1.3 Heterologous expression of putative PMO in *E.coli* BL21

The genes encoding four subunits of the putative propane monooxygenase were cloned into the *E. coli* expression vector pQE-30. The successful translation of each peptide was confirmed by SDS-PAGE (data not shown). However, propane or 1,4-dioxane degradation activity by this clone was not detected.

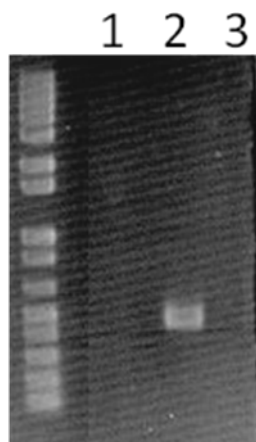


Figure 61. **Gene expression analysis of *alkB*, soluble diiron monooxygenase, and cytochrome P450 in *Nocardia* sp. strain ENV425 after growth on propane.** Total RNA was extracted from cells grown in MSB media with propane as a sole carbon source. 5ng of RNA was used for each RT-PCR reaction using degenerate primers. The amplification cycle was following: 1) 50°C for 30 min, (2) 30 cycles of 94°C for 30 sec, 55°C for 30 sec, 72°C for 30 sec and (3) 72°C for 5 min. The RT-PCR product of *alkB* (lane 1), diiron monooxygenase (lane 2) and cytochrome P450 (lane 3) was run on 1% agarose gel by electrophoresis .



Figure 62. **Gene expression analysis of soluble diiron monooxygenase and cytochrome P450 in response to NDMA (N -Nitrosodimethylamine) in *Nocardia* sp. strain ENV425.** Total RNA was extracted from cells grown in MSB media supplemented with glucose (lane 1, 2,3,4), glucose and NDMA (N-Nitrosodimethylamine) (lane 5,6,7,8), or propane (lane 9,10) as a sole carbon source. The RNA was extracted from cells at exponential phase (OD₆₀₀ 0.5) or at early stationary phase (OD₆₀₀ 0.7). 5ng of RNA was used for each RT-PCR reaction amplifying diiron monooxygenase (PMO) (lane 1,3,5,7,9) or cytochrome P450 (lane 2,4,6,8,10).

5.2 Identification and analysis of alkane monooxygenase (AlkB) and cytochrome P450 gene in *Rhodococcus* sp. ENV425

PCR using *alkB* degenerate primers amplified a fragment most similar to *alkB* in a number of *Rhodococcus* and *Mycobacterium* strains. It also shares 88% and 76% protein sequence identity to *alkB* in two known propane degraders, *Rhodococcus* sp. strain RHA1 and *Mycobacterium* sp. strain Ty-6, respectively.

RT-PCR was performed using RNA extracted from cells grown in propane. RT-PCR reaction did not yield a product, indicating that *alkB* is not expressed in propane grown ENV425 (Figure 61).

The above mentioned primers for cytochrome P450 gene were used to examine the presence of cytochrome P450 gene in strain ENV425. Although one or more cytochrome P450 genes were shown to be present in this organism, none of these genes were expressed during growth on propane (Figure 61).

5.3 Discussion

Strain ENV425 is another strain capable of oxidizing 1,4-dioxane after growth on propane. All three oxygenases were also identified in this strain by the degenerate primer approach. RT-PCR experiments showed that only a soluble diiron monooxygenase was expressed in propane grown cells. The expression of this BMM is also induced by the presence of N-Nitrosodimethylamine (NDMA). The deduced amino acid sequence of the

soluble diiron monooxygenase showed that it belongs to the Group 5-2 subfamily (Figure 59). A total 8 kb DNA sequence of a fragment containing monooxygenase subunits, alcohol dehydrogenase, chaperonin, and two genes with unknown functions were verified. They showed high sequence similarity and gene order to that of *Rhodococcus* sp. RHA-1. In strain RHA-1, a knockout mutant of PMO was constructed using homologous recombination. This mutant no longer utilizes propane.

Since the construction of knockout mutants in strain ENV425 was not possible, 1,4-dioxane oxidation activity of the enzyme was examined by heterologous expression of monooxygenase components in an *E. coli* host. Two expression clones were constructed, one containing only the monooxygenase subunits and another containing the entire 8 kb fragment mentioned above. 1,4-dioxane oxidation activity was not observed with either clone. The failure to show any activity in expression clones is consistent with other studies on propane-inducible monooxygenases. It had been suggested that this lack of activity is due to the necessity for a specific molecular chaperon for constructing a functional oxygenase from multiple subunits. In the butane-utilizing *Pseudomonas butanovora*, random mutagenesis identified a mutation on a chaperonin that prohibited its growth on butane.

5.4 Conclusion for PART-A

Three 1,4-dioxane degrading strains were screened and shown to possess multiple oxygenases (Table 16). Moreover, in strain ENV421 and ENV478, multiple oxygenases

Table 16. Summary of three oxygenases in *Mycobacterium* sp. strain ENV421, *Pseudonocardia* sp. strain ENV478 and *Nocardia* sp. strain ENV425.

Gene	ENV421		ENV425		ENV478	
	PCR	RT-PCR	PCR	RT-PCR	PCR	RT-PCR
P450	+	+	+	-	+	+
AlkB	+	+	+	-	-	-
Diiron MO	+	+	+	+	+	+

were expressed under 1,4-dioxane degrading conditions. Induction of a number of oxygenases by xenobiotics seems to be common phenomena in many different organisms. The simultaneous expression of multiple oxygenases was seen in another propane degrading bacteria, *Rhodococcus* sp. strain RHA1-1 (Sharp et al., 2007). In the RHA-1 strain, expression of both AlkB and PMO was shown to be induced by propane. Only PMO is essential for propane oxidation in RHA-1. In a fungus, a variety of xenobiotics can induce an expression of two tandem cytochrome P450 genes (Doddapaneni and Yadav, 2004).

So far only two propane hydroxylases have been genetically characterized and they belong to different subfamilies of diiron monooxygenases (BMM). Interestingly, all three strains in this study carried one or more BMM (Figure 63). The BMM in strain ENV421 and ENV425 are each similar to different propane monooxygenases. The BMM in strain ENV478 is similar to THF-induced BMM in *Pseudonocardia* sp. K1. In this project, 1,4-dioxane oxidation capability was only verified in BMM from strain ENV478. BMMs in strain ENV421 and ENV425 are also possibly capable of 1,4-dioxane oxidation, however, reconstituting an active oxygenase complex in a heterologous host is possibly hindered because of the lack of a proper molecular chaperon to facilitate subunit interactions. Thus, in the future when direct genetic manipulation is possible in these two organisms, we will be able to analyze the importance of these BMMs.

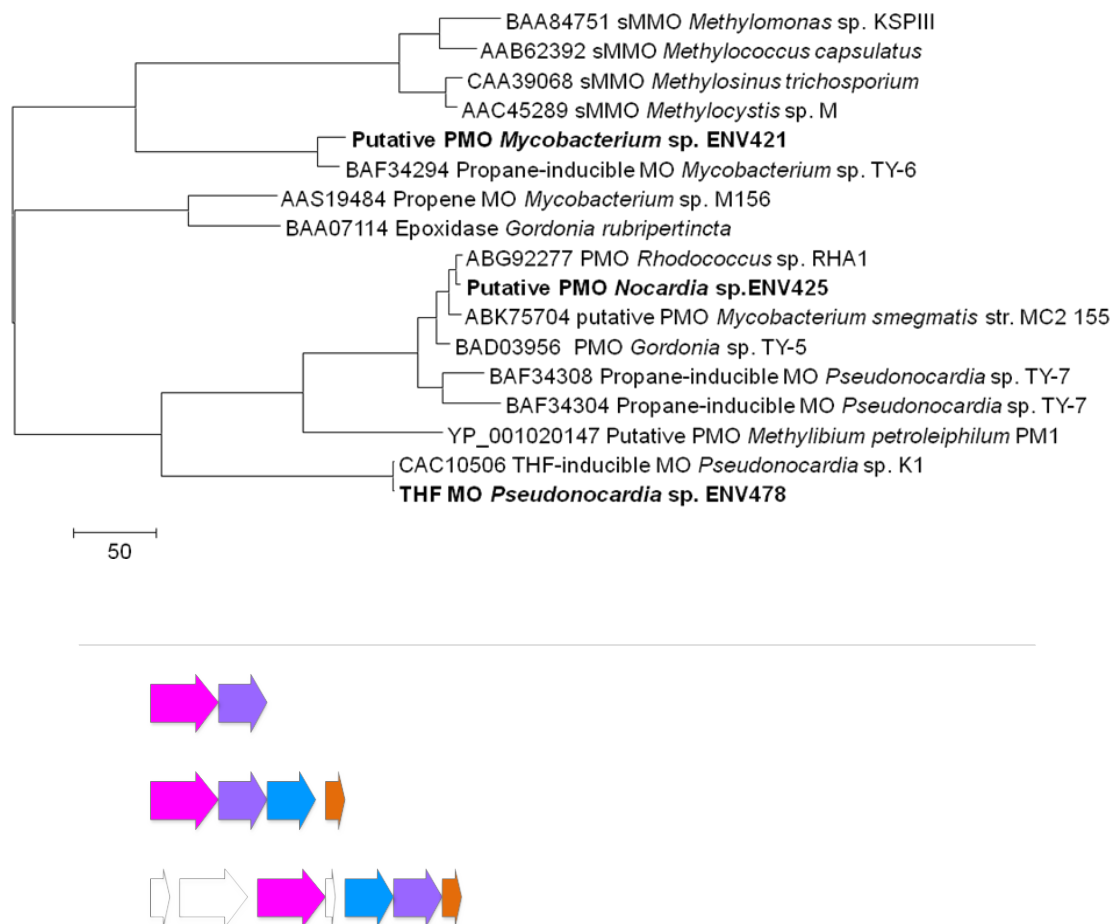


Figure 63. **Phylogenetic and gene organization analysis of soluble diiron monooxygenase α -subunit identified in *Mycobacterium* sp. strain ENV421, *Pseudonocardia* sp. strain ENV478 and *Nocardia* sp. strain ENV425.** The enzymes are abbreviated as soluble methane monooxygenase (sMMO), propane monooxygenase (PMO), and THF monooxygenase (THF MO).

PART-B

6.0 Isolation and characterization of *Aquabacterium njensis* sp. nov., a novel member of the β -*Proteobacteria* active in liquid and solid alkane degradation

Abstract:

A novel liquid and solid alkane-degrading bacterium was isolated from hydrocarbon-contaminated soil in New Jersey, USA. The morphological, genomic, and metabolic properties of this organism were examined, including observation with scanning electron microscopy, DNA-DNA hybridization, and nutritional screening of aliphatic compounds as the sole source of carbon for growth. The preliminary screen of known alkane oxidation enzymes identified two alkane monooxygenase (AlkB) genes, and no cytochrome P450 genes in the HMGZ-01^T strain.

The isolate is a gram negative rod, oxidase positive, and catalase negative. It utilizes liquid and solid alkanes, alkyl alcohols and alkyl carboxylic acids. It showed anaerobic growth with nitrate as an electron acceptor.

The 16S rRNA sequence analysis showed that it has the highest similarity to members of the genus *Aquabacterium*, which belongs to β -proteobacteria. The ability to hydrolyze urea and gelatin, NaCl tolerance, substrate utilization pattern and anaerobic growth distinguish the isolate from other members of this genus. We proposed the new species, *Aquabacterium njensis*, to be created with a single member and a type strain (HMGZ-01^T).

6.1 Introduction

Petroleum hydrocarbons are widely released into the environment by man-made industry and accidents such as oil spills, causing serious environmental problems around the world. Traditionally, large scale incineration plants have been utilized for remediation. Biological treatments for hydrocarbon remediation have also been attracting attention as an alternative green technology in recent years.

More than a decade of studies on alkane degradation revealed that bacterial degradation of linear alkanes is a common reaction in soil and water. Isolation of liquid-alkane degrading bacteria from the environmental samples is relatively easy. The degradation of long chain alkanes, particularly solid alkanes, however, is difficult due its low bioavailability to organisms. Thus, the physiological basis for long chain alkane degradation is less understood and more investigations are necessary. Long chain alkane degradation can be carried out by both gram negative and positive bacteria, and the majority cluster in the genera *Acinetobacter*, *Rhodococcus*, and *Gordonia*.

The initial and rate-limiting step of alkane degradation is a hydroxylation reaction by an oxygenase. Non-heme iron containing, membrane bound, alkane monooxygenase (AlkB) is the best studied enzyme so far for alkane oxidation.

Understanding the reaction mechanism of AlkB is of particular interest because the oxygenation reaction that AlkB can catalyze is hard to achieve by chemistry. So far, the x-ray crystal structure of AlkB is not available, thus the detailed studies of AlkB are limited to mutational screening and alignment of *alkB* sequences. These studies have

resulted in identification of an amino acid possibly important for determining the substrate range or an amino acid that is a part of an active site (van Beilen et al., 2005).

alkB is present in a variety of bacteria capable of growing on alkanes ranging from C₆ to C₃₀. However, the molecular study of *alkB* is limited to that of *P. putida* GPO1 for C₅-C₁₂ and *P. fluorescens* CHA0 for C₁₂-C₁₆. To better understand *alkB*, discovering AlkB enzymes with different substrate ranges is crucial.

HMGZ-01^T was isolated while searching for new *alkB* homologues that have low similarity to known *alkB* sequences. It was originally isolated as a fast octane degrader. It forms a thick lawn of cells on solid medium within two days when a mid-chain length alkane, such as octane, is provided as the sole source of carbon. It also grows rapidly on solid alkane (C₂₂) as a sole source of carbon. The growth was observed not only directly on the alkane particle but also on the media without direct contact with the solid particle. This suggests the production of surfactants which possibly increase the bioavailability of the solid alkane.

16S rRNA sequence analysis showed that the strain belongs to the genus *Aquabacterium*. HMGZ-01^T shares many physiological features with related members of this genus, including rapid growth on alkanes, alkyl alcohol, and carboxylic acids. It possesses a single flagellum and large inclusion bodies. In this study, alkane utilization was observed for the first time in this genus. This feature was shown to be a common trait in the genus *Aquabacterium* and they may share a common genetic basis for alkane utilization.

Preliminary screening of *alkB* showed that all of the *Aquabacterium* strains tested carried one or more copies of *alkB*. In HMGZ-01^T, two copies of *alkB* were found; both

share less than 60% protein sequence similarities to *alkB* sequences on the database.

Three related *Aquabacterium* strains also contain an *alkB* highly similar to these novel *alkB*, forming a new clade in the phylogenetic tree.

In this study, the physiological and phylogenetic properties of our strain were examined, and we proposed that it is a representative of a new species, *Aquabacterium njensis* sp. nov. (type strain HMGZ-01^T).

6.2 Methods

6.2.1 Bacterial strains, media and culture conditions

The strain HMGZ01^T was isolated in 2005 from contaminated New Jersey soil. The bacterium was isolated on MSB agar with octane provided in the gas phase as a sole carbon source. Three strains of *Aquabacterium*, *A. citratiphilum* sp. B4^T, *A. parvum* sp. B6^T, and *A. commune* sp. B8^T, were obtained from DSMZ culture collection for comparison. All three strains were isolated from the biofilm in the Berlin drinking water system (Kalmbach et al., 1999).

For cultivation of the B4^T, B6^T and HMGZ01^T strains, MSB medium supplemented with octane as a carbon source was used. For cultivation of the B8^T strain, modified R2A medium (replacing starch with 0.1% (v/v) Tween 80) was used (0.5 g yeast extract, 0.5 g peptone, 0.5 g casamino acids, 0.5 g glucose, 1ml Tween 80, 0.3 g Na-pyruvate, 0.3 g K₂HPO₄, 0.05 g MgSO₄•7H₂O, 15 g noble agar in 1L dH₂O).

All strains were grown at room temperature. Growth was tested either on solid medium or in liquid medium with constant agitation (100 r.p.m.). Complex media used in our work were trypticase soy agar, R2A agar, and LB (Difco, Franklin Lakes, NJ). The chemically defined medium used was MSB medium (Stanier et al., 1966).

6.2.2 Morphological and physiological characterization

Microscopic observations were made and photomicrographs were taken with an Amray 1840 scanning electron microscope with PGT Imix x-ray detector and analyzer at the Food Science Department of Rutgers University, NJ.

Nutritional screening was performed using MSB medium. Carbon substrates were added from an autoclaved or filter-sterilized stock solution to a final concentration of 10 mM or 0.1%. Volatile substrates were supplied in gas phase using small glass tubes with a cotton plug and plates were sealed with parafilm.

Cytochrome oxidase activity was determined by dark color development using an oxidase kit (Sigma-Aldrich, Switzerland). Catalase production was tested by mixing 3% (v/v) H₂O₂ solution with liquid culture (Murray et al., 1998). Hydrolysis of urea was determined by examining the change in pH after the incubation of cells grown in MSB medium supplemented with octane with 2% (w/v) urea. The hydrolysis of starch was determined on MSB agar containing 0.2% (w/v) soluble starch and octane in the gas phase. After cell growth, the plate was flooded with iodine solution. Hydrolysis of casein was tested on casein agar (double-strength, MSB agar was combined with an equal volume of sterile skimmed milk). The incubation period for tests mentioned above was 5

days. Gelatin hydrolysis was determined by method that previously described (Gerhardt et al. 1994).

The NaCl tolerance range (0 to 2% w/v) was examined in MSB medium supplemented with octane in the gas phase. The pH tolerance range (pH 5 to 13) was tested in modified R2A medium. To examine pH tolerance, MSB medium was supplemented with 10 mM phosphate buffer (pH 5-7) or with 10 mM Tris- buffer (pH 7.5-13). The pH was adjusted with HCl or NaOH. After 5 days of incubation, growth was examined spectroscopically.

The use of KNO₃, KNO₂, NaClO₃, Na₂SO₄, and iron (III) citrate as an electron acceptor was examined under anaerobic conditions in MSB medium containing butyrate as a carbon source. An electron acceptor and a carbon source were added to a final concentration of 10 mM. All cultures were grown under argon atmosphere for 7 days and growth was examined by monitoring the change in optical density (OD₆₀₀).

6.2.3 Nucleic acid techniques

Isolation of genomic DNA and DNA-DNA hybridization were performed at the DSMZ (Braunschweig, Germany). DNA was isolated using a French pressure cell (Thermo Spectronic) and purified with chromatography on hydroxyapatite (Cashion et al. 1977). DNA-DNA hybridization was performed as described by De Dey and colleagues with slight modification (De Ley et al., 1970, Huss et al., 1983).

Genomic DNA was extracted using the UltraCleanTM Microbial DNA isolation kit (MO BIO Laboratories, Inc, Carlsbad, CA). The 16S rRNA gene was amplified by PCR using the 27F and 1522R primers under standard conditions. PCR products were purified

using the GeneClean® SPIN Kit (MP Biomedicals, Solon, OH) and used directly for DNA sequencing. DNA sequence was obtained using 3130xl Genetic Analyzers (Applied Biosystems) with the primers 27F, 357F, 704F, 1242F, 342R, 685R, 907R, 1522R. Primer sequences are as described by Johnson (Johnson et al., 1994). The nucleotide sequences were aligned using CLUSTAL V in the Lasergene software package (DNASTar) and visually inspected. Phylogenetic analysis was performed with the MEGA version 4 software package (Tamura et al., 2007). Distances (according to the Kimura two-parameter model) and clustering with the neighbor-joining and maximum-parsimony methods were calculated using bootstrap values of 1000 replications.

Partial fragments of *alkB* were amplified by PCR using degenerate primers. A set of primers, DSalkF (AATACHGVCAYGAGCTCRGYCAYAAR) and DSalkR (GCRTGRTGATCAGARTGHCGYTG) were developed based on conserved sequences in multiple sequence alignment of *alkB* copies. PCR products were cloned into the pGEM-T vector (Promega, Madison, WI) and the plasmid DNA was isolated with the Nucleospin® Plasmid kit (Macherey-Nagel, Bethlehem, PA). DNA sequences of each clone were obtained using SP6 (ATTTAGGTGACACTATAG) and T7 (TAATACGACTCACTATAGG) primers, and sequences were analyzed as described above.

6.3 Results

6.3.1 Morphology and colony characteristics

The cells were small, Gram-negative rods, 0.75 μm ×1.25 μm in size, occurring singly (Figure 64). The cells were motile by means of a single polar flagellum

A)



B)

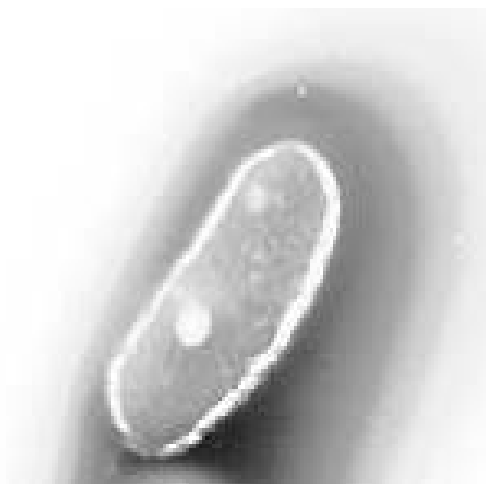


Figure 64. **Scanning electron microscopy of *Aquabacterium njensis* HMGZ01^T**. The cells were grown on octane until they reached exponential phase. SEM photographs were taken using scanning electron microscopy by Dr. Simon at Plant Science Department of Rutgers University. A) live cell B) lysed cell

(approximately twice the length of the bacterium). The cells contain inclusion bodies but their chemical nature was not characterized. The morphology of HMGZ01^T was very similar to that of three other species of *Aquabacterium*; *A. citratiphilum* sp. B4^T, *A. parvum* sp. B6^T, and *A. commune* sp. B8^T.

When streaked onto MSB agar supplemented with octane in the gas phase and incubated for 3 days, HMGZ01^T forms white, flat colonies with smooth margins and a diameter of 1.5-2.0 mm.

6.3.2 Physiological properties

The physiological characteristics of HMGZ01^T and its close relatives, *A. citratiphilum* sp. B4^T, *A. parvum* sp. B6^T, and *A. commune* sp. B8^T were examined and compared.

All of the strains were oxidase positive and catalase negative. HMGZ01^T, B4^T, and B6^T hydrolyze urea. None of the strains hydrolyzed starch or casein. HMGZ01^T and B4^T have gelatinase activity. Lipase activity (Tween 80 hydrolysis) was present in all strains as shown by the growth on modified R2A medium. pH and NaCl range for growth of the strains is given in Table 17.

The optimal temperature of growth was about 30°C, while no significant growth was observed above 37°C. All strains showed limited growth on rich media. None of the strains grew on LB media, and only HMGZ01^T strain grew well in Tryptic Soy Agar (TSA) media. Strain B8^T grew well on modified R2A media, in which starch was replaced by Tween80. HMGZ01^T and other two strains showed relatively slow growth in

Characteristics	B4 ^T	B6 ^T	B8 ^T	HMGZ-01 ^T
Oxidase test	+	+	+	+
Catalase	-	-	-	-
Anaerobic reduction of				
NO ₃ ⁻	-	-	-	+
NO ₂ ⁻ , Fe ³⁺ , SO ₄ ²⁻ , ClO ₃ ⁻	-	-	-	-
Hydrolysis of				
Urea	+	+	-	+
Casein	-	-	(-)	-
Starch	-	-	-	-
Gelatin	(+)	-	-	+
NaCl concentration (% w/v)	0-1.8	0-1.0	0-0.4	0-0.4
pH range	5-12	6-10	6.5-9.5	6-11
Substrate utilization				
Asparagine, glutamate	-	-	+	-
Lactate, glycerol	+	-	-	+
Cosamino acid, propionate	+	-	+	-
Citrate	+	-	-	-

Table 17. **Summary of physiological characteristics of *Aquabacterium njensis* HMGZ-01^T, *Aquabacterium*, *A. citratiphilum* sp. B4^T, *A. parvum* sp. B6^T, and *A. commune* sp. B8^T.** Substrates that were utilized by all four strains included Tween 80, acetate, butyrate, adipate, pyruvate, succinate, butanol, 1-octanol, dodecanol, hexadecanol, tetradecanone, octane, dodecane, hexadecane, hexacosane, D-fructose. Substrates none of the four strains utilized include D-mannose, D-mannitol, L-arabinose, D-glucose, D-maltose, sucrose, D-xylose, D-ribose, L-rhamnose, D-lactose, D-galactose, D-trehalose, D-ribulose, D-melibiose, N-acetylglucosamine, gluconate, galacturonate, glutamine, aspartate, threonine, isoleucine, phenylalanine, leucine, cysteine, valine, alanine, glycine, proline, serine, arginine, ascorbic acid, (benzoate), hydroxybenzoate, ethylene glycol, polyethylene glycol, phenol, ethanol, 2-propanol, and hexane.

this medium. Growth of all of the strains was fastest on MSB medium supplemented with aliphatic carbon sources, particularly with alkanes.

6.3.3 Substrate utilization

The substrate utilization pattern by strains HMGZ01^T, B4^T, B6^T, and B8^T is summarized in Table 17. All four strains utilized a variety of mid-chain length liquid and solid alkanes (C₈-C₂₆), with no growth on short chain alkanes. HMGZ01^T showed growth on pentane after a month. No growth of any of the four strains was observed with propane.

During growth on long chain liquid alkanes in liquid media, a layer of material formed between the aqueous medium and aliphatic alkanes. Also, when the cells were incubated on solid MSB medium with solid alkanes, growth was observed on media without direct contact with solid alkane particles. This may be an indication of production of surfactant. The nature of this material has not been determined. Growth on alkane, alkyl alcohol, and alkyl carboxylic acids with mid to long chain length is a newly found common trait of bacteria in this genus.

All strains did not grow on carbohydrates except for fructose. Only HMGZ01^T grew on formamide, albeit at a slow rate. Growth on MSB medium which was supplemented with a carbon source also indicated that organic growth factors are not required.

6.3.4 Electron acceptor

When nitrate was supplied as an alternative electron acceptor in liquid culture, HMGZ01^T exhibited anaerobic growth. The three related strains did not show growth in the same conditions. No anaerobic growth was observed with KNO₂, NaClO₃, Na₂SO₄, or iron (III) citrate as an electron acceptor.

6.3.5 DNA-DNA hybridization

DNA-DNA hybridization experiments were performed between HMGZ01^T and three *Aquabacterium* strains, B4^T, B6^T, and B8^T at DSMZ. The % DNA-DNA similarity between *A. njensis* HMGZ01^T and *A. citratiphilum* sp. B4^T, *A. parvum* sp. B6^T, and *A. commune* sp. B8^T was 16.6, 23.5, and 14.0%, respectively.

6.3.6 Phylogenetic analysis of 16S rRNA sequence

Almost complete (1492 nt) 16S rRNA gene sequences were determined for HMGZ01^T using the 27F and 1522R PCR primers. The closest 16S rRNA gene sequences of verified organisms in the GenBank database are those of *Aquabacterium* strains B4^T, B6^T, and B8^T, which belong to the β 1 subclass of proteobacteria (Figure 65). The comparison of 16S rRNA sequence of HMGZ01^T with these three strains showed that it had 98%, 97%, and 98% identity to *Aquabacterium* B4^T, B6^T, and B8^T, respectively. The phylogenetic tree of 16S rRNA of HMGZ01^T and its closest relative shows that HMGZ01^T together with the uncharacterized oral clone *Leptothrix* AV011a-1

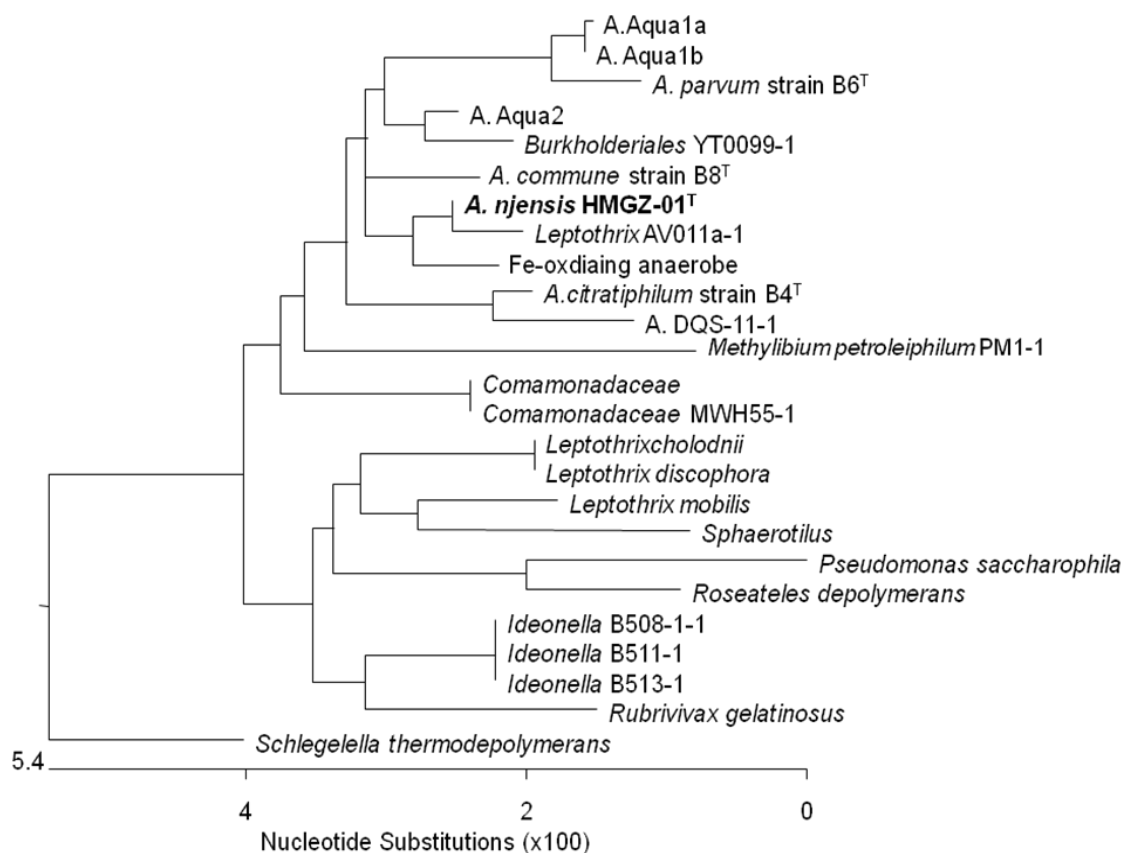


Figure 65. Phylogenetic analysis of 16S rRNA gene of *Aquabacterium njensis* sp. HMGZ-01^T and other β -proteobacteria strains.

(AF385528) and denitrifying Fe<II>-oxidizing bacterium (DFU51102) forms a clade separate from the B4^T, B6^T, and B8^T strains.

6.3.7 Phylogenetic analysis of *alkB*

All four strains carry *alkB*. PCR products were cloned and DNA sequences of several clones were determined for each strain. B4^T and HMGZ01^T carry 2 copies while B6^T and B8^T carry one copy of *alkB*. The phylogenetic analysis of these copies is shown in Figure 66. The two copies of HMGZ01^T *alkB* share only 72% protein sequence identity to each other and they showed only 68% identity to known *alkB* sequences in the database. *alkB* from HMGZ01^T, B6^T, B8^T and one of the copies from B4^T themselves form a new distinct clade in the *alkB* phylogenetic tree.

The high sequence similarity of at least one *alkB* from four *Aquabacterium* species and their identical growth patterns on alkanes indicate possible involvement of these AlkB in alkane metabolism in *Aquabacterium* strains.

6.4 Discussion

Strain HMGZ01^T and three strains of *Aquabacterium* did not grow well on rich media. No growth was observed on LB and the growth on TSA was faint. On the other hand, the growth on low nutrient (R2A) medium or MSB medium supplemented with organic carbon was rapid. Combined with the observation of fast growth on alkyl acids and alcohol and the lack of growth on sugars, it is reasonable to assume that the

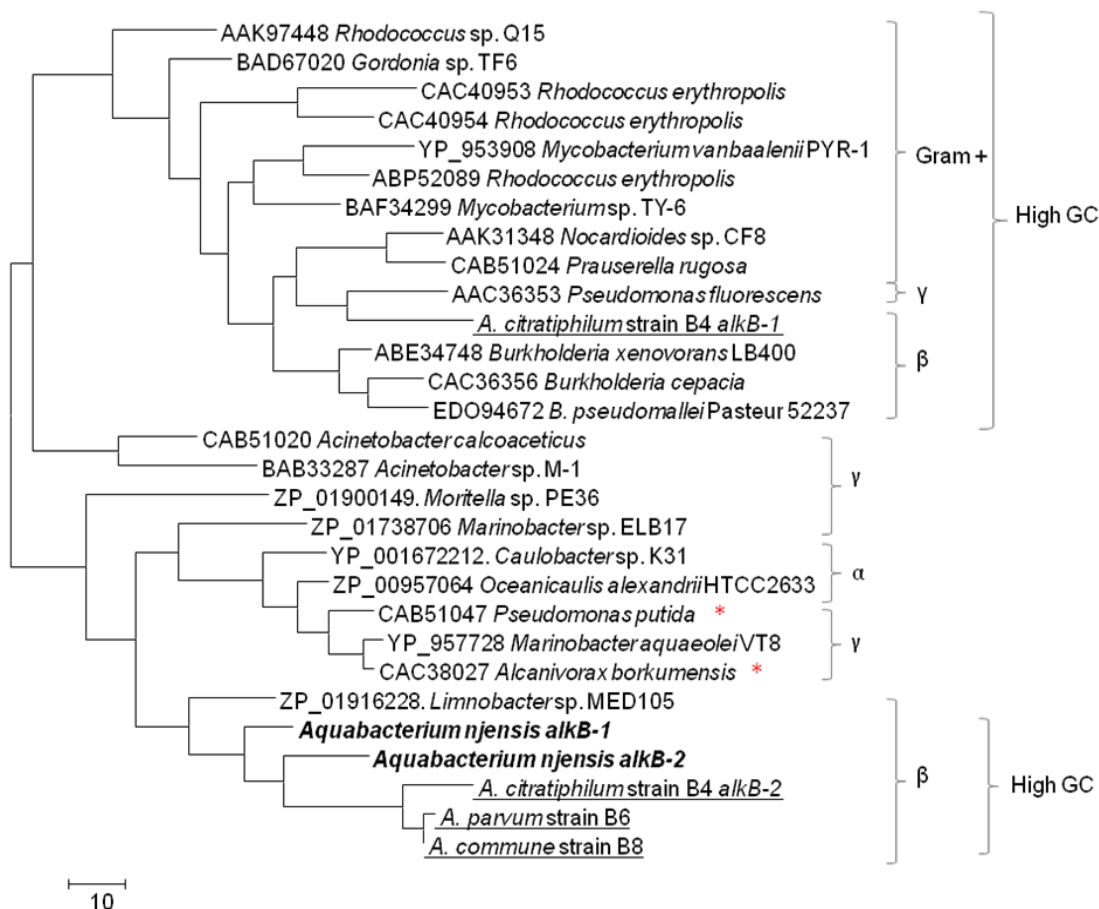


Figure 66. Phylogenetic analysis of *alkB* protein sequences in *Aquabacterium njensis* HMGZ-01^T, *A. citratiphilum* strain B4^T, *A. parvum* strain B6^T, and *A. commune* strain B8^T.

* liquid alkane oxidizing activity is verified (Smits et al., 1999; Smits et al., 2002)

Table 18. List of alkane monooxygenases with known substrate range.

Organism	Substrate range	Reference
<i>P. putida</i> GPO1	C6-12	Smits et al., 2002
<i>Alcanivorax borkumensis</i>	C8-12	Smits et al., 1999
<i>Pseudomonas fluorescens</i> CHA0	C12-16	Smits et al., 2002

Aquabacterium strains favor life in a low nutrient and low salt environment. Three characterized strains of *Aquabacterium* were isolated as prominent members of bacteria that exist in the biofilm in drinking water in Berlin, Germany. Strain HMGZ01 was isolated from a hydrocarbon contaminated soil, which is also expected to be a low nutrient environment.

Despite the large number of bacteria that can grow on liquid alkanes as a sole carbon source, solid alkane degraders are rare. This is proposed to be due to the low accessibility of solid alkanes to organisms. In order to overcome this issue, some bacteria produce biosurfactants. The types of properties of biosurfactant which are important for biodegradation of hydrophobic materials are: effects on surface and interfacial tensions, emulsification and pseudosolubilization capacities (Bouchez-Naïtali and Vandecasteele, 2008). The role of surfactants varies among bacteria. For example, in two hexadecane degraders, *Pseudomonas aeruginosa* GL1 and *Rhodococcus equi* ou2, different roles of surfactants in hexadecane degradation were observed. In *Pseudomonas aeruginosa* GL1, the biosurfactant has an effect on pseudosolubilization capacity and allows bacteria to uptake hexadecane from micelles. In *Rhodococcus equi* ou2, the biosurfactant has a minor role in hexadecane degradation, and bacteria uptake hexadecane via direct interfacial accession. It is proposed that the effect of surfactants in the second case is to change bacterial cell surface hydrophobicity.

Using a non-biological surfactant, the effect of surfactant on bacteria with different surface hydrophobicity was examined. The effect of surfactant on biodegradation capability of bacteria depends on the hydrophobicity of the cell surface (Churchill and Churchill, 1997). In the absence of surfactant, bacteria with a hydrophobic

cell surface can oxidize octadecane faster than bacteria with hydrophilic cell surfaces. The rate of octadecane degradation in bacteria with hydrophilic cell surfaces can be greatly enhanced by the addition of surfactant, while surfactant had no effect on the rate of degradation in bacteria with a hydrophobic cell surface.

Based on the observation of rapid growth on distant solid alkanes and the formation of micelles in liquid culture, it is proposed that the biosurfactant produced by HMGZ-01^T is secreted extracellularly and plays a role to increase alkane solubility, hence increased availability. The most well known type of biosurfactant is a glycolipid. The above mentioned hexadecane degraders are known to produce glycolipid as a surfactant. Therefore, the biosurfactant produced by the *Aquabacterium njensis* HMGZ-01^T could be a glycolipid type biosurfactant.

In the presence of abundant carbon sources, under limited phosphorus or nitrogen conditions, cells often produce 3-hydroxybutyryl-CoA. This will be polymerized by PHA synthase and form granules (Jurasek et al., 2004). Then, phasin molecules will be produced and they will attach themselves to the growing granules. A known PHA producing bacterium, *Ralstonia eutropha*, produces on average, ten such PHA granules whose diameters are about 500 nm (Anderson and Dawes, 1990; Ballard et al., 1987).

Scanning electron microscopy of lysed HMGZ-01^T cells showed the possible presence of inclusion bodies. Further analysis of these inclusion bodies by SEM is limited. In the paper describing three *Aquabacterium* strains, the nature of inclusion bodies was examined using transmission electron microscopy (Kalmbach et al., 1999). Both polyalkanoate and polyphosphate were present in all three *Aquabacterium* strains. Thus, it is likely that HMGZ01^T also carries these two types of inclusion bodies.

HMGZ-01^T is a facultative anaerobe. Only nitrate can be used as an alternative electron acceptor to support its growth under anaerobic conditions. Previously, the microaerophilic growth of three strains of *Aquabacterium* was observed using deep agar cultures (Kalmbach et al., 1999). Nitrate reduction was also observed in all three strains under this condition. However, in our study, anaerobic growth of these strains was not observed.

DNA-DNA percent similarity between HMGZ-01^T and the three strains of *Aquabacterium* was 16.6, 23.5, and 14.0%, which is significantly below the conventional threshold of 75% for defining two distinct species of bacteria (Wayne et al., 1987).

Aquabacterium njensis HMGZ-01^T and other *Aquabacterium* strains belong to the β -proteobacteria, more specifically in families *Burkholderiaceae*. *Burkholderiales* contains five families, three of which are well-known genera, *Burkholderiaceae*, *Alcaliginaceae*, and *Comamonadaceae*. *Burkholderiaceae* contains the genus *Burkholderia*. The physiological characteristics of *Aquabacterium* resemble those of other members of this family: gram-negative, aerobic, nonfermentative, non-spore forming, mesophilic, straight rods; motile with single flagellum or a tuft of polar flagella; catalase-positive, use poly- β -hydroxybutyrate as carbon reserve. *Alcaliginaceae* and *Comamonadaceae* are known to have some characteristics that are not seen in *Aquabacterium*. *Alcaliginaceae* is a coccobacillus and a chemoorganotroph. Some members of *Comamonadaceae* have a sheath, a hollow tubelike structure surrounding a chain of cells. Thus, both 16S rRNA sequence data and physiological characteristics indicate that the newly isolated strain is a member of the genus *Aquabacterium*, which is a subclass of *Burkholderia*.

Although there are a large number of *alkB* sequences in the database, they are mainly sequences that have been amplified using metagenomic DNA as a template. The functions of very few *alkB* genes have been experimentally verified. In this study, in addition to experimentally characterized *alkB*, *alkB* sequences amplified from alkane degrading bacteria and those present in whole genome sequences were used for phylogenetic analysis.

The *alkB* from four strains of *Aquabacterium* have the highest similarity to *alkB* in a genome sequence of β -proteobacteria, *Limnobacter* sp. strain MED105. These sequences form a separate group from a cluster containing the well studied *alkB* from *P. putida* GPo1 (CAB51050). Interestingly, this second cluster contains *alkB* genes from a variety of α and γ -proteobacteria. *alkB* genes in other β -proteobacteria strains are very different from these *alkB* genes. It is most similar to the *alkB* found in gram positive bacteria. This indicates the possibility of horizontal gene transfer in *alkB* transmission.

The GC content and localization of these *alkB* genes were then analyzed. The GC% of the whole genome was also analyzed to see if there is any difference from that of *alkB*. Based on the nucleotide sequence and GC content, *alkB* sequences that are similar to *Aquabacterium* can be categorized into 4 subgroups (Figure 66): the high GC gram positive (group 1), high GC gram negative (group 2), relatively low GC gram negative (group 3), and high GC gram negative that are not similar to gram positive *alkB* (group 4). Group 4 includes the *alkB* from *Aquabacterium* strains.

In groups 1 and 2, the GC content of *alkB* and the whole genome matches. This implies the possibility that the acquisition of *alkB* by these organisms is historical. On the other hand, the third group showed mixed results. The GC content of *alkB* and the whole

genome is not the same as in group 3. This may indicate the recent acquisition of *alkB* by these organisms.

The GC content of *alkB* and that of the whole genome matches in *Aquabacterium* strains (group 4). Also, the GC content of these *alkB* is consistently higher than that of group 3, which sets them apart as a different group from group 3. The small discrepancy of *alkB*'s GC content between HMGZ01^T strain (60%) and three aqua strains (~65%) could be explained either by 1) the sequences were too short for accurate analysis, or by 2) the time since *alkB* acquisition was long enough to adjust to the GC content of the rest of the genome. And HMGZ01^T's GC content (unknown) is lower than that of other strains (65%).

The AlkB with known substrate ranges were identified in *P. putida* (CAB51047) and *Alcanivorax borkumensis* (CAC38027), and *Pseudomonas fluorescens* CHA0 (sequence not available). Their substrate ranges are summarized in Table 18. Although *Pseudomonas fluorescens* can grow on C₁₀-C₂₈ alkanes, AlkB is only shown to be involved in C₁₂-C₁₆ alkane utilization. The two *alkB* in the HMGZ01^T strain are distantly related to any of these genes, only sharing less than 30% sequence identity.

Thus, *alkB* in *A. njensis* HMGZ01^T strain and its related *Aquabacterium* strains are new types of *alkB*, sharing very low sequence similarity to known *alkB*. This will make *alkB* from HMGZ01^T an interesting new type of *alkB* to study further, because of its potential ability to oxidize mid to long chain alkanes.

REFERENCES

- Allen, J. R., and S. A. Ensign.** 1999. Two short-chain dehydrogenases confer stereoselectivity for enantiomers of epoxyp propane in the multiprotein epoxide carboxylating systems of *Xanthobacter* strain Py2 and *Nocardia corallina* B276. *Biochemistry* **38**:247-56.
- Allenby, N. E., N. O'Connor, Z. Pragai, N. M. Carter, M. Miethke, S. Engelmann, M. Hecker, A. Wipat, A. C. Ward, and C. R. Harwood.** 2004. Post-transcriptional regulation of the *Bacillus subtilis* pst operon encoding a phosphate-specific ABC transporter. *Microbiology* **150**:2619-28.
- Altschul, S. F., T. L. Madden, A. A. Schaffer, J. Zhang, Z. Zhang, W. Miller, and D. J. Lipman.** 1997. Gapped BLAST and PSI-BLAST: a new generation of protein database search programs. *Nucleic Acids Res* **25**:3389-402.
- Anderson, A. J., and E. A. Dawes.** 1990. Occurrence, metabolism, metabolic role, and industrial uses of bacterial polyhydroxyalkanoates. *Microbiol Rev* **54**:450-72.
- Andreoni, V., S. Bernasconi, M. Colombo, J. B. van Beilen, and L. Cavalca.** 2000. Detection of genes for alkane and naphthalene catabolism in *Rhodococcus* sp. strain 1BN. *Environ Microbiol* **2**:572-7.
- Appel, D., S. Lutz-Wahl, P. Fischer, U. Schwaneberg, and R. D. Schmid.** 2001. A P450 BM-3 mutant hydroxylates alkanes, cycloalkanes, arenes and heteroarenes. *J Biotechnol* **88**:167-71.
- Arp, D. J.** 1999. Butane metabolism by butane-grown '*Pseudomonas butanovora*'. *Microbiology* **145** (Pt 5):1173-80.
- Ashraf, W., A. Mihdhir, and J. C. Murrell.** 1994. Bacterial oxidation of propane. *FEMS Microbiol Lett* **122**:1-6.
- Ayoubi, P. J., and A. R. Harker.** 1998. Whole-cell kinetics of trichloroethylene degradation by phenol hydroxylase in a *ralstonia eutropha* JMP134 derivative. *Appl Environ Microbiol* **64**:4353-6.
- Ballard, D. G. H., P. A. Holmes, and P. J. Senior.** 1987. Formation of polymers of beta-hydroxybutyric acid in bacterial cells and a comparison of the morphology of growth with the formation of polyethylene in the solid state. *Recent Adv Mech Synth Aspects Polym*:293-314.

- Bertoni, G., M. Martino, E. Galli, and P. Barbieri.** 1998. Analysis of the gene cluster encoding toluene/o-xylene monooxygenase from *Pseudomonas stutzeri* OX1. *Appl Environ Microbiol* **64**:3626-32.
- Bouchez-Naïtali, M., and J. P. Vandecasteele.** 2008. Biosurfactants, an help in the biodegradation of hexadecane? The case of *Rhodococcus* and *Pseudomonas* strains. *World Journal of Microbiology and Biotechnology* **24**:1901-1907.
- Brodsky L.I., I. V. V., Kalai dzidis Ya.L., Leontovich A.M., Nikolaev V.K., Feranchuk S.I., Drachev V.A.** 1995. GeneBee-NET:Internet-based server for analyzing biopolymers structure. *Biochemistry* **60**:923-928.
- Byrne, A. M., J. J. Kukor, and R. H. Olsen.** 1995. Sequence analysis of the gene cluster encoding toluene-3-monooxygenase from *Pseudomonas pickettii* PKO1. *Gene* **154**:65-70.
- Cadwallader, K., R. J. Braddock, M. E. Parish, and D. P. Higgins.** 1989. Bioconversion of (+)-limonene by *Pseudomonas gladioli*. *J Food Sci* **54**:1241-1245.
- Chauvaux, S., F. Chevalier, C. Le Dantec, F. Fayolle, I. Miras, F. Kunst, and P. Beguin.** 2001. Cloning of a genetically unstable cytochrome P-450 gene cluster involved in degradation of the pollutant ethyl tert-butyl ether by *Rhodococcus ruber*. *J Bacteriol* **183**:6551-7.
- Cheong, T. K., and P. J. Oriel.** 2000. Cloning and expression of the limonene hydroxylase of *Bacillus stearothermophilus* BR388 and utilization in two-phase limonene conversions. *Appl Biochem Biotechnol* **84-86**:903-15.
- Churchill, P., and S. Churchill.** 1997. Surfactant-enhanced biodegradation of solid alkanes. *J Environ Sci Health* **32**:371-377.
- Colby, J., D. I. Stirling, and H. Dalton.** 1977. The soluble methane mono-oxygenase of *Methylococcus capsulatus* (Bath). Its ability to oxygenate n-alkanes, n-alkenes, ethers, and alicyclic, aromatic and heterocyclic compounds. *Biochem J* **165**:395-402.
- Condon, C.** 2003. RNA processing and degradation in *Bacillus subtilis*. *Microbiol Mol Biol Rev* **67**:157-74.
- De Ley, J., H. Cattoir, and A. Reynaerts.** 1970. The quantitative measurement of DNA hybridization from renaturation rate. 133-142.
- Denison, M. S., and J. P. Whitlock, Jr.** 1995. Xenobiotic-inducible transcription of cytochrome P450 genes. *J Biol Chem* **270**:18175-8.

- Doddapaneni, H., and J. S. Yadav.** 2004. Differential regulation and xenobiotic induction of tandem P450 monooxygenase genes pc-1 (CYP63A1) and pc-2 (CYP63A2) in the white-rot fungus *Phanerochaete chrysosporium*. *Appl Microbiol Biotechnol* **65**:559-65.
- Doughty, D. M., L. A. Sayavedra-Soto, D. J. Arp, and P. J. Bottomley.** 2006. Product repression of alkane monooxygenase expression in *Pseudomonas butanovora*. *J Bacteriol* **188**:2586-92.
- Eremina, S. S., O. Asperger, and H. P. Kleber.** 1987. [Cytochrome P-450 and the respiratory activity of *Acinetobacter calcoaceticus* growing on n-nonane]. *Mikrobiologiya* **56**:764-9.
- Feenstra, K. A., E. B. Starikov, V. B. Urlacher, J. N. Commandeur, and N. P. Vermeulen.** 2007. Combining substrate dynamics, binding statistics, and energy barriers to rationalize regioselective hydroxylation of octane and lauric acid by CYP102A1 and mutants. *Protein Sci* **16**:420-31.
- Fosdike, W. L., T. J. Smith, and H. Dalton.** 2005. Adventitious reactions of alkene monooxygenase reveal common reaction pathways and component interactions among bacterial hydrocarbon oxygenases. *Febs J* **272**:2661-9.
- Fox, B. G., J. G. Borneman, L. P. Wackett, and J. D. Lipscomb.** 1990. Haloalkene oxidation by the soluble methane monooxygenase from *Methylosinus trichosporium* OB3b: mechanistic and environmental implications. *Biochemistry* **29**:6419-27.
- Fox, B. G., K. K. Surerus, E. Munck, and J. D. Lipscomb.** 1988. Evidence for a mu-oxo-bridged binuclear iron cluster in the hydroxylase component of methane monooxygenase. Mossbauer and EPR studies. *J Biol Chem* **263**:10553-6.
- Fujii, T., T. Narikawa, F. Sumisa, A. Arisawa, K. Takeda, and J. Kato.** 2006. Production of alpha, omega-alkanediols using *Escherichia coli* expressing a cytochrome P450 from *Acinetobacter* sp. OC4. *Biosci Biotechnol Biochem* **70**:1379-85.
- Gillam, E. M., L. M. Notley, H. Cai, J. J. De Voss, and F. P. Guengerich.** 2000. Oxidation of indole by cytochrome P450 enzymes. *Biochemistry* **39**:13817-24.
- Green, J., and H. Dalton.** 1989. Substrate specificity of soluble methane monooxygenase. Mechanistic implications. *J Biol Chem* **264**:17698-703.
- Grosse, S., L. Laramee, K. D. Wendlandt, I. R. McDonald, C. B. Miguez, and H. P. Kleber.** 1999. Purification and characterization of the soluble methane monooxygenase of the type II methanotrophic bacterium *Methylocystis* sp. strain WI 14. *Appl Environ Microbiol* **65**:3929-35.

- Groves, J. T.** 2006. High-valent iron in chemical and biological oxidations. *J Inorg Biochem* **100**:434-47.
- Hardison, L. K., S. S. Curry, L. M. Ciuffetti, and M. R. Hyman.** 1997. Metabolism of diethyl ether and cometabolism of methyl tert-butyl ether by a filamentous fungus, a *Graphium* sp. *Appl Environ Microbiol* **63**:3059-3067.
- Hristova, K. R., R. Schmidt, A. Y. Chakicherla, T. C. Legler, J. Wu, P. S. Chain, K. M. Scow, and S. R. Kane.** 2007. Comparative transcriptome analysis of *Methylobium petroleiphilum* Pm1 exposed to the fuel-oxygenates methyl-tert-butyl ether and ethanol. *Appl Environ Microbiol* **73**:7347-57.
- Hur, H., L. M. Newman, L. P. Wackett, and M. J. Sadowsky.** 1997. Toluene 2-monooxygenase-dependent growth of *Burkholderia cepacia* G4/PR1 on diethyl ether. *Appl Environ Microbiol* **63**:1606-1609.
- Huss, V. A. R., H. Festl, and K. H. Schleifer.** 1983. Studies on the spectrophotometric determination of DNA hybridization from renaturation rates. *Syst Appl Microbiol* **4**: 184-192.
- Hyman, M. R., C. L. Page, and D. J. Arp.** 1994. Oxidation of methyl fluoride and dimethyl ether by ammonia monooxygenase in *Nitrosomonas europaea*. *Appl Environ Microbiol* **60**:3033-5.
- Johnson, E. L., and M. R. Hyman.** 2006. Propane and n-butane oxidation by *Pseudomonas putida* GPo1. *Appl Environ Microbiol* **72**:950-2.
- Johnson, G. R., and R. H. Olsen.** 1995. Nucleotide sequence analysis of genes encoding a toluene/benzene-2-monooxygenase from *Pseudomonas* sp. strain JS150. *Appl Environ Microbiol* **61**:3336-46.
- Johnson, J. L.** 1994. Similarity analyses of rRNAs. American Society for Microbiology, Washington, DC.
- Jurasek, L., and R. H. Marchessault.** 2004. Polyhydroxyalkanoate (PHA) granule formation in *Ralstonia eutropha* cells: a computer simulation. *Appl Microbiol Biotechnol* **64**:611-7.
- Kalmbach, S., W. Manz, J. Wecke, and U. Szewzyk.** 1999. *Aquabacterium* gen. nov., with description of *Aquabacterium citratiphilum* sp. nov., *Aquabacterium parvum* sp. nov. and *Aquabacterium commune* sp. nov., three in situ dominant bacterial species from the Berlin drinking water system. *Int J Syst Bacteriol* **49 Pt 2**:769-77.
- Kampfer, P., U. Kohlweyer, B. Thiemer, and J. R. Andreesen.** 2006. *Pseudonocardia tetrahydrofuranoxydans* sp. nov. *Int J Syst Evol Microbiol* **56**:1535-8.

- Kim, Y. H., and K. H. Engesser.** 2004. Degradation of alkyl ethers, aralkyl ethers, and dibenzyl ether by *Rhodococcus* sp. strain DEE5151, isolated from diethyl ether-containing enrichment cultures. *Appl Environ Microbiol* **70**:4398-401.
- Kim, Y. H., K. H. Engesser, and S. J. Kim.** 2007. Physiological, numerical and molecular characterization of alkyl ether-utilizing rhodococci. *Environ Microbiol* **9**:1497-510.
- Kohlweyer, U., B. Thiemer, T. Schrader, and J. R. Andreesen.** 2000. Tetrahydrofuran degradation by a newly isolated culture of *Pseudonocardia* sp. strain K1. *FEMS Microbiol Lett* **186**:301-6.
- Kotani, T., Y. Kawashima, H. Yurimoto, N. Kato, and Y. Sakai.** 2006. Gene structure and regulation of alkane monooxygenases in propane-utilizing *Mycobacterium* sp. TY-6 and *Pseudonocardia* sp. TY-7. *J Biosci Bioeng* **102**:184-92.
- Kotani, T., T. Yamamoto, H. Yurimoto, Y. Sakai, and N. Kato.** 2003. Propane monooxygenase and NAD⁺-dependent secondary alcohol dehydrogenase in propane metabolism by *Gordonia* sp. strain TY-5. *J Bacteriol* **185**:7120-8.
- Kubota, M., M. Nodate, M. Yasumoto-Hirose, T. Uchiyama, O. Kagami, Y. Shizuri, and N. Misawa.** 2005. Isolation and functional analysis of cytochrome P450 CYP153A genes from various environments. *Biosci Biotechnol Biochem* **69**:2421-30.
- Kulikova, A. K., and A. M. Bezborodov.** 2001. [Assimilation of propane and properties of propane monooxygenase from *Rhodococcus erythropolis* 3/89]. *Prikl Biokhim Mikrobiol* **37**:186-9.
- Kumar, S., K. Tamura, I. B. Jakobsen, and M. Nei.** 2001. MEGA2: molecular evolutionary genetics analysis software. *Bioinformatics*:1244 - 1245.
- Landthaler, M., A. Yalcin, and T. Tuschl.** 2004. The human DiGeorge syndrome critical region gene 8 and its *D. melanogaster* homolog are required for miRNA biogenesis. *Curr Biol* **14**:2162-7.
- Leahy, J. G., P. J. Batchelor, and S. M. Morcomb.** 2003. Evolution of the soluble diiron monooxygenases. *FEMS Microbiol Rev* **27**:449-79.
- Li, Q. S., U. Schwaneberg, P. Fischer, and R. D. Schmid.** 2000. Directed evolution of the fatty-acid hydroxylase P450 BM-3 into an indole-hydroxylating catalyst. *Chemistry* **6**:1531-6.

- Liu, W., and D. A. Saint.** 2002. A new quantitative method of real time reverse transcription polymerase chain reaction assay based on simulation of polymerase chain reaction kinetics. *Anal Biochem* **302**:52-9.
- Lopes Ferreira, N., D. Labbe, F. Monot, F. Fayolle-Guichard, and C. W. Greer.** 2006. Genes involved in the methyl tert-butyl ether (MTBE) metabolic pathway of *Mycobacterium austroafricanum* IFP 2012. *Microbiology* **152**:1361-74.
- Lopes Ferreira, N., H. Mathis, D. Labbe, F. Monot, C. W. Greer, and F. Fayolle-Guichard.** 2007. n-Alkane assimilation and tert-butyl alcohol (TBA) oxidation capacity in *Mycobacterium austroafricanum* strains. *Appl Microbiol Biotechnol* **75**:909-19.
- Lund, J., and H. Dalton.** 1985. Further characterisation of the FAD and Fe₂S₂ redox centres of component C, the NADH:acceptor reductase of the soluble methane monooxygenase of *Methylococcus capsulatus* (Bath). *Eur J Biochem* **147**:291-6.
- Lund, J., M. P. Woodland, and H. Dalton.** 1985. Electron transfer reactions in the soluble methane monooxygenase of *Methylococcus capsulatus* (Bath). *Eur J Biochem* **147**:297-305.
- Lupien, S., F. Karp, M. Wildung, and R. Croteau.** 1999. Regiospecific cytochrome P450 limonene hydroxylases from mint (*Mentha*) species: cDNA isolation, characterization, and functional expression of (-)-4S-limonene-3-hydroxylase and (-)-4S-limonene-6-hydroxylase. *Arch Biochem Biophys* **368**:181-92.
- Mahendra, S., and L. Alvarez-Cohen.** 2006. Kinetics of 1,4-dioxane biodegradation by monooxygenase-expressing bacteria. *Environ Sci Technol* **40**:5435-42.
- Maier, T., H. H. Forster, O. Asperger, and U. Hahn.** 2001. Molecular characterization of the 56-kDa CYP153 from *Acinetobacter* sp. EB104. *Biochem Biophys Res Commun* **286**:652-8.
- Malachowsky, K. J., T. J. Phelps, A. B. Teboli, D. E. Minnikin, and D. C. White.** 1994. Aerobic mineralization of trichloroethylene, vinyl chloride, and aromatic compounds by *Rhodococcus* species. *Appl Environ Microbiol* **60**:542-548.
- Marin, M. M., L. Yuste, and F. Rojo.** 2003. Differential expression of the components of the two alkane hydroxylases from *Pseudomonas aeruginosa*. *J Bacteriol* **185**:3232-7.
- McClay, K., B. G. Fox, and R. J. Steffan.** 1996. Chloroform mineralization by toluene-oxidizing bacteria. *Appl Environ Microbiol* **62**:2716-22.
- McClay, K., B. G. Fox, and R. J. Steffan.** 2000. Toluene monooxygenase-catalyzed epoxidation of alkenes. *Appl Environ Microbiol* **66**:1877-82.

- McLean, K. J., A. J. Dunford, R. Neeli, M. D. Driscoll, and A. W. Munro.** 2007. Structure, function and drug targeting in *Mycobacterium tuberculosis* cytochrome P450 systems. *Arch Biochem Biophys* **464**:228-40.
- Muller, R., O. Asperger, and H. P. Kleber.** 1989. Purification of cytochrome P-450 from n-hexadecane-grown *Acinetobacter calcoaceticus*. *Biomed Biochim Acta* **48**:243-54.
- Murray, P. R., K. S. Rosenthal, G. Kobayashi, and M. A. Pfaller.** Medical microbiology. 3rd ed. St. Louis, Mo., 1998: 180.
- Murrell, J. C., B. Gilbert, and I. R. McDonald.** 2000. Molecular biology and regulation of methane monooxygenase. *Arch Microbiol* **173**:325-32.
- Murrell, J. C., I. R. McDonald, and B. Gilbert.** 2000. Regulation of expression of methane monooxygenases by copper ions. *Trends Microbiol* **8**:221-5.
- Nelson, D. R., L. Koymans, T. Kamataki, J. J. Stegeman, R. Feyereisen, D. J. Waxman, M. R. Waterman, O. Gotoh, M. J. Coon, R. W. Estabrook, I. C. Gunsalus, and D. W. Nebert.** 1996. P450 superfamily: update on new sequences, gene mapping, accession numbers and nomenclature. *Pharmacogenetics* **6**:1-42.
- Newman, L. M., and L. P. Wackett.** 1997. Trichloroethylene oxidation by purified toluene 2-monooxygenase: products, kinetics, and turnover-dependent inactivation. *J Bacteriol* **179**:90-6.
- Nodate, M., M. Kubota, and N. Misawa.** 2006. Functional expression system for cytochrome P450 genes using the reductase domain of self-sufficient P450RhF from *Rhodococcus* sp. NCIMB 9784. *Appl Microbiol Biotechnol* **71**:455-62.
- Noma, Y., S. Yamasaki, and Y. Asakawa.** 1992. Biotransformation of limonene and related compounds by *Apergillus cellulosa*. *Phytochemistry* **31**:2725-2727.
- Notomista, E., A. Lahm, A. Di Donato, and A. Tramontano.** 2003. Evolution of bacterial and archaeal multicomponent monooxygenases. *J Mol Evol* **56**:435-45.
- Ochman, H., A. S. Gerber, and D. L. Hartl.** 1988. Genetic applications of an inverse polymerase chain reaction. *Genetics* **120**:621-3.
- Omura, T.** 1999. Forty years of cytochrome P450. *Biochem Biophys Res Commun* **266**:690-8.
- Parales, R. E., J. E. Adamus, N. White, and H. D. May.** 1994. Degradation of 1,4-dioxane by an actinomycete in pure culture. *Appl Environ Microbiol* **60**:4527-30.

- Pfaffl, M. W.** 2001. A new mathematical model for relative quantification in real-time RT-PCR. *Nucleic Acids Res* **29**:e45.
- Pieper, D. H., K. Stadler-Fritzsche, H. J. Knackmuss, K. H. Engesser, N. C. Bruce, and R. B. Cain.** 1990. Purification and characterization of 4-methylmuconolactone methylisomerase, a novel enzyme of the modified 3-oxoadipate pathway in the gram-negative bacterium *Alcaligenes eutrophus* JMP 134. *Biochem J* **271**:529-34.
- Quiros, L., S. Jarque, R. Lackner, P. Fernandez, J. O. Grimalt, and B. Pina.** 2007. Physiological response to persistent organic pollutants in fish from mountain lakes: analysis of CYP1A gene expression in natural populations of *Salmo trutta*. *Environ Sci Technol* **41**:5154-60.
- Rojo, F.** 2005. Specificity at the end of the tunnel: understanding substrate length discrimination by the AlkB alkane hydroxylase. *J Bacteriol* **187**:19-22.
- Sawers, R. G.** 2006. Differential turnover of the multiple processed transcripts of the *Escherichia coli* *focA-pflB* operon. *Microbiology* **152**:2197-205.
- Sharp, J. O., C. M. Sales, J. C. LeBlanc, J. Liu, T. K. Wood, L. D. Eltis, W. W. Mohn, and L. Alvarez-Cohen.** 2007. An inducible propane monooxygenase is responsible for N-nitrosodimethylamine degradation by *Rhodococcus* sp. strain RHA1. *Appl Environ Microbiol* **73**:6930-8.
- She, Q., R. K. Singh, F. Confalonieri, Y. Zivanovic, G. Allard, M. J. Awayez, C. C. Chan-Weiher, I. G. Clausen, B. A. Curtis, A. De Moors, G. Erauso, C. Fletcher, P. M. Gordon, I. Heikamp-de Jong, A. C. Jeffries, C. J. Kozera, N. Medina, X. Peng, H. P. Thi-Ngoc, P. Redder, M. E. Schenk, C. Theriault, N. Tolstrup, R. L. Charlebois, W. F. Doolittle, M. Duguet, T. Gaasterland, R. A. Garrett, M. A. Ragan, C. W. Sensen, and J. Van der Oost.** 2001. The complete genome of the crenarchaeon *Sulfolobus solfataricus* P2. *Proc Natl Acad Sci U S A* **98**:7835-40.
- Shields, M. S., S. O. Montgomery, P. J. Chapman, S. M. Cuskey, and P. H. Pritchard.** 1989. Novel pathway of toluene catabolism in the trichloroethylene-degrading bacterium G4. *Appl Environ Microbiol* **55**:1624-1629.
- Shingler, V., F. C. Franklin, M. Tsuda, D. Holroyd, and M. Bagdasarian.** 1989. Molecular analysis of a plasmid-encoded phenol hydroxylase from *Pseudomonas* CF600. *J Gen Microbiol* **135**:1083-92.
- Small, F. J., and S. A. Ensign.** 1997. Alkene monooxygenase from *Xanthobacter* strain Py2. Purification and characterization of a four-component system central to the bacterial metabolism of aliphatic alkenes. *J Biol Chem* **272**:24913-20.

- Smith, C. A., and M. R. Hyman.** 2004. Oxidation of methyl tert-butyl ether by alkane hydroxylase in dicyclopropylketone-induced and n-octane-grown *Pseudomonas putida* GP01. *Appl Environ Microbiol* **70**:4544-50.
- Smith, C. A., K. T. O'Reilly, and M. R. Hyman.** 2003. Characterization of the initial reactions during the cometabolic oxidation of methyl tert-butyl ether by propane-grown *Mycobacterium vaccae* JOB5. *Appl Environ Microbiol* **69**:796-804.
- Smits, T. H., S. B. Balada, B. Witholt, and J. B. van Beilen.** 2002. Functional analysis of alkane hydroxylases from gram-negative and gram-positive bacteria. *J Bacteriol* **184**:1733-42.
- Smits, T. H., M. Rothlisberger, B. Witholt, and J. B. van Beilen.** 1999. Molecular screening for alkane hydroxylase genes in Gram-negative and Gram-positive strains. *Environ Microbiol* **1**:307-17.
- Stanier R. Y., N. J. Palleroni, and M Doudoroff.** 1966. The aerobic *Pseudomonas*: a taxonomic study. *J Gen Microbiol* **43**:159-271.
- Stover, C. K., X. Q. Pham, A. L. Erwin, S. D. Mizoguchi, P. Warrenner, M. J. Hickey, F. S. Brinkman, W. O. Hufnagle, D. J. Kowalik, M. Lagrou, R. L. Garber, L. Goltry, E. Tolentino, S. Westbrook-Wadman, Y. Yuan, L. L. Brody, S. N. Coulter, K. R. Folger, A. Kas, K. Larbig, R. Lim, K. Smith, D. Spencer, G. K. Wong, Z. Wu, I. T. Paulsen, J. Reizer, M. H. Saier, R. E. Hancock, S. Lory, and M. V. Olson.** 2000. Complete genome sequence of *Pseudomonas aeruginosa* PA01, an opportunistic pathogen. *Nature* **406**:959-64.
- Tamura, K., J. Dudley, M. Nei, and S. Kumar.** 2007. MEGA4: Molecular Evolutionary Genetics Analysis (MEGA) software version 4.0. *Mol Biol Evol* **24**:1596-9.
- Tao, Y., W. E. Bentley, and T. K. Wood.** 2005. Phenol and 2-naphthol production by toluene 4-monooxygenases using an aqueous/dioctyl phthalate system. *Appl Microbiol Biotechnol* **68**:614-21.
- Tao, Y., A. Fishman, W. E. Bentley, and T. K. Wood.** 2004. Oxidation of benzene to phenol, catechol, and 1,2,3-trihydroxybenzene by toluene 4-monooxygenase of *Pseudomonas mendocina* KR1 and toluene 3-monooxygenase of *Ralstonia pickettii* PKO1. *Appl Environ Microbiol* **70**:3814-20.
- Teramoto, M., H. Futamata, S. Harayama, and K. Watanabe.** 1999. Characterization of a high-affinity phenol hydroxylase from *Comamonas testosteroni* R5 by gene cloning, and expression in *Pseudomonas aeruginosa* PAO1c. *Mol Gen Genet* **262**:552-8.

- Thierner, B., J. R. Andreessen, and T. Schrader.** 2003. Cloning and characterization of a gene cluster involved in tetrahydrofuran degradation in *Pseudonocardia* sp. strain K1. *Arch Microbiol* **179**:266-77.
- Vainberg, S., K. McClay, H. Masuda, D. Root, C. Condee, G. J. Zylstra, and R. J. Steffan.** 2006. Biodegradation of ether pollutants by *Pseudonocardia* sp. strain ENV478. *Appl Environ Microbiol* **72**:5218-24.
- van Beilen, J. B., and E. G. Funhoff.** 2007. Alkane hydroxylases involved in microbial alkane degradation. *Appl Microbiol Biotechnol* **74**:13-21.
- van Beilen, J. B., E. G. Funhoff, A. van Loon, A. Just, L. Kaysser, M. Bouza, R. Holtackers, M. Rothlisberger, Z. Li, and B. Witholt.** 2006. Cytochrome P450 alkane hydroxylases of the CYP153 family are common in alkane-degrading eubacteria lacking integral membrane alkane hydroxylases. *Appl Environ Microbiol* **72**:59-65.
- van Beilen, J. B., R. Holtackers, D. Luscher, U. Bauer, B. Witholt, and W. A. Duetz.** 2005. Biocatalytic production of perillyl alcohol from limonene by using a novel *Mycobacterium* sp. cytochrome P450 alkane hydroxylase expressed in *Pseudomonas putida*. *Appl Environ Microbiol* **71**:1737-44.
- van Beilen, J. B., T. H. Smits, L. G. Whyte, S. Schorcht, M. Rothlisberger, T. Plaggemeier, K. H. Engesser, and B. Witholt.** 2002. Alkane hydroxylase homologues in Gram-positive strains. *Environ Microbiol* **4**:676-82.
- van Beilen, J. B., M. G. Wubbolts, and B. Witholt.** 1994. Genetics of alkane oxidation by *Pseudomonas oleovorans*. *Biodegradation* **5**:161-74.
- van der Werf, M., H. Swarts, and J. de Bont.** 1999. *Rhodococcus erythropolis* DCL14 contains a novel degradation pathway for limonene. *Appl Environ Microbiol* **65**:2092-102.
- van Hylckama Vlieg, J. E., H. Leemhuis, J. H. Spelberg, and D. B. Janssen.** 2000. Characterization of the gene cluster involved in isoprene metabolism in *Rhodococcus* sp. strain AD45. *J Bacteriol* **182**:1956-63.
- van Rensburg, E., N. Moleleki, J. P. van der Walt, P. J. Botes, and M. S. van Dyk.** 1997. Biotransformation of (+)limonene and (-)piperitone by yeasts and yeast-like fungi *Biotechnology letters* **19**:779-782.
- Wackett, L. P., G. A. Brusseau, S. R. Householder, and R. S. Hanson.** 1989. Survey of microbial oxygenases: trichloroethylene degradation by propane-oxidizing bacteria. *Appl Environ Microbiol* **55**:2960-4.

- Wayne, L. G., Brenner, D. J., Colwell, R. R., Grimont, P. A. D., Kandler, O., Krichevsky, M. I., Moore, L. H., Moore, W. E. C., Murray, R. G. E., Stackebrandt, E., Starr, M. P. & Trüper, H. G. . 1987.** Report of the ad hoc committee on reconciliation of approaches to bacterial systematics. *Int J Syst Bacteriol* **463**:463-464.
- White, G. F., N. J. Russell, and E. C. Tidswell. 1996.** Bacterial scission of ether bonds. *Microbiol Rev* **60**:216-32.
- Woodland, M. P., and H. Dalton. 1984.** Purification and characterization of component A of the methane monooxygenase from *Methylococcus capsulatus* (Bath). *J Biol Chem* **259**:53-9.
- Yang, J. E., Y. J. Park, and H. C. Chang. 2007.** Cloning of four genes involved in limonene hydroxylation from *Enterobacter cowanii* 6L. *J Microbiol Biotechnol* **17**:1169-76.
- Yen, K. M., M. R. Karl, L. M. Blatt, M. J. Simon, R. B. Winter, P. R. Fausset, H. S. Lu, A. A. Harcourt, and K. K. Chen. 1991.** Cloning and characterization of a *Pseudomonas mendocina* KR1 gene cluster encoding toluene-4-monooxygenase. *J Bacteriol* **173**:5315-27.

CURRICULUM VITAE

Hisako Masuda

2002-2003 Teaching assistant, Hiram College, OH

2003 B.A. Biochemistry, Hiram College, OH

2003 B.A. Chemistry, Hiram College, OH

2003 Phi Beta Kappa Society

2003-2005 The H. Boyd and Jeanette Woodruff Microbiology Fellowship

2003-2008 Graduate Assistant, Rutgers the State University of New Jersey, NJ

2007 Teaching assistant, Rutgers the State University of New Jersey, NJ

2008 Ph.D. Microbiology and Molecular Genetics

Vainberg S, McClay K, Masuda H, Root D, Condee C, Zylstra GJ, Steffan RJ. 2006. Biodegradation of Ether Pollutants by *Pseudonocardia* sp. Strain ENV478. AEM:5218.